1976

Histochemical and ultrastructural studies of Quinqueserialis quinqueserialis (Trematoda: Notocotylidae)

Darwin Donald Wittrock
Iowa State University

Histochemical and ultrastructural studies of *Quinqueserialis quinqueserialis* (Trematoda: Notocotylidae)

by

Darwin Donald Wittrock

A Dissertation Submitted to the
Graduate Faculty in Partial Fulfillment of
The Requirements for the Degree of
DOCTOR OF PHILOSOPHY

Department: Zoology
Major: Zoology (Parasitology)

Approved:

Signature was redacted for privacy.

In Charge of Major Work

Signature was redacted for privacy.

For the Major Department

Signature was redacted for privacy.

For the Graduate College

Iowa State University
Ames, Iowa

1976

TABLE OF CONTENTS

INTRODUCTION

Histochemical and ultrastructural studies of trematodes have provided useful data in understanding the biology and host-parasite relationships of these organisms. However, most of these studies have dealt with economically important species, such as Fasciola hepatica and Schistosoma mansoni, and only recently have helminthologists begun to investigate the various organ systems of wildlife parasites.

There exists within the Trematoda a large family of monostomes, the Notocotylidae, parasitic in wild birds and mammals. These trematodes are distinguished from other monostomes by the presence of longitudinal rows of papillae on the ventral surface. A notocotylid possessing five rows of ventral papillae, Quinqueserialis quinqueserialis (Barker and Laughlin, 1911), is a common parasite of muskrats (Ondatra zibethicus) in lakes and marshes near the Iowa Lakeside Laboratory in northwestern Iowa. Infected hosts in this region contained a large number of worms, providing an abundant source of material for subsequent histochemical and ultrastructural investigations.

This dissertation is concerned with detailed studies on various organ systems of Quinqueserialis quinqueserialis. Data were gathered utilizing techniques in light microscopy, histochemistry, and scanning and transmission electron microscopy. A major emphasis of these studies involves determining

structure and chemical composition of the ventral papillae. A complete study of the male and female reproductive systems was also undertaken to elucidate structural relationships of components of these systems. Additionally, various aspects of the digestive, osmoregulatory, and supportive systems were investigated.

Data gained from these studies should provide information useful in understanding the biology of this organism and in elucidating the structural and physiological roles of trematode organ systems.

HISTORICAL REVIEW

The family Notocotylidae Lühe, 1909, whose members parasitize both birds and mammals, comprises the largest group of monostomate trematodes. Although the family has worldwide distribution, most species have been described from localities in Europe and North America.

Although trematodes possessing a single sucker were observed as early as 1782, the genus Monostoma was not established until 1800 when Zeder created the genus based on descriptions of five species including a notocotylid. The group was first organized by Rudolphi (1819), who described two additional notocotylids based on the presence of three rows of ventral papillae. These species were separated from other monostomes by Diesing (1839) and placed in the new genus Notocotylus with Notocotylus triserialis, a parasite of European ducks, as the type species. Diesing, however, confused dorsal and ventral aspects, and, as the generic name implies, regarded the characteristic papillae as dorsal. The first major revision of the group was presented by Kossack (1911), who subdivided the Notocotylidae into two subfamilies: the Notocotylinae, including the genera Notocotylus, Catatropis, and Paramonostomum; and the Ogmogasterinae, represented by the single species Ogmogaster plicatus. An additional subfamily, the

Nudocotylinae, was erected by Barker (1916) to contain Nudocotyle novicia. Harrah (1922) catalogued all North American notocotylid species and included a thorough review of the early history of the family in his monograph. A complete revision and keys to the American species of the subfamily Notocotylinae were presented by Harwood (1939), who recognized five genera as occurring in North America. These genera, identified on the basis of the arrangement of ventral papillae, included Paramonostomum (papillae absent), Hofmonostomum (single median ridge), Catatropis (median ridge and two lateral rows), Notocotylus (three rows), and Quinqueserialis (five rows). A sixth genus, Uniserialis, containing a single median row of papillae, was described by Beverly-Burton (1958).

According to Harwood (1939), characteristic features of the Notocotylidae include in addition to longitudinal rows or ridges of ventral papillae: flattened, ovoid to elongate body; pharynx absent; testes extracaecal and opposite, near posterior end of body; lobed ovary, median between testes; large Mehlis' gland, cephalic to ovary; vitellaria in lateral clusters; metraterm and cirrus pouch well developed; eggs with bipolar filaments.

A notocotylid trematode possessing five rows of ventral papillae, recovered from the caecum of a muskrat, Fiber (=Ondatra) zibethicus, in Nebraska, was described as

Notocotyle quinqueseriale by Barker and Laughlin (1911). Additional descriptions were reported by Barker (1915), Harrah (1922), and Law and Kennedy (1932). A second species, Notocotylus hassalli, separated from N. quinqueseriale by differences in the vitellaria, was reported from the meadow vole, Microtus pennsylvanicus, by McIntosh and McIntosh (1934). To distinguish notocotylids possessing five rows of papillae, Skvortsov (1934) erected the genus Quinqueserialis with Q. quinqueserialis (Barker and Laughlin, 1911) as the type species, and described an additional species, Quinqueserialis wolgaensis, from a vole, Arvicola terrestris. Rausch (1952) described an extremely small species, Quinqueserialis floridensis, from the round-tailed muskrat, Neofiber alleni. A fifth species, Quinqueserialis zibethicai, was described by Gupta (1962) from a single specimen taken from the duodenum of a muskrat in Canada.

Of the five species of Quinqueserialis, all parasitizing microtine (arvicoline) rodents, only three (Q. quinqueserialis, Q. wolgaensis, and Q. floridensis) appear to be valid at present. Kinsella (1971), studying intraspecific variation in Q. quinqueserialis, found that characters used in distinguishing Q. quinqueserialis from Q. hassalli were host-dependent and declared Q. hassalli to be a synonym of

Q. quinqueserialis. He also questioned the validity of Q. zibethicai and considered it as a species inquirenda until the description is confirmed by collection of additional material. Although Q. wolgaensis has been considered by various authors (Rausch, 1952; Smith, 1954; Gupta, 1962) as a synonym of Q. quinqueserialis or Q. hassalli, Kinsella (loc. cit.) retained Q. wolgaensis as a separate species based on differences in sucker size and metraterm length.

The life history of Q. quinqueserialis, involving gyraulid snails as intermediate hosts, was delineated by Herber (1962).

The importance of ventral papillae as a taxonomic character is well established, yet little is known of their function. They have been referred to as ventral glands by some investigators and as ventral papillae by others. Histochemical and ultrastructural observations of these structures to determine their possible function(s) are the focal point of this investigation. References to histochemical and ultrastructural studies on various organ systems of trematodes are presented within subsequent sections of this dissertation.

MATERIALS AND METHODS

Adult Quinqueserialis quinqueserialis were obtained from naturally infected muskrats, Ondatra zibethicus, and meadow voles, Microtus pennsylvanicus, collected by shooting or trapping in areas near the Iowa Lakeside Laboratory, including Miller's Bay on Lake West Okoboji, Crossroads Pond, Garlock Slough and Spring Run Preserve, all in Dickinson County. Anderson Lake and Little Wall Lake in Hamilton County, Skunk Creek in Story County, and farmlands north of Slater in Boone County provided additional collection sites. Hosts were brought into the laboratory where the intestines and caecae were removed and examined for parasites. Dissections were made in white enamel pans where worms could readily be observed due to their reddish coloration.

Light Microscopy and Histochemistry

Upon removal from the host, worms were washed in mammalian saline and fixed for whole mounts by applying AFA with camel-hair brushes. After worms were rigid, a coverslip was applied and the area flooded with AFA. This method prevented flattening of the ventral papillae so that they could be easily observed. Specimens were stained with

Mayer's paracarmine, counterstained with fast green, dehydrated, cleared, and mounted in a synthetic medium (Permount or Kleermount). In addition, some specimens were fixed in 4% formalin, washed in distilled water and 30% acetic acid, and mounted, unstained, in polyvinylpyrrolidine (PVP) for demonstration of the ventral papillae.

Specimens to be sectioned for general morphology and histochemistry were fixed in 10% neutral buffered formalin, 3% glutaraldehyde, Carnoy's, Zenker's, or AFA, dehydrated through tertiary-butyl alcohol, and embedded in Paraplast or Tissuemat at 56-58°C. Serial sections of worms were cut at 8-12 µm on an AO Spencer microtome, affixed to slides with Haupt's gelatin adhesive, and processed according to standard histological and histochemical procedures. For frozen sections, worms were fixed in cold 10% formol calcium, frozen in distilled water, and sectioned at 10 µm in an AO cryostat microtome.

Sections were stained with Harris' hematoxylin with eosin counterstain, Mallory's triple connective tissue stain, and Heidenhain's azan modification of Mallory's triple stain for general morphology. Various histochemical techniques reported by Pearse (1960), Bancroft (1967), Chayen, Bitensky, and Butcher (1973), and H. T. Horner, Jr. (Department of Botany, I.S.U., unpublished lab manual) were

employed on paraffin-embedded and frozen sections of adult Q. quinqueserialis.

To demonstrate total carbohydrates, the periodic acid-Schiff (PAS) test was performed. Control sections consisted of no periodic acid oxidation or digestion with amylase or salivary diastase. Alcian blue at pH 2.5 and Hale's dialyzed iron were used for acid mucopolysaccharides, and Best's carmine was utilized to localize glycogen.

The mercuric bromphenol blue, naphthol yellow S, and ninhydrin-Schiff methods were used for basic proteins. Control procedures included digestion with pepsin, deamination with sodium nitrate, and acetylation with acetic anhydride in pyridine. To demonstrate histones associated with nucleic acids, the fast green-eosin Y method was employed.

For the demonstration of DNA and RNA, the azure B and gallocyanin-chromalum methods were utilized. Control sections were treated with perchloric acid to differentially remove DNA and RNA. In addition, paraffin sections stained with acridine orange for nucleic acid localization were examined with a Leitz fluorescent microscope.

The acetone-Sudan black B method on paraffin sections was used to detect lipids bound to tissue protein. Neutral

fats were localized using Sudan black B and oil red O staining of frozen sections.

For the detection of acid and alkaline phosphatase, azo dye coupling techniques using sodium α-naphthyl phosphate as the substrate were employed. Diazonium salts (Roboz Surgical Instrument Co., Washington, D.C.) used to determine sites of enzyme activity included fast red TR for alkaline phosphatase and fast garnet GBC for acid phosphatase. Substrate was omitted from controls. Nonspecific esterase activity was demonstrated using α-naphthol acetate and the diazonium salt fast blue B. Controls consisted of inhibition of esterase activity by preincubation in 10^{-2}M silver nitrate.

In addition to these histochemical tests, an aldehyde-fuchsin technique (Cameron and Steele, 1959) was employed for morphological localization of presumed neurosecretory cells.

For purposes of orientation and critical study of areas examined with the electron microscope, plastic (epon) sections cut at 1-2 μm with glass knives on an ultramicrotome and stained with methylene blue-azure II at 56°C for one hour were examined with the light microscope. Stained sections were mounted in high viscosity immersion oil to prevent curling of sections normally caused by

synthetic mounting media. Slides were made permanent by ringing coverslips with Permount.

All light photomicrographs were made using Pantomic-X and Kodachrome II type A roll film in a Leitz M-1 or Canon FTb single lens reflex camera mounted on a Leitz Labolux research microscope. Drawings were made with the aid of a Leitz microprojector.

Electron Microscopy

Specimens for transmission electron microscopy were fixed and embedded using protocol given by Lumsden (1970), and summarized as follows: Immediately after removal from the host, worms were fixed for 2 to 3 hours at 4°C in a solution of 3% glutaraldehyde and Sorenson's phosphate buffer. After initial fixation, specimens were washed for 2 to 4 hours with three changes of cold buffer and post-fixed with 1% osmium tetroxide (OsO_4) in buffer for 1 to 2 hours at 4°C. Dehydration in an ethanol-propylene oxide series was followed by infiltration and embedding in Luft's epon mixture. After polymerization of the epon with heat (45°C for one day and 60°C for two days), blocks were trimmed for sectioning, and thin sections (60 to 90 nm) displaying gray to silver interference colors were cut with a Dupont diamond knife on a Reichart OmU2 ultramicro-

tome. Sections, mounted on uncoated 200 mesh copper grids, were doubly stained with uranyl acetate in absolute methanol for 10 to 20 minutes and Reynold's lead citrate for 5 to 10 minutes. Examinations of stained preparations were carried out using Hitachi HS-8 and HU-11C transmission electron microscopes operating at 50 kilovolts. Negatives were taken on Dupont Cronar film at magnifications from 2,500X to 45,000X and photographically enlarged with an Omega D5-V enlarger.

Specimens for scanning electron microscopy were initially washed in Hedon-Fleig saline (Dawes, 1954) and fixed in phosphate-buffered 3% glutaraldehyde followed by post-fixation in 1% osmium tetroxide. Specimens were then washed in three changes of buffer and dehyrated through a graded ethanol series. Dehydrated specimens were transferred to freon TF and dried using critical point drying techniques. Dried specimens were coated with carbon and gold in a Varian vacuum evaporator. Preparations were viewed with a JEOL JSM-S1 scanning electron microscope operating at 10 KV or a JEOL JSM-35 scanning microscope operating at 15 KV. Micrographs were recorded on Kodak Ektapan 4162 negative film or Polaroid type 105 positive/ negative film.

NATURAL INFECTIONS AND SUMMARY OF LIFE CYCLE

The primary hosts of Quinqueserialis quinqueserialis in North America are muskrats (Ondatra zibethicus L.) and meadow voles (Microtus pennsylvanicus (Ord)). In addition, this parasite has been recovered from the mountain vole (Microtus montanus (Peale)), prairie vole (Microtus ochrogaster Wagner), meadow jumping mouse (Zapus hudsonius Zimmermann), woodchuck (Marmota monax L.), and northern pocket gopher (Thomomys talpoides Merriam). Records of Q. quinqueserialis from 22 states and 4 Canadian provinces in North America are summarized in Table 1. This species has also been reported commonly from muskrats and voles in Czechoslovakia and Russia (Lavrov, 1953; Tenora, 1956; Erhardova, 1958; Machulskii, 1959).

During the course of this study, 123 rodents belonging to five families were examined for Quinqueserialis (Table 2). In Iowa, muskrats appear to be the most important hosts as evidenced by their high infection rate and large number of specimens per infected host. Infections in meadow voles are less frequent, probably due to the variety of terrestrial habitats they may occupy where the snail intermediate host does not exist.

Edwards (1949) and Rausch (1952) noted that specimens

Table 1. Records of Quinqueserialis quinqueserialis from North America

Host	Locality	Reference
Ondatra zibethicus and Microtus pennsylvanicus	Maryland	Stiles and Hassall, 1894
Ondatra zibethicus	Nebraska	Barker and Laughlin, 1911; Barker, 1915
Ondatra zibethicus	Washington	Harrah, 1922
Ondatra zibethicus	Ontario	Law and Kennedy, 1932; Sweatman, 1952
Microtus pennsylvanicus	Maryland and Virginia	McIntosh and McIntosh, 1934
Zapus hudsonius	Michigan	Erickson, 1938
Ondatra zibethicus	Iowa, Montana, and Maryland	Harwood, 1939
Microtus pennsylvanicus	Minnesota	Harwood, 1939
Marmota monax	Wisconsin	Rausch and Tiner, 1948
Ondatra zibethicus, Microtus ochrogaster, & Microtus pennsylvanicus	Wisconsin, Indiana, Michigan, and Ohio	Rausch and Tiner, 1949
Ondatra zibethicus	New York	Edwards, 1949
Ondatra zibethicus	Maine	Meyer and Reilly, 1950
Microtus pennsylvanicus and Microtus montanus	Wyoming	Kuns and Rausch, 1950
Ondatra zibethicus	British Columbia	Knight, 1951
Ondatra zibethicus	Colorado	Ball, 1952; Burnett, 1956

Table 1 (Continued)

Host	Locality	Reference
Microtus pennsylvanicus	Alaska	Rausch, 1952
Microtus montanus	Wyoming and Colorado	Smith, 1954
Microtus pennsylvanicus	New Mexico and Colorado	Smith, 1954
Thomomys talpoides	Wyoming	Smith, 1954
Microtus pennsylvanicus and Zapus hudsonius	Quebec and Labrador	Schad, 1954
Ondatra zibethicus	Illinois	Gilford, 1954; Arata, 1959
Ondatra zibethicus	Oregon	Senger and Neiland, 1955
Ondatra zibethicus	Alaska	Dunagan, 1957
Ondatra zibethicus	Utah	Senger and Bates, 1957; Grundmann and Tsai, 1967
Ondatra zibethicus	Pennsylvania	Anderson and Beaudoin, 1966
Ondatra zibethicus	Ohio	Beckett and Gallicchio, 1967
Microtus pennsylvanicus and Ondatra zibethicus	Montana	Kinsella, 1967, 1971
Ondatra zibethicus	Maryland	Abram, 1969
Ondatra zibethicus and Microtus pennsylvanicus	Iowa	Present study

Table 2. Incidence of Quinqueserialis quinqueserialis in rodent hosts collected in Iowa from 1971-1975

Host	Number Examined	Number Infected	Number of specimens per host	Percent Infection
Family Cricetidae				
Ondatra zibethicus	17	14	2-∿5,000	82.4
Microtus pennsylvanicus	59	8	1-26	13.6
Peromyscus leucopus	22	0	-	0.0
Peromyscus maniculatus	5	0	-	0.0
Reithrodontomys megalotis	1	0	-	0.0
Family Zapodidae				
Zapus hudsonius	9	0	-	0.0
Family Sciuridae				
Tamias striatus	5	0	-	0.0
Marmota monax	1	0	-	0.0
Family Castoridae				
Castor canadensis	1	0	-	0.0
Family Muridae				
Mus musculus	2	0	-	0.0
Rattus norvegicus	1	0	-	0.0

from these two hosts varied in size, larger worms occurring in voles and smaller worms occurring in muskrats. Age of worms was suggested as a possible reason for such differences (Rausch, 1952). In experimental studies by Kinsella (1971) on intraspecific variation in Quinqueserialis, specimens of known ages from Microtus and muskrats were compared. He found specimens from Microtus pennsylvanicus (mean length 4.147 mm) and M. montanus (5.541 mm) to be consistently larger than specimens from Ondatra (3.844 mm). In this study, gravid specimens from M. pennsylvanicus measured from 1.80-4.30 mm in length ($\bar{x}$ 3.02) whereas specimens from Ondatra measured from 2.40-3.58 mm ($\bar{x}$ 2.88). Although ages of worms in these natural infections were unknown, these measurements are somewhat smaller than those reported by Kinsella. It was also noted that from one M. pennsylvanicus (host no. 133), which harbored 26 gravid worms in the caecum, specimens measured from 1.80-2.88 mm ($\bar{x}$ 2.33). Although age may certainly be a factor contributing to their small size, crowding, shown by Read (1951) and Holmes (1961) to cause size reductions in cestodes, may have also played a role, effects of which were not taken into account by Kinsella. Even though worms from these natural infections were gravid, such comparisons may have little validity, as Kinsella reported that growth continues

considerably past sexual maturity.

No variation was shown between numbers of ventral papillae in the two hosts. Numbers of papillae ranged from 15-18 in the lateral and paramesal rows and 13-16 in the median row.

The life history of Q. quinqueserialis was delineated by Herber (1962), and summarized as follows: Embryonated filamentous eggs, released by adult worms into the caecal contents and passed out with the feces, must be ingested by the snail intermediate host Gyraulus parvus (Say). Within the intestine, miracidia hatch, penetrate the intestinal wall, and transform into sac-like mother sporocysts in the mantle and tissue surrounding the intestine. Within each mother sporocyst, four mother rediae develop. These migrate to the hepatopancreas where daughter rediae develop rapidly. Twenty-three days following ingestion, immature cercariae emerge through the birth pores of the daughter rediae and remain in the hepatopancreas an additional three days before maturity is reached. At day 26, tri-ocellate monostomate cercariae emerge from snails primarily between 9 and 11 AM. They readily encyst on vegetation and transform into metacercariae. The process of encystment is completed in 3-5 minutes, after which the metacercariae are infective.

Metacercariae ingested by muskrats and voles excyst in

the intestine and migrate to the caecum. According to Kinsella (1971), worms mature sexually in 15 days in Microtus montanus, 18 in M. pennsylvanicus, and 28 in Ondatra zibethicus.

DORSAL TEGUMENT

The nature of the trematode body covering has attracted the attention of helminthologists for many decades. Early investigators concluded that the body lacks an epidermal covering and is instead covered with a resistant cuticle (see review of early literature by Odlaug, 1948). The origin of the cuticle became the subject of considerable controversy, and several theories were advanced, summarized by Hyman (1951) as follows: (1) the cuticle is a degenerate epidermis, (2) it is the basement membrane of a former epidermis, (3) it is the outer layer of an epidermis, cells of which have sunk beneath the subcuticular musculature, and (4) it is the secretion of mesenchymal (parenchymal) cells. Hyman concluded that the fourth theory was the most acceptable.

With the development of the electron microscope and its subsequent application to studies of trematode morphology, controversies concerning the structure and origin of the 'cuticle' have been resolved. In the first published electron microscopic study of the trematode body covering based on observations of Schistosoma mansoni, Senft, Philpott, and Pelofsky (1961) described this structure as "an acellular amorphous" layer. Threadgold (1963), in a detailed description of the body wall of Fasciola hepatica,

however, demonstrated the cytoplasmic syncytial nature of this layer and proposed the term tegument to replace the now inappropriate term cuticle. In addition, Threadgold observed an underlying layer of nucleated cells connected to the syncytial tegument by means of cytoplasmic tubules. Such findings have shown that Hyman's third theory concerning the origin of the tegument was essentially correct.

Subsequent studies on the ultrastructure of the teguments of adult trematodes are numerous (Table 3) and confirm the syncytial nature of the tegument and its connection with underlying subtegumental cells. In general, the ultrastructure of the tegument of Quinqueserialis is similar to that described in other digenetic trematodes. Considerable variation in structure exists, however, between the teguments of the ventral and dorsal surfaces. Portions of the ventral tegument have become modified as ventral papillae, observations of which will be presented in a subsequent section of this dissertation. In the following observations on the ultrastructure and histochemistry of the dorsal tegument, the terminology of Kritsky and Kruidenier (1976), who termed the outer confluent surface the syntegument and the underlying subtegumental cells the cytotegument, will be used.

The dorsal syntegument (Figs. 39-43) varies in thick-

Table 3. Ultrastructural descriptions of teguments of adult trematodes

Trematode	Reference
Monogenea	
Acanthocotyle elegans	Lyons, 1970a
Entobdella soleae	Lyons, 1970a
Gyrodactylus sp.	Lyons, 1970b
Amphibdella flavolineata	Lyons, 1971
Diclidophora merlangi	Morris and Halton, 1971
Plectanocotyle gurnardi	Lyons, 1972
Rajonchocotyle emarginata	Lyons, 1972
Polystomoides spp.	Rhode, 1975
Gyrodactylus eucaliae	Kritsky and Kruidenier, 1976
Aspidobothrea	
Aspidogaster conchicola	Bailey and Tompkins, 1971 Halton and Lyness, 1971
Multicotyle purvisi	Rhode, 1971a
Digenea	
Schistosoma mansoni	Senft et al., 1961 Lee, 1966 Morris and Threadgold, 1968 Silk et al., 1969 Smith et al., 1969 Miller et al., 1972 Hockley, 1973 Wilson and Barnes, 1974
Fasciola hepatica	Threadgold, 1963, 1967b Björkman and Thorsell, 1964a

Table 3 (Continued)

Trematode	Reference
Haematoloechus medioplexus	Burton, 1964
Acanthoparyphium spinulosum	Bils and Martin, 1966
Gorgoderina sp.	Burton, 1966a
Cyathocotyle bushiensis	Erasmus, 1967a
Posthodiplostomum minimum	Bogitsh and Aldridge, 1967
Haplometra cylindracea	Threadgold, 1968a
Megalodiscus temperatus	Bogitsh, 1968 Nollen and Nadakavukaren, 1974
Leucochloridiomorpha constantiae	Harris et al., 1974
Schistosoma haematobium	Kuntz et al., 1976

ness from 7 μm in the anterior regions to 3 μm in the posterior region. Its external surface is convoluted and consists of numerous shallow (0.5 μm) infoldings (Figs. 39, 40). The cytoplasmic ground substance stains intensely with ultrastructural stains (uranyl acetate and lead citrate) and contains numerous inclusions and a few mitochondria. These inclusions, distributed throughout the cytoplasm, are of two types: (1) dense, rod-shaped bodies (DB, Figs. 45, 46) (0.16 μm in length) lacking a limiting membrane, and (2) electron-lucent circular to ovoid vesicles (VB, Fig. 41) (0.9 μm by 0.12 μm) limited by a

distinct unit membrane. A dense particulate material is commonly observed in inclusions of the latter type. Small ovoid mitochondria (M, Fig. 41) (0.2 - 0.5 μm in length), containing few cristae, are sparse in the basal cytoplasm. Presumed ciliated sensory structures with attendent rootlet fibers (RT, Fig. 42) are rarely observed in this region. No evidence of tegumental spines, Golgi complexes, endoplasmic reticulum, or ribosomes are seen in the dorsal syntegument.

Histochemically, the syntegument stains intensely with P.A.S. (diastase fast) (Fig. 12) and mercuric bromphenol blue (Fig. 19), indicating the presence of glycoproteins. Similar observations have been reported in a number of other trematodes (Lal and Shrivastava, 1960; Smith et al., 1969; Watertor and Van Landingham, 1976; Wheater and Wilson, 1976).

Internally, the syntegument is limited by a basal (basement) membrane and amorphous basal lamina (B, Figs. 41, 42). Numerous hemidesmosomes (HD, Fig. 41) secure the membrane to the lamina. Underlying the lamina is a conspicuous layer of fibrous interstitial connective tissue (F, Figs. 39, 42, 43, 68) composed of granules and intertwined fibers. Numerous bands of circular muscle (CM, Figs. 39, 68) and a layer of longitudinal muscle

(LM) are embedded within the fibrous tissue.

Lying below the tegumental muscles are nucleated cells (cytons) forming the cytotegument (Figs. 39, 44-46). This region is connected to the overlying syntegument by means of thin cytoplasmic tubules or internuncial processes (IP, Fig. 43). Each cyton (Fig. 44), irregularly ovoid and 6-10 μm in length, is characterized by a distinct nucleus (N) containing a dense granular nucleolus (NU) and peripheral patches of heterochromatin (H). The cytoplasm contains a high concentration of ribosomes (R, Fig. 46) and an extensive system of granular endoplasmic reticulum (ER, Figs. 44, 45). A few Golgi complexes and mitochondria are present. Clusters containing large numbers of inclusions, identical to those observed in the syntegument, are scattered throughout the cytoplasm (Figs. 44-46). Although ovoid vesicles are present, dense rod-shaped bodies (DB) predominate within each cluster.

The ultrastructural organization of the cytotegument is indicative of cells involved in protein synthesis. Histochemical tests confirm these observations, for the cytotegument stains with azure B for RNA (Figs. 25, 27) and mercuric bromphenol blue for proteins (Fig. 19). The primary sites of protein synthesis in the cytotegument of Quinqueserialis appear to be the ribosomes and granular

endoplasmic reticulum, because Golgi complexes are rarely observed. The granular endoplasmic reticulum is apparently involved in the production of the two types of tegumental inclusions noted above. In other trematodes, however, cytotegumental Golgi complexes are numerous and generally associated with the secretion of these inclusions (Burton, 1966a; Threadgold, 1967b).

The dorsal tegument of Quinqueserialis appears to function primarily as a protective covering. Large numbers of secretory inclusions, particularly the dense rod-shaped bodies produced by the cytotegument, form the cytoplasmic ground substance of the cytotegument. Similar observations were reported by Burton (1966a) and Wilson and Barnes (1974), who suggested that the dense bodies merge to form the ground substance once they reach the syntegument. Because the production of these bodies is continuous, a thick protective surface stratum is maintained.

VENTRAL PAPILLAE

Quinqueserialis quinqueserialis is characterized by the presence of conspicuous papillae on the ventral surface. Although Barker and Laughlin (1911), in their description of Q. quinqueserialis, termed these structures papillae, other authors describing notocotylid trematodes have referred to ventral glands and the terms have been used interchangeably. Smith (1954), in a revision of the genus Quinqueserialis, examined histological sections of papillae and was unable to find any evidence of glandular structures or secretions. He suggested ventral papillae as a preferable term; however, his suggestion has gone largely unnoticed by recent workers. In preliminary ultrastructural observations on ventral papillae of Q. quinqueserialis, Beverly-Burton and Logan (1976) were unable to detect secretory organelles or products in cells associated with them. These authors, in studying paraffin sections of worms in situ, noted that these papillae, often closely applied to the host's caecal epithelium, may function as specialized, nonglandular adhesive organs. Unfortunately, their ultrastructural observations lend little support to this hypothesis.

Because the structure and function of the ventral papillae of Quinqueserialis remain unclear, extensive

studies utilizing techniques in electron microscopy and light-level histochemistry were undertaken to resolve these questions.

Structural Observations

In whole mount specimens of Q. quinqueserialis examined with the scanning electron microscope, the five characteristic longitudinal rows of papillae are prominent on the ventral surface (Figs. 47, 48). Each papilla is circular to ovoid and measures 65-80 μm in diameter. Numbers of papillae range from 15-18 in the lateral and paramesal rows and from 13-16 in the median row. These counts compare favorably with those reported for this species by Barker and Laughlin (1911), McIntosh and McIntosh (1934), Smith (1954), and Kinsella (1971).

Papillae of Q. quinqueserialis are histologically similar to those of the notocotylid Ogmogaster plicatus as illustrated by Führmann (1928). Each contains large numbers of nuclei concentrated in numerous eosinophilic, pyriform cells extending into the body of the parasite (Fig. 5). These cells measure from 95-125 μm in length and 10-16 μm in width at the base. In one micrometer epon (plastic) sections stained with methylene blue-azure II, each papilla consists of a thin outer tegument supported by underlying circular and longitudinal muscles and several

large pyriform cells (PC, Figs. 4, 8). Commonly, small osmoregulatory (excretory) ducts (OD, Figs. 4, 8) branch from large collecting ducts and extend into each papilla.

Electron microscope observations of ventral papillae reveal the specific components of these structures, including: (1) a thin outer syntegument showing regional variations in structure, (2) large pyriform cells underlying the syntegument but joined to it by thin cytoplasmic projections and junctional complexes, and (3) osmoregulatory ducts associated with the pyriform cells.

Syntegument

When viewed with the SEM, this region (Figs. 49, 50) appears highly convoluted and devoid of spines in the apical region of each papilla but becomes spinose along the marginal surface and throughout the general ventral body surface. Infoldings of the syntegument (TI, Fig. 49) form two deep depressions near the apex of each papilla, but there is no histological evidence that these open inward.

The ventral syntegument (Figs. 51-58) consists of a thin (2-3 μm) cytoplasmic layer containing a few small mitochondria (M, Figs. 52, 57, 58) and two types of tegumental inclusions, similar to those described from the dorsal tegument. One type (DB, Fig. 58) consists of

electron-lucent to dense, dumbbell-shaped bodies (1500 Å in length by 300 Å in width) situated near the surface plasmalemma. The second type (VB, Fig. 57) includes circular electron-lucent vesicles (900 Å in diameter) located in the basal portion of the syntegument.

Although the apical region of each papilla is convoluted and devoid of spines, the syntegument of the remaining ventral surface is characterized by the presence of large numbers of paracrystalline spines (SP, Figs. 50, 58) measuring from 1.3 - 1.6 μm long and generally not extending deeply into the cytoplasmic ground substance. The paracrystalline substructure consists of parallel electron-dense bands traversing the spine longitudinally. This configuration closely resembles that of a cylindrical protein lattice crystal and appears to be uniform in all trematodes (Burton, 1964; Erasmus, 1967a; Smith et al., 1969).

Two types of presumed sensory receptors are observed within the syntegument of the ventral papillae. The most common type, the bulbous receptor (Figs. 54, 57) contains numerous synaptic vesicles (VS, Fig. 54) (500 Å in diameter) lying within a bulbous ending in the basal portion of the syntegument. The entire receptor is covered with tegumental cytoplasm, and there is no direct contact with the external medium. Structurally, this

receptor resembles the "lateral bulbous ending" described in the miracidium of Fasciola hepatica by Wilson (1970) and "type III sensory receptor" observed in the tegument of adult Fibricola cratera by Jansma (1971). A bulging of the syntegument at the site of this receptor, noted in the two aforementioned studies, was not observed in Quinqueserialis.

A second type of sensory structure, the ciliated receptor, is rarely observed in the apical syntegument of the papillae. When viewed with the SEM, this receptor appears as a dome-shaped structure containing a single cilium projecting from a central depression (CS, Fig. 50). The cilium (0.21 μm in diameter) possesses an outer ring of nine doublet microtubule units and nine single microtubules randomly arranged inside this ring (Fig. 55). This unusual 9+9 microtubule arrangement has previously been undescribed in ciliated sensory structures of trematodes, although some variation from the typical 9+2 arrangement has been reported. Wilson (1970) described a 7+2 arrangement from the tip of a cilium in the miracidial tegument of Fasciola, and Short and Gagné (1975) reported patterns of 9+0, 8+2, and 8+0 from cilia of possible photoreceptors in Schistosoma mansoni cercariae.

Internally, the syntegument is limited by a convoluted basal membrane and lamina (B, Figs. 52, 56). Under-

lying the lamina is an irregular layer of fibrous interstitial connective tissue (F, Fig. 58) containing bands of circular muscle (CM, Fig. 56) and layer of longitudinal muscle (LM). These muscle bands are commonly interrupted by cytoplasmic processes extending to the syntegument from underlying pyriform cells (Fig. 53). No nucleated elements of a cytotegument were observed within the ventral papillae.

Major chemical components of the ventral syntegument are glycoproteins, as indicated by positive histochemical tests with P.A.S. (diastase fast) for carbohydrates (Figs. 11, 13) and mercuric bromphenol blue for proteins (Fig. 17).

Pyriform cells

Underlying the tegumental musculature are large pyriform cells (="flask-shaped cells" reported by Beverly-Burton and Logan (1976) (Figs. 51, 59-61) forming the bulk of each papilla. Interspersed between them are parenchymal cells (PA, Fig. 51), each containing a large nucleus. Such nuclei apparently constitute many of those observed within each papilla in paraffin sections stained with hematoxylin and eosin (Fig. 5).

The cytoplasm of each pyriform cell is characterized by the presence of large numbers of elongate mitochondria

(M, Figs. 59-61), significantly larger than those of other cell types in Quinqueserialis and measuring up to 4 μm in length with an average diameter of 0.32 μm. Each mitochondrion is bounded by a double unit membrane (75 Å thick) and contains numerous elongate, villiform cristae (CR, Figs. 59, 61) measuring 220 Å in width. These are continuous with the inner unit membrane and extend far into the mitochondrial matrix.

Other cytoplasmic components include a sparse amount of granular endoplasmic reticulum (ER, Figs. 59, 60) and occasional circular osmiophilic inclusions (I, Fig. 60) measuring 0.45 - 0.60 μm in diameter. The peripheral cytoplasm commonly contains cytoplasmic rods or microfilaments (RC, Figs. 53, 61) aligned in parallel rows. These rods, exceeding one or more micrometers in length with a diameter of 300 Å, stain uniformly, and there is no evidence of a tubular configuration. The remaining cytoplasm consists of a dense, finely granular ground substance containing very few free ribosomes. No evidence of Golgi complexes or secretory products was seen in these cells.

The nucleus (Fig. 59) is irregularly shaped and contains scattered patches of heterochromatin, an ovoid, finely granular nucleolus, and an occasional paracrystalline inclusion. A double membrane containing pores (NP) ap-

proximately 500 Å in diameter envelopes the nucleoplasm.

Narrow cytoplasmic projections of each pyriform cell extend between the tegumental muscles and connect with the syntegument by means of junctional complexes or tight junctions (J, Fig. 52). Such junctions (175 Å wide) consist of dense, parallel plasma membranes separated by a narrow intercellular space containing a dense line. Similar junctions are observed connecting pyriform cells with adjacent parenchymal cells and osmoregulatory ducts.

Results of histochemical tests employed on pyriform cells indicate that proteins or protein-bound substances form the major chemical components. These cells stain an intense blue with mercuric bromphenol blue (Fig. 17) and a pale magenta using the ninhydrin-Schiff method (Fig. 23), indicating the presence of basic proteins. A positive reaction for protein-bound lipids, shown by the acetone-Sudan black B method using paraffin sections, is also elicited by these cells (Fig. 32). Although they are proteinaceous, such cells do not appear to be involved in the production or secretion of hydrolytic enzymes, as positive reactions for acid phosphatase, alkaline phosphatase, and nonspecific esterase could not be demonstrated. Additional histochemical tests for carbohydrates, mucosubstances, neutral lipids, and RNA were negative.

Osmoregulatory ducts

These (Figs. 62-67) extend into each papilla from large collecting ducts running lengthwise through the organism. Each duct is formed by an epithelium containing distinct cells separated by septate desmosomes (D, Fig. 64). Although the cytoplasmic volume of these cells is limited within a thin layer, free ribosomes (R, Fig. 63), mitochondria (M, Figs. 63, 67), and Golgi complexes (G, Fig. 67) are present. The cytoplasmic layer becomes greatly distended by the presence of a large ovoid nucleus (N, Fig. 65).

Each epithelial cell is characterized by the presence of long lamellae (LA, Figs. 62-66) forming a continuous border along the luminal surface. Commonly, these lamellae fuse laterally to form stacks (Fig. 66). Each lamella is thin (300 Å) and enclosed by a double membrane. A narrow strip of cytoplasm, continuous with the general epithelial cytoplasm, may be seen within each lamella.

No fat droplets or excretory concretions, common in the lumen of osmoregulatory ducts in Cyathocotyle bushiensis by Erasmus (1967b), were observed in Quinqueserialis.

The basal membrane of the epithelium is surrounded by a layer of fibrous interstitial tissue (F, Fig. 62) interrupted in a few areas where the plasma membranes of

the epithelium and adjacent pyriform cells are joined by junctional complexes (J, Figs. 62, 63).

The ultrastructure of these osmoregulatory ducts corresponds to that described for Schistosoma mansoni by Senft et al. (1961), for Fasciola hepatica by Pantelouris and Threadgold (1963) and Gallagher and Threadgold (1967), and for Cyathocotyle bushiensis by Erasmus (1967b).

Functional Considerations

Evaluation of ultrastructural observations and histochemical tests indicates that the ventral papillae of Q. quinqueserialis are nonglandular. Ultrastructurally, trematode gland cells are characterized by the presence of numerous secretory organelles (such as granular endoplasmic reticulum and Golgi complexes) and accumulated secretory products (Erasmus and Öhman, 1965; Halton and Dermott, 1967; Dorsey and Stirewalt, 1971). These cells may be divided into two generalized groups based upon their reactions to certain histochemical stains. P.A.S.-positive cells which stain for mucosubstances, such as postacetabular gland cells of cercariae, function in the production of mucous for protection or adhesion (Stirewalt, 1965). Gland cells which stain for proteins and RNA and exhibit proteolytic or hydrolytic enzyme activity, such as the

holdfast cells of strigeoids, function in breakdown of host tissue for extracorporeal digestion (Erasmus and Öhman, 1963; Erasmus, 1970; Johnson et al., 1971). Because the pyriform cells constituting each papilla do not contain mucosubstances or hydrolytic enzymes and lack secretory organelles characteristic of trematode gland cells, the term "ventral gland" should be discarded.

Although ultrastructural and histochemical observations on the ventral papillae of Quinqueserialis confirm those presented by Beverly-Burton and Logan (1976), evidence for their hypothesis that papillae function as specialized adhesive organs is sparse. These authors based their hypothesis on observations of papillae associated with the host's caecal wall, such papillae causing depressions distorting the epithelium. In the present study, however, most worms recovered at autopsy were found lying free within the caecal contents. Although some worms were attached to the caecal wall by the oral sucker, this attachment was weak and worms could easily be detached with a camel-hair brush.

Additionally, papillae lack specialized structures associated with adhesion. The major adhesive organs of trematodes, the acetabula or suckers, are extensively muscularized. Another type of adhesive structure, the strigeoid holdfast organ, consists of numerous unicellular

glands. Strigeoid trematodes are commonly deeply embedded in the intestinal mucosa of their hosts, and host tissue may actually be drawn into the holdfast (Erasmus, 1969). Superficially, the ultrastructure of papillae resembles that of the holdfast of Diplostomum phoxini, as described by Erasmus (1970), who observed narrow cytoplasmic processes of holdfast cells extending into the tegument and noted a close association between the holdfast and reserve excretory system. Holdfast cells, however, contain secretory organelles which actively synthesize and secrete hydrolytic enzymes for extracorporeal digestion of host tissue. Because Q. quinqueserialis is rarely attached to the caecal wall and its ventral papillae lack the extensive musculature or enzyme-secreting gland cells of known adhesive organs, the hypothesis that papillae are adhesive appears to have little validity.

On the basis of ultrastructural observations presented in this dissertation, two functions for the ventral papillae of Q. quinqueserialis are suggested: (1) absorption of nutrients, and (2) osmoregulation.

The absorption of nutrients through the thin, highly convoluted apical syntegument of each papilla and the subsequent transport of these nutrients throughout the organism is proposed as one possible function. The role of the trematode tegument in the absorption of nutrients,

especially monosaccharides, has been well documented. In autoradiographic studies, direct evidence for the uptake of glucose by the tegument was demonstrated in Philophthalmus megalurus by Nollen (1968a), Haematoloechus medioplexus and Gorgoderina sp. by Parkening and Johnson (1969), and Alaria marcianae by Bhatti and Johnson (1971). Although tyrosine and leucine are absorbed by teguments of some trematodes (Isseroff and Read, 1969; Bhatti and Johnson, 1971), for most, the gastrodermis appears to be the primary site of amino acid absorption (Nollen, 1968a; Pappas, 1971). Lumsden (1975), in a review of ultrastructural studies of helminth surfaces, noted that the topography of trematode teguments involved in nutrient absorption is generally highly convoluted because of extensive invaginations of the outer plasma membrane. On the other hand, teguments having a smooth topography devoid of specializations for surface area amplification, such as that of Megalodiscus temperatus, are impermeable to hexose sugars and amino acids (Shannon and Bogitsh, 1971).

Nutrients such as glucose which are absorbed into the trematode tegument cross the surface membrane either by simple diffusion or by a mediated system of transport such as facilitated diffusion or active transport (see review by Read, Rothman, and Simmons, 1963). According to Kilejian (1970), helminths generally utilize mediated

transport, i.e., active transport when the metabolite is absorbed against a concentration gradient, or facilitated diffusion when concentrations within the parasite and the outside medium are equal. Metabolic energy must be expended by the parasite if mediated transport is to occur. Glucose has been shown by Phifer (1960a, b) to be actively absorbed by the cestode Hymenolepis diminuta, and, recently, such transport has been demonstrated in the trematode Haematoloechus medioplexus by McCracken (1972), who noted that active transport occurs only at low concentrations, whereas at high concentrations glucose is absorbed by simple diffusion. Although the concentration of glucose in the caecum of hosts infected with Quinqueserialis is unknown, it is probably quite low, and, if absorbed, active transport mechanisms would be required. The occurrence of numerous mitochondria in the pyriform cells of each papilla is indicative of a high degree of metabolic activity necessary for such a process.

Light and electron microscope studies by Erasmus and Öhman (1963), Öhman (1966), and Erasmus (1970) on the strigeoid holdfast have revealed an intimate association between holdfast gland cells and lacunae of the reserve excretory system. These authors suggested that this system may function in the transport of soluble material throughout the organism in the absence of a true circulatory system.

Support for this view was presented by Bhatti and Johnson (1971), who found labelled glucose and tyrosine within excretory spaces of Alaria marcianae. A similar relationship between the pyriform cells of the papillae and epithelial cells forming osmoregulatory ducts may exist in Quinqueserialis. Junctional complexes, shown to be highly permeable to ion transport (Loewenstein and Kanno, 1964; Politoff, Socalar, and Loewenstein, 1967), form connections between these cell types, and may facilitate movement of absorbed nutrients through these structures and throughout the organism.

Although ultrastructural observations on ventral papillae of Q. quinqueserialis are suggestive of an absorptive function, autoradiographic studies are necessary to determine their role, if any, in nutrient absorption.

A second possible function of papillae is that of osmoregulation. Typically, trematodes contain a protonephridial system assumed to function in excretion and/or osmoregulation. Evidence for excretion of lipids was presented by Erasmus (1967b), who reported large fat droplets and excretory concretions in the reserve excretory system of Cyathocotyle bushiensis. Demonstration by Halton (1967b) of hydrolytic enzyme activity in the osmoregulatory systems of eight digenetic trematodes provides evidence for a secretory function associated either with excretion

or nutrient transport. Öhman (1966) suggested that this system may also serve as a hydrostatic skeleton. Although a major function ascribed to this system is osmoregulation, there is no direct confirmatory evidence. To the contrary, experiments by Knox and Pantelouris (1966) and Wilson (1967b) indicate that trematodes are able to tolerate wide ranges of osmotic pressures and that they carry out little water regulation.

The basic unit of the osmoregulatory system is the flame cell (protonephridium), functioning either as a site of filtration of body fluids (Kümmel, 1959) or in the production of hydrostatic pressure within osmoregulatory ducts (Wilson, 1969a). Although flame cells have been observed in early stages of cercarial development in notocotylids (Rothschild, 1938), no descriptions of these cells in adult Q. quinqueserialis are available nor were any observed in the present study. In the apparent absence of flame cells in this trematode, the relationship between pyriform cells and osmoregulatory ducts suggests that papillae may be involved in filtration of body fluids entering or leaving the organism. However, until experimental evidence is obtained, the precise function of notocotylid ventral papillae must remain speculative.

MUSCULATURE

Studies on the fine structure of helminth muscle tissue are numerous, and include investigations on turbellarians (MacRae, 1963, 1965; Morita, 1965), monogeneans (Lyons, 1970b), adult digeneans (Burton, 1966a; Silk and Spence, 1969), miracidia (Wilson, 1969b), cercariae (Kruidenier and Vatter, 1958; Cardell and Philpott, 1960; Lumsden and Foor, 1968; Chapman, 1973; Rees, 1974), cestodes (Lumsden and Byram, 1967), and nematodes (Rosenbluth, 1965; Lee and Miller, 1967). Although variations exist, particularly in interfibrillar structures, these accounts have revealed a basic similarity in the structure of the contractile units, the myofilaments. Myofibrils typically contain two size classes of parallel myofilaments, one with a diameter of 250 Å, the other with a diameter of 50 Å. Such myofilaments do not differ significantly in structure from those described by Huxley (1960) for vertebrate skeletal tissue; thus, it appears that the mechanism of contraction may correspond essentially to Huxley's sliding filament model. Ultrastructural studies on the musculature of Quinqueserialis reveal structures similar to those of other platyhelminths and are consistent with the relatively slow body movements typical of this organism.

Networks of muscle fibers are present throughout the

body of Quinqueserialis, but are primarily concentrated in the oral sucker and parenchyma, beneath the tegument, and surrounding the reproductive structures. Muscles of the body wall consist of outer circular (CM) and inner longitudinal (LM) bands of myofibers lying below the basal lamina and fibrous interstitial layer of the tegument (Figs. 56, 68). There is little difference between musculature of the ventral and dorsal surfaces. Numerous bands of circular muscle form the outer walls of the terminal male reproductive structures, especially the cirrus pouch (Figs. 69, 73).

The contractile portion of the muscle cell consists of a single, elongate myofiber surrounded by a plasma membrane or sarcolemma (SL, Fig. 69). Fibrous interstitial connective tissue (F, Figs. 69, 73) surrounds each myofiber. Within each myofiber are numerous thick (TK) and thin (TN) myofilaments (Fig. 70). Thick myofilaments are dispersed throughout the myofiber; the more numerous thin filaments are interspersed between the thick filaments or appear in areas where thick filaments are absent. There is no geometrical association between these two types of myofilaments.

Mitochondria (M, Figs. 68, 69), containing few cristae, are located along the periphery of each myofiber near the sarcolemma. Sac-like cisternae of sarcoplasmic reticulum

(SR, Fig. 70) (agranular endoplasmic reticulum) are also distributed in this region. No actual contact between the sarcoplasmic reticulum and sarcolemma is evident. Because platyhelminth muscle fibers lack transverse tubule or T-systems (MacRae, 1965; Lumsden and Byram, 1967; Lumsden and Foor, 1968; Rees, 1974), MacRae (loc. cit.) suggested that the sarcoplasmic reticulum with its close association to the sarcolemma may function as the equivalent of the vertebrate T-system in transferring stimuli from one myofiber to another.

Desmosomes (D, Fig. 69) form connections between the sarcolemma and myofilaments. Associated with these desmosomes (or more frequently scattered throughout the sarcoplasm of the myofiber) are irregularly-shaped patches of electron-dense material (DP, Figs. 70, 71). Crossbands of these patches, termed dense bodies by numerous authors, have been reported commonly in invertebrate and vertebrate smooth muscle (see review by Lumsden and Byram, 1967). Dense bodies, possibly equivalent to a fragmented Z-disc, have been suggested to function as attachment sites of thin myofilaments, thus serving as points of insertion from which contraction may be initiated (MacRae, 1965; Lumsden and Foor, 1968). The desmosomal connections between the dense bodies and the sarcolemma serve as means by which mechanical energy generated by the

movement of the myofilaments may be transferred to the surface of the myofiber for subsequent movement of the worm (Lumsden and Foor, 1968).

Myofibers are of the nonstriated type, as seen in longitudinal section in Figure 73. Thick and thin filaments, exceeding one or more microns in length, are not segregated into A or I bands, as in vertebrate skeletal muscle. It is also apparent that the dense bodies are randomly distributed, and there is no "striation" due to an orderly arrangement of dense bodies forming crossbands, as found in the axial musculature of cercariae (Kruidenier and Vatter, 1958; Cardell and Philpott, 1960; Lumsden and Foor, 1968; Chapman, 1973).

Microtubules (MT, Fig. 72), ranging from 200-300 Å in diameter, are occasionally observed in small groups in the periphery of the myofiber. These tubules are consistently oriented parallel to the myofilaments, and have been reported in the sarcoplasm of both vertebrate and invertebrate myofibers (Behnke, 1964; Lumsden and Byram, 1967). In addition, aggregations of microtubules (Fig. 73), perpendicular to the myofibers, are prominent in the musculature surrounding the reproductive ducts. Such aggregations, surrounded by a double membrane, have not been reported in previous studies on the ultrastructure of helminth muscle. Functionally, these structures may be

involved in cytological movements associated with muscle contraction as materials are passed through the reproductive ducts or as cytoskeletal elements maintaining structural form.

PARENCHYMA

Before the advent of electron microscopy, parenchyma was considered to be a packing tissue of mesenchymal cells filling spaces between internal organs. In cestodes and digenetic trematodes, this tissue was believed to be a syncytial meshwork of branched mesenchymal cells enclosing fluid-filled spaces, whereas in the Monogenea, it was thought to consist of discrete cells closely packed together (Hyman, 1951). Recent electron microscopic studies have clearly shown that the parenchyma of cestodes and trematodes is composed of individual, polymorphic cells separated from one another and embedded in a homogeneous matrix of fibrous interstitial tissue (Threadgold and Gallagher, 1966; Lumsden, 1966). On the basis of these studies, Gallagher and Threadgold (1967) suggested three possible functions for parenchymal cells, namely: (1) synthesis and secretion of the fibrous interstitial tissue, (2) storage of glycogen to be mobilized and resynthesized when required, and (3) transport of substances throughout the parasite in the absence of a circulatory system. In addition to protein and carbohydrate synthesis, parenchymal cells may be important sites of lipid metabolism (Lumsden and Harrington, 1966).

Ultrastructural studies have shown glycogen to be a

major cytoplasmic component of platyhelminth parenchymal cells, thus confirming previous histochemical studies. Glycogen has been demonstrated throughout the parenchyma of both trematodes and cestodes by use of various histochemical techniques (Axmann, 1947; von Brand and Mercado, 1961; Burton, 1962; Waitz, 1963; Waitz and Schardein, 1964; Halton, 1967a; Bibby and Rees, 1971). Similar tests performed on Quinqueserialis demonstrate large quantities of carbohydrate substances, believed to be glycogen, in the parenchyma. An intense reaction throughout the parenchyma with the P.A.S. technique indicates the presence of carbohydrates in this region (Fig. 12). After treatment with amylase and diastase, digestion of these substances, shown by a negative P.A.S. reaction, suggests that these carbohydrates are simple polysaccharides such as glycogen. Further evidence of glycogen is demonstrated by an intense staining reaction throughout this area with Best's carmine, a selective stain for glycogen (Fig. 16). Unfortunately, ultrastructural studies do not substantiate these findings, as glycogen was extracted during dehydration as specimens were prepared for electron microscopy.

The parenchyma of Quinqueserialis also contains large amounts of protein, as indicated by mercuric bromphenol blue, ninhydrin-Schiff reaction, and naphthol yellow S. Concentrations of protein are common in large, ovoid cells

found throughout the parenchyma. Although protein synthesis does not appear to be characteristic of helminth parenchyma, its occurrence in the parenchyma of Quinqueserialis suggests that this region may be involved in protein synthesis, as well as a primary site of glycogen storage.

In ultrastructural studies, parenchymal cells have been shown to be highly variable in their size and shape. In Quinqueserialis there appears to be two distinct types of parenchymal cells (herein designated A and B), based on differences in size and cytological components.

Type A Parenchymal Cells

These cells (Figs. 74-78), measuring from 5-10 µm in length, are polymorphic, varying from ovoid to long and slender with many cytoplasmic projections. No syncytial arrangement of cells is observed; plasma membranes are separated from each other by electron-dense intercellular spaces or fibrous interstitial connective tissue. These cells are ultrastructurally similar to those described by Threadgold and Gallagher (1966) and Threadgold and Arme (1974) from Fasciola hepatica and by Lumsden (1966) from the trypanorhynch cestode Lacistorhynchus tenius, and confirm these authors' conclusions that parenchyma of trematodes and cestodes is composed of discrete cytological

units.

Each type A cell contains an irregularly-shaped nucleus (N, Figs. 74, 75) normally located near the cell center. The nucleoplasm, enclosed by a double membrane, is variable in its composition. An amorphous nucleoplasm containing sparse chromatin and a well-defined, finely-granular nucleolus (NU, Fig. 74) is evident in some nuclei. Other nuclei contain large amounts of electron-dense heterochromatin (H, Fig. 75) and no distinct nucleolus.

Scattered throughout the cytoplasm are numerous ribosomes, a moderate number of Golgi complexes, mitochondria, narrow cisternae of granular endoplasmic reticulum, and various types of inclusion bodies. Golgi complexes (G, Figs. 74, 75) consist of 3 to 5 flattened, parallel sacs, somewhat swollen terminally, and numerous small vesicles (GV), some of which are electron-dense, others with internal areas of low density. These complexes are frequently found in association with granular endoplasmic reticulum (ER, Figs. 74, 76) which is most extensive in the peripheral cytoplasm. Numerous ribosomes (R, Fig. 76) are attached to the endoplasmic cisternae or occur free in the adjacent cytoplasm. Mitochondria (M, Fig. 74), often occurring in groups, are small (<1 μm) and either ovoid or circular. Cristae are few, and membranes of each crista are widely

separated forming a conspicuous clear zone. Cytoplasmic inclusions include lipid droplets (L, Fig. 76), membraneous whorls (MW), and small electron-dense vesicles, possibly lysosomes.

Observation of a variety of cellular organelles in type A parenchymal cells suggests a diversity of metabolic functions. The presence of Golgi complexes, free ribosomes, and granular endoplasmic reticulum provides a potential for protein synthesis. As hypothesized by Threadgold and Gallagher (1966), trematode parenchymal cells may be involved in the synthesis and secretion of proteinaceous materials forming the interstitial connective tissue found throughout the parenchyma, beneath the tegument, and surrounding the musculature. This material, composed of fibers similar to elastic fibers, is thought to act as a type of skeletal system, allowing considerable distortion of the body but maintaining general body shape upon relaxation of the muscles. Production of interstitial tissue by a type A cell is shown in Figure 75. Within the peripheral cytoplasm are two Golgi complexes and numerous free ribosomes. Closely associated with these organelles is a quantity of fibrous tissue. There is no evidence of a unit membrane between the cytoplasm and fibrous tissue. These relationships imply that secretions from the Golgi

may be synthesized by ribosomes producing the proteinaceous interstitial tissue. Certainly these cells have the requisite cellular morphology, numbers, and distribution to account for the large amounts of interstitital tissue found in this fluke.

Lipid droplets appear to be a common type of inclusion in platyhelminth parenchymal cells (Waitz and Schardein, 1964; Threadgold and Gallagher, 1966; Lumsden, 1966; Lumsden and Harrington, 1966; Threadgold and Arme, 1974). Investigations by Lumsden and Harrington (1966) and King and Lumsden (1969), using autoradiography and electron microscopy, have revealed parenchymal cells of Hymenolepis diminuta as major sites of lipid metabolism. Although lipids were once thought of as waste products of carbohydrate metabolism (von Brand, 1952), Lumsden and Harrington consider cestodes to be capable of actively absorbing lipids, storing these substances in the medullary parenchymal cells. However, evidence that lipids serve as potential energy reserves is inconclusive (Lumsden, 1966). The end products of lipid metabolism are large, osmiophilic inclusions. These occur commonly in type A cells in Quinqueserialis (Fig. 76). They possess the characteristic morphology of lipid droplets, in that they are large, ovoid structures containing a homogeneous, electron-opaque substance. The lipid content of these inclusions is

further verified by staining of portions of the parenchyma with oil red O. Frequently found in association with lipid inclusions are whorled membranous bodies consisting of numerous concentric folds. These structures have been reported in the gastrodermis of a variety of trematodes and are suspected to be remnants of lipid metabolism (Shannon and Bogitsh, 1969).

Although parenchymal cells are sites of protein synthesis and lipid metabolism, they are believed to play a central role in carbohydrate metabolism as well. Lumsden (1966) reported that the parenchymal cells of Lacistorhynchus are involved in synthesis and degradation of glycogen in addition to serving as storage sites. Specific features of these cells include glycogen inclusions, agranular (smooth) endoplasmic reticulum, large and numerous mitochondria, and lipid droplets. Similar features of cellular organization were described in the parenchymal cells of Fasciola hepatica by Threadgold and Arme (1974), who concluded these cells are involved in both glycogenolysis and glycogenesis. Additionally, many of the enzymes associated with carbohydrate metabolism have been demonstrated in Fasciola parenchyma by Prichard and Schofield (1968, 1969).

Although histochemical tests demonstrate large quantities of glycogen in the parenchyma, there is no evidence of such inclusions in the type A cells of Quinqueserialis. It

is, however, possible that much of the glycogen could have been extracted during dehydration as specimens were prepared for electron microscopy. Nevertheless, the absence of smooth endoplasmic reticulum and presence of few mitochondria would imply that participation in some type of carbohydrate metabolism is unlikely. Although these mitochondria, with their poorly developed cristae, are similar to those from the parenchymal cells of Fasciola as described by Björkman and Thorsell (1962), they are not nearly as abundant in parenchymal cells of Quinqueserialis, nor are there any significant size differences between parenchymal mitochondria and those of other cell types. Such size differences were observed by Lumsden (1966), who noted that in Lacistorhynchus the parenchymal mitochondria, containing enzymes necessary for glycogenesis, are significantly larger and more numerous than those of other cells.

Evidence that parenchymal cells function in the transport of substances in the absence of a recognizable circulatory system has been presented by Gallagher and Threadgold (1967) and Threadgold and Read (1970). Although cells are normally separated by interstitial connective tissue, in localized regions there is intimate contact between cells via junctional complexes or tight junctions (J, Fig. 77), consisting of dense, parallel plasma membranes

(PM) separated by a narrow intercellular space containing a dense line. Such junctions appear commonly throughout the parenchyma of Quinqueserialis, where they form connections with cells of the gastrodermis, osmoregulatory ducts, musculature, and tegument, thus facilitating the transport of chemical substances between these organs systems.

Of considerable interest is the presence of paracrystalline inclusions (PI, Figs. 78, 95) in various cells in Q. quinqueserialis. Proteinaceous inclusions similar to these have been reported from a wide spectrum of animals, but only recently, have they been observed in trematodes, specifically Q. quinqueserialis and Notocotylus urbanensis by Beverly-Burton and Sweeny (1972), Paragonimus kellicotti by Byram et al. (1975), and Schistosoma mansoni by Dike (1971). Observations of Beverly-Burton and Sweeny are confirmed in this study, as similar inclusions occur commonly in cells of the parenchyma, ventral papillae, and reproductive system. Although described as intranuclear bodies by Beverly-Burton and Sweeny, there is evidence of their cytoplasmic location in Figure 78. Ultrastructurally, the paracrystalline pattern appears honeycomb-like with numerous hexagonal, electron-dense granules (Fig. 79). In sagittal section, a wavelike pattern of parallel, electron-lucid lines is observed (Fig. 80). There is no

evidence of an enclosing membrane. The precise nature of these inclusions is not yet fully understood, but Beverly-Burton and Sweeny have speculated that these structures may represent protein storage sites, or, because of their resemblance to rodlike RNA viruses, may be associated with a virus infection. The latter possibility has also been suggested by Byram et al. (1975), who found extreme nucleolar disruption and alterations of the endoplasmic reticulum in caecal epithelial cells of Paragonimus containing a paracrystalline array of viruslike particles.

Type B Parenchymal Cells

Found throughout the parenchymal region of Quinqueserialis are numerous large, ovoid cells (Figs. 81-84), heretofore apparently undescribed from platyhelminths. Termed type B parenchymal cells, they are easily observed in paraffin and plastic sections by light microscopy due to their extreme size (up to 20 µm in width and 40 µm in length).

In addition to their size, type B cells are characterized by a large, circular nucleus (N, Figs. 81, 82) (diameter 6-9 µm) located in the cell center. Contained within the nucleus is an amorphous, lightly-staining nucleoplasm and a distinct, centrally located nucleolus (NU, Fig. 82). Chromatin material is not evident.

The cytoplasm of these cells contains extensive amounts of granular endoplasmic reticulum, cisternae of which appear as wide lakes (EL, Figs. 81, 83, 84) containing a moderately dense material, and smooth endoplasmic reticulum (ER, Figs. 83, 84) with narrow cisternae. Commonly associated with the endoplasmic reticulum are small Golgi complexes (G, Fig. 83) consisting of small vesicles. Ribosomes are dispersed through the cytoplasmic ground substance. Mitochondria (M, Fig. 84) are small and few in number.

Much of the cytoplasm, however, lacks organelles and contains an amorphous ground substance, but areas devoid of this ground substance occur frequently through the cytoplasm. Glycogen is suspected to have been contained in these areas, but is believed to have been extracted during processing of the tissue for electron microscopy. Evidence that these cells once contained glycogen is shown histochemically with the P.A.S. test. The presence of smooth endoplasmic reticulum, abundant in parenchymal cells of Lacistorhynchus and Fasciola (Lumsden, 1966; Threadgold and Arme, 1974), also suggests that glycogen is a normal component of type B cells. Although this evidence is indirect, it appears that these cells are involved, at least in part, in glycogen metabolism.

Type B cells are also believed to be involved in protein

synthesis. Presence of basic proteins in the cytoplasm is demonstrated histochemically by staining with mercuric bromphenol blue. Specific sites of protein synthesis are thought to be the lakes of granular endoplasmic reticulum and Golgi complexes. The moderately-staining substance within the endoplasmic lakes is believed to represent accumulation of a newly synthesized protein, presumably prior to further processing by the Golgi bodies (Toner and Carr, 1971). This type of endoplasmic reticulum, common in a variety of vertebrate cells (Threadgold, 1967a), has been reported from the excretory bladder epithelium of intraredial cercariae of Cryptocotyle lingua by Krupa, Cousineau, and Bal (1969) and from the gastrodermis of numerous adult digeneans (Dike, 1967; Davis, Bogitsh, and Nunnally, 1968; Davis and Bogitsh, 1971a).

CAECUM

Investigations on the nutrition of digenetic trematodes have been numerous. Utilizing a variety of histochemical and ultrastructural techniques, workers have recently shown the digestive tract, specifically the caecum, to be chemically complex and highly variable in structure. The caecum is thought to function simultaneously in absorption, secretion, and digestion. Much current research is concerned with determining specific sites and mechanisms involved in these activities.

Although detailed investigations on the digestive tract of Quinqueserialis were not conducted, evidence presented in this dissertation suggests that the caecum of this fluke is essentially similar in structure and chemical components to those described from other digenetic trematodes.

The digestive tract of Q. quinqueserialis (Fig. 1) consists of a well-developed oral sucker (250-480 µm in diameter) surrounding the mouth. The latter opens into a small, weakly muscularized structure (32-50 µm in diameter) resembling a prepharynx. This structure, previously unreported in descriptions of members of the Notocotylidae, is commonly observed in whole mount specimens and appears in sectioned material as a thickening of

the esophageal epithelium. The esophagus (50-150 μm in length) bifurcates just anterior to the genital opening into two unbranched caeca (intestinal crura). These extend posteriad lateral to the uterine coils, turn mesiad immediately anterior to the testes, and pass between testes and ovary, ending blindly posterior to the testes.

In one micrometer-thick plastic sections, the darkly-staining caecal epithelium shows evidence of numerous projections extending into a lightly-staining lumen (Fig. 7). Within the epithelium are many unstained inclusions. The dorsal position of the caecum in such sections is evident.

Ultrastructural descriptions of caeca of digenetic trematodes are summarized in Table 4. In addition, histochemical and cytochemical observations on a variety of species have been presented by Halton (1967b, d), Bogitsh, Davis, and Nunnally (1968), Threadgold (1968b), Davis, Bogitsh, and Nunnally (1969), Dike (1969), Bogitsh and Shannon (1971), Davis and Bogitsh (1971a), and Bogitsh (1972, 1973).

The caecum of digenetic trematodes is composed of a single layered gastrodermis which may be syncytial (appearing as a modified tegument in the gorgoderids and schistosomes), or, more commonly, composed of epithelial

Table 4. Ultrastructural descriptions of caeca (digestive tracts) of digenetic trematodes

Trematode	Reference
Fasciola hepatica	Gresson and Threadgold, 1959 Thorsell and Björkman, 1965b Robinson and Threadgold, 1975
Schistosoma mansoni	Senft et al., 1961 Morris, 1968 Spence and Silk, 1970 Dike, 1971 Ernst, 1975
Schistosoma haematobium	Sodeman et al., 1972
Schistosomatium douthitti	Shannon and Bogitsh, 1969
Gorgodera amplicava	Dike, 1967
Gorgoderina attenuata	Davis and Bogitsh, 1971a
Haematoloechus medioplexus	Dike 1967, 1969 Davis et al., 1968
Paragonimus kellicotti	Dike, 1969
Megalodiscus temperatus	Bogitsh, 1972 Morris, 1973

cells (low columnar or cuboidal) with distinct lateral cell boundaries (see review by Davis and Bogitsh, 1971a). In Quinqueserialis, the gastrodermis (Figs. 85-89) contains distinct cells separated from one another by plasma membranes observed in junctional complexes (J) or large desmosomes (D, Fig. 89). Septate desmosomes, marking points of gastrodermal cell attachment in many trematodes,

are not evident.

The gastrodermal cytoplasm demonstrates an extensive system of randomly arranged narrow cisternae of granular endoplasmic reticulum (ER, Fig. 87). Golgi complexes (G, Fig. 89), consisting of small, smooth-membraned vesicles, occur occasionally along the luminal surface. Mitochondria (M, Figs. 87, 89), also concentrated in this region, possess few cristae, and, in some sections, no cristae are evident. The basal gastrodermis (Fig. 87) contains many lamellar structures (LA) which may represent infoldings of the basal lamina (B). Muscle bands (MU) and fibrous interstitial connective tissue (F) surround the gastrodermis (Fig. 85).

Conspicuous in the luminal portion of the gastrodermis are large membrane-bound lipid inclusions (L, Fig. 86), similar to those described by Dike (1969) from Paragonimus. These inclusions stain intensely with oil red O (Figs. 29, 30) and Sudan black B (Fig. 31) in cryostat sections, confirming the presence of lipids.

A prominent feature of the gastrodermis is the presence of numerous cytoplasmic projections or microvilli (MV, Figs. 85, 86, 88) extending into the gut lumen. These structures, ubiquitous in digenetic trematodes, may be digitiform or lamelloid and serve to increase the absorptive surface area. Halton (1966), in studies on microvilli of seven trematode species, calculated that these

increase the surface area of the caecum at least 100 times. In addition to enhancing surface area, Morris (1968) hypothesized that microvilli may function in entrapping food particles which are subsequently taken in by endocytosis. Although there is no evidence of endocytosis or intracellular digestion in the gastrodermis (Bogitsh, 1975a), extracellular digestion within the lumen has been suggested by many authors (Thorsell and Björkman, 1965b; Halton, 1967d; Bogitsh et al., 1968; Davis and Bogitsh, 1971a; Bogitsh and Shannon, 1971) due to the occurrence of acid phosphatase along the microvillus border. Specific sites of extracellular digestion may be represented by superficial vacuoles (VA, Figs. 85, 88) formed by microvilli. These structures, shown to contain acid phosphatase secreted from microvilli (Bogitsh et al., 1968; Dike, 1969), may be homologous to intracellular food vacuoles of other animals. Foodstuffs are hydrolyzed within the vacuoles, and end products of digestion diffuse across the microvillar membrane into the gastrodermis (Bogitsh et al., 1968).

Acid phosphatase activity has been demonstrated within the gastrodermal cytoplasm as well as within microvilli. Localized sites of activity include cytoplasmic vesicles (Dike, 1969; Bogitsh and Shannon, 1971; Davis and Bogitsh, 1971a), Golgi bodies (Dike, 1969), rough endoplasmic

reticulum (Dike, 1969; Bogitsh, 1973), and infoldings of the basal plasma membrane (Threadgold, 1968b; Bogitsh and Shannon, 1971; Bogitsh, 1972, 1973). Thus, it is apparent that much of the gastrodermis is involved in the synthesis and secretion of this enzyme for extracellular digestion. This is evident in Quinqueserialis, where in cryostat sections subjected to a modified azo dye coupling technique for acid phosphatase, the enzyme is demonstrated throughout the gastrodermis (Fig. 33). Reaction products were so intense that specific areas of activity could not be ascertained.

The microvillus border and apical cytoplasm also stain with P.A.S. for carbohydrates (Fig. 13) and Alcian blue and Hale's dialyzed iron for acid mucopolysaccharides (Fig. 14). The thick particulate coating or glycocalyx (GC, Fig. 89) associated with the microvillar membranes apparently represents the primary reaction site. Davis and Bogitsh (1971b) demonstrated cytochemically the presence of macromolecular diglycols (a mucopolysaccharide) in the microvillar coatings of Gorgoderina and Haematoloechus. They concluded that the surface coating is a true glycocalyx, a term describing extracellular mucopolysaccharide coatings on plasma membranes. Functionally, the glycocalyx may be involved in binding high molecular weight materials allowing for subsequent digestion by hydrolytic

enzymes at the glycocalyx-plasmalemma interface. Resulting smaller molecules then enter the gastrodermis by diffusion or active transport. Bogitsh (1972) postulated that the mucopolysaccharide component of the glycocalyx is synthesized and packaged in Golgi complexes found along the luminal surface. Since these organelles are similarly located in Quinqueserialis, this may account for the positive Alcian blue and dialyzed iron reactions in the apical cytoplasm.

Although the trematode gastrodermis functions concomitantly in absorption and secretion, correlations of these functions with cellular morphology have led to confusion as to the cell types involved and whether or not these activities occur simultaneously or cyclically. Gresson and Threadgold (1959) proposed a cyclical alteration between absorptive and secretory cell types. Expanding this hypothesis, Dawes (1962) and Thorsell and Björkman (1965b) suggested that absorptive cells develop from degenerating secretory cells which have released their secretory products. Recent evidence by Robinson and Threadgold (1975) indicates that gastrodermal cells of Fasciola are of a single cell type having three different functional states (absorptive, secretory, and transportative). A cyclical, nonsynchronous transformation between functional states results in constant secretion of enzymes for

extracellular digestion and continuous absorption of end products of digestion. Histochemical and ultrastructural observations on the gastrodermis of Quinqueserialis lend support to this interpretation.

FEMALE REPRODUCTIVE SYSTEM

Egg production in digenetic trematodes is a complex phenomenon requiring coordination and interaction of activities by components of the female reproductive system. This system, highly developed in all trematodes, comprises much of the internal structure of Q. quinqueserialis, and appears in whole mount specimens (Fig. 1) as follows: The deeply lobed ovary (O), averaging 315 µm in width and 340 µm in length, is situated between the caeca at the level of the testes. Leading from the anterior end of the ovary is a short oviduct (OV), joined by the common vitelline duct to form the oötype surrounded by the Mehlis' gland (MG). A receptaculum seminis uterinum (RS) leads from the Mehlis' gland and forms the first uterine loop. The egg-filled uterus (U), consisting of 12-15 transverse loops lying between the caeca, extends anteriad to the level of the cirrus sac. A thick-walled, glandular metraterm (ME), 750 µm in length, extends to the common genital opening (GO). Vitellaria (V), arranged in lateral clusters, are extracaecal extending anteriad from the testes. At the level of the Mehlis' gland, the two vitelline ducts (VT) join to form a vitelline reservoir leading to the common vitelline duct. A Laurer's canal is absent.

Although a comprehensive study of all components of the female reproductive system of Quinqueserialis quinqueserialis was not undertaken, histochemical and ultrastructural observations were made on the ovary, Mehlis' gland, vitellaria, uterus, and eggs.

Ovary

Although studies on egg shell formation by digenetic trematodes are numerous, few histochemical and ultrastructural studies on the ovary have been published. These include observations on the ovary and oocytes of Fasciola hepatica by Govaert (1960), Gresson (1962, 1964), and Björkman and Thorsell (1964b) and of Schistosoma mansoni by Spence and Silk (1971) and Erasmus (1973).

The ovary of Quinqueserialis (Figs. 90-92) contains a large number of gonial cells (GN, Fig. 90) surrounded by an ovarian wall consisting of a basement membrane and basal lamina (B). Underlying the lamina are occasional muscle fibers (MU).

Gonial cells, occurring in different states of maturation, vary in size from 5-10 μm in diameter. Commonly, smaller cells representing oogonia are found along the periphery of the ovary, whereas the larger oocytes occur in the central region. However, no major differences, other

than size, have been observed in ultrastructural studies on these cell types (Björkman and Thorsell, 1964b; Gresson, 1964).

Characterizing each gonial cell is a large, ovoid nucleus (N, Fig. 91) containing a distinct nucleolus (NU). Aggregations of heterochromatin (H) are dispersed throughout the nucleoplasm. Commonly associated with the nuclear membrane are narrow perinuclear spaces (PS, Fig. 92). Major cytoplasmic constituents are clusters of mitochondria (M, Figs. 90-92), containing sparse cristae, and small cortical granules (CG, Fig. 92), conspicuous in the perinuclear cytoplasm. These granules, common in the oocytes of Fasciola and Schistosoma, have been shown by Björkman and Thorsell (1964b) to be polysaccharide in nature and are thought to serve as nutritive bodies (Gresson, 1964). In close association with these granules are long, thin cisternae of smooth endoplasmic reticulum (ER, Fig. 92), continuous with the nuclear membrane. Since Golgi complexes are few, it appears that the smooth endoplasmic reticulum is involved in the production of the cortical granules.

Previous histochemical and autoradiographic studies have indicated that the major chemical components of gonial cells are proteins and nucleic acids. Govaert (1960) reported a positive Millon reaction in cytoplasm of oocytes of Fasciola hepatica, and Thorsell, Björkman, and

Appelgren (1966) demonstrated incorporation of labelled amino acids, precursors of protein, by these cells. Incorporation of ^{3}H-thymidine into DNA in the nucleus of gonial cells in two species of Philophthalmus was observed by Nollen (1968b) and Moseley and Nollen (1973). In Q. quinqueserialis, the cytoplasm of gonial cells stains with azure B for nucleic acids (Fig. 27) and with mercuric bromphenol blue for basic proteins (Fig. 20), confirming previous histochemical studies.

Mehlis' Gland

Histochemical and ultrastructural studies on the Mehlis' gland of trematodes are numerous, yet the precise function of this structure is still the subject of controversy. Early investigators believed the Mehlis' gland to be primarily responsible for secretion of the egg shell, but this hypothesis was discarded when recent workers (Stephenson, 1947; Smyth and Clegg, 1959; Burton, 1963, 1967a) determined that the bulk of the egg shell is formed from protein globules arising from the vitelline cells. Dawes (1940) and Burton (1963) theorized that the Mehlis' gland secretes a primary membrane around an oocyte and several vitelline granules, the latter coalescing upon the membrane to form the egg shell. Lipoprotein membranes, secreted by the Mehlis' gland, were demonstrated on the

inner and outer surfaces of egg shells of Fasciola by Clegg (1965), who concluded that these membranes serve as templates for the deposition of shell material. Studies by Gönnert (1962), Thorsell and Björkman (1965a), Threadgold and Irwin (1970), and Irwin and Threadgold (1972) using Fasciola and by Burton (1967a) using Haematoloechus medioplexus have revealed the presence of two secretory cell types within the Mehlis' gland. One cell type, referred to as DB-cell (Burton, 1967a) or S_2 cell (Threadgold and Irwin, 1970), occurs near the ootype and synthesizes a dense secretory product termed dense body. The second cell type, termed MB-cell or S_1 cell, is more numerous and secretes a membranous body.

These two types of secretory cells are also evident in the Mehlis' gland of Q. quinqueserialis. The DB-cells surround the ootype and contain many electron-dense secretory bodies (SG, Fig. 93). Occasional mitochondria, granular endoplasmic reticulum, and membranous whorls characterize the DB-cell cytoplasm.

The peripherally located MB-cells (Figs. 94-96) are more numerous and distinguished from the DB-cells by the presence of large numbers of cytoplasmic vacuoles containing membranous secretory bodies (MS, Figs. 95, 96). These bodies, consisting of small vesicles and membranous residues, have been shown to contain acid phosphatase

(Bogitsh, 1970) and may represent autolysosomes in the process of hydrolyzing excess secretory material. Golgi complexes (G, Figs. 94, 95) are closely associated with the membranous bodies and appear to be involved in their secretion. Endoplasmic reticulum (ER, Figs. 95, 96) is frequently observed surrounding the nucleus or adjacent to the outer plasma membrane. Small ovoid to elongate mitochondria (M, Fig. 96), containing few cristae, often occur in groups scattered throughout the cytoplasm.

The MB-cell nucleus (N, Fig. 94) is irregular in outline and contains a distinct nucleolus (NU). Intranuclear paracrystalline inclusions (PI, Fig. 95) are common.

In histochemical tests, the MB-cells stain for nucleic acids (RNA) (Fig. 27) and nonspecific esterase (Fig. 37) confirming their secretory function. Esterase activity has been demonstrated in the Mehlis' gland cells of Fasciola hepatica by Halton (1967c), but its role in secretory activities is not known.

A number of possible functions for the Mehlis' gland and its secretions have been proposed. Burton (1967a) suggested that the secretion of the DB-cells may lubricate the uterus or stimulate the spermatozoa, whereas the MB-cell secretions may induce the expulsion of protein granules from the vitellaria. Irwin and Threadgold (1972)

hypothesized that secretions from the MB-cells lower the surface tension of shell protein globules allowing them to unite more easily in forming the trematode egg shell. Additionally, secretions of either of these cell types may play a part in the actual tanning process of the egg shell, either by triggering the enzymatic process or by adding some essential co-factor to the process (Threadgold and Irwin, 1970).

Vitellaria

The role of vitellaria in the production of protein globules which eventually form the trematode egg shell is well documented (see reviews by Smyth and Clegg, 1959; and Irwin and Threadgold, 1970). The precursors of egg shell sclerotin (basic proteins, phenols, and phenolase) have been demonstrated histochemically in these globules. Ultrastructural observations have revealed additional features, particularly an extensive system of granular endoplasmic reticulum, consistent with a high degree of protein synthesis. Moreover, vitelline cells appear to be involved in glycogen synthesis and provide a food store for the developing miracidium.

The vitellaria of Q. quinqueserialis (V, Fig. 1) are composed of lateral clusters, consisting of follicles containing vitelline cells in various stages of development

(Fig. 8). Four developmental stages, categorized by Erasmus (1975a), are evident. Immature cells (stage 1) (Fig. 97) are characterized by a large nucleus (N) and cytoplasm containing scattered ribosomes (R) and a few mitochondria (M). Granular endoplasmic reticulum is poorly developed. Cells of increasing maturity (stage 2) (Fig. 99) contain an extensive system of granular ER and small globules of shell protein (PG), the latter occurring singly within membrane-bound spheres found throughout the cytoplasm. Yolk droplets (Y, Fig. 99) are common in stage 2 cells. Stage 3 cells (Figs. 100, 101) contain numerous free ribosomes (R), an extensive system of granular ER arranged in parallel series, and protein globules (PG) accumulated within membrane-bound clusters. The cytoplasm of mature cells (stage 4) (Figs. 102, 103) is displaced to the cell periphery by large clusters of globules. Each cluster contains 15-20 small globules (PG, Fig. 102) well separated from one another. Small amounts of glycogen (GY, Fig. 103), remnants of ER, and occasional Golgi complexes also occur within these cells.

The nucleus (N, Figs. 97, 100) of cells in any stage is similar, containing large amounts of chromatin material. A distinct nucleolus was not observed.

In addition to developing vitelline cells, each follicle contains nurse cells (Fig. 98) located along the

perimeter. These cells are similar in structure to stage 1 cells but possess cytoplasmic projections extending between developing vitelline cells. Nurse cells apparently function in transport of nutritive materials from the parenchyma to the developing vitelline cells (Irwin and Threadgold, 1970).

These findings indicate that vitelline cells of Quinqueserialis undergo a continuous developmental process resulting in the progressive accumulation of protein globules. Ultrastructural observations of vitelline cells undergoing morphological changes during maturation have been recorded for Haematoloechus medioplexus by Tulloch and Shapiro (1957), for Fasciola hepatica for Björkman and Thorsell (1963) and Irwin and Threadgold (1970), for Schistosoma mansoni by Erasmus (1975a), and for three species of monogeneans by Halton, Stranock, and Hardcastle (1974).

The granular endoplasmic reticulum (GER) in cells of stages 2 and 3 is apparently the site of synthesis and packaging of protein globules. Evidence presented by Erasmus (1975b), who precisely localized labelled tyrosine in the GER and protein globules of vitelline cells of S. mansoni, substantiates this view. Irwin and Threadgold (1970) suggested that although protein globules are synthesized by the GER, they are concentrated into

membrane-bound packages by Golgi complexes. Erasmus (1975b), however, was unable to localize tyrosine in Golgi complexes but indicated that only newly formed globules could be labelled. Although Golgi complexes are abundant in maturing vitelline cells of Fasciola and Schistosoma, they occur only occasionally in mature stage 4 cells of Quinqueserialis and appear to play a minor role in the production of protein globules.

As vitelline cells mature to stage 4, protein synthesis ceases due to degeneration of GER, and small amounts of glycogen become evident. Apparently these cells serve as storage sites of accumulated shell protein and glycogen. Glycogen may exist in the form of rosettes or within yolk droplets (Irwin and Threadgold, 1970; Halton et al., 1974), but concentrations in Quinqueserialis are low and undetectable with light-level histochemistry. Specific sites of glycogen synthesis are unknown. Hanna (1976), in electron autoradiographic studies, noted rapid incorporation of galactose and glucose into glycogen within maturing vitelline cells of Fasciola, but was unable to associate any cell organelle with its synthesis. He concluded that previously formed glycogen might act as a template for further synthesis.

In histochemical studies, Smyth and Clegg (1959), Burton (1963), Fried and Stromberg (1971), and Nollen

(1971) have demonstrated the presence of basic protein, phenols, and phenolase, precursors of a quinone tanning system, within vitelline cells of a variety of trematodes. The major component of the basic protein is tyrosine, which is readily incorporated in the vitelline cells and later detected in egg shells (Nollen, 1971; Moseley and Nollen, 1973). In Quinqueserialis, basic protein was identified in vitellaria using mercuric bromphenol blue (Fig. 19). Intense staining with azure B for nucleic acids was also observed (Fig. 26). Although histochemical tests for phenols and phenolase were not conducted, the occurrence of a quinone tanning system in egg shells of Quinqueserialis is suspected. This type of system is commonly reported in trematodes inhabiting the digestive systems of their hosts and is believed to represent a digestion resistant device (Llewellyn, 1965).

Uterus

The most obvious component of the female reproductive system of Quinqueserialis is the egg-filled uterus (U, Fig. 1). In addition to functioning as a conduit for the passage of eggs to the exterior, the uterus provides a passageway for spermatozoa to the ootype where fertilization occurs. In the absence of a Laurer's canal and distinct seminal receptacle, that portion of the uterus forming the first uterine loop is

modified as a receptaculum seminis uterinum for storage of spermatozoa. Evidence provided by Coil (1966) indicates that the uterus of notocotylid trematodes is also involved in the formation of polar egg filaments.

Surprisingly, the ultrastructure of the trematode uterus is poorly known. In a comprehensive examination of the female reproductive system of Schistosoma mansoni, Spence and Silk (1971) described the lining of the uterus as a typical tegumental structure. This is clearly not the case in Quinqueserialis. The uterine wall (Figs. 104-109) appears as a thin epithelium, 1-2 μm in thickness, containing distinct cells separated from one another by desmosomes (D, Fig. 106). The basal portion of these cells is bordered by a thin basal lamina (B, Figs. 106, 107) underlaid by a thin layer of circular muscle (MU, Fig. 107). Parenchymal cells (PA, Fig. 104) are commonly interspersed between adjacent uterine walls. The plasma membrane along the luminal edge is commonly infolded in areas where secretory products are released into the lumen (Figs. 107, 109). In other regions, filiform cytoplasmic projections (CE, Fig. 106) extend into the lumen. Flattened, elongate nuclei (N, Fig. 104) are centrally located and contain chromatin along the periphery.

A high degree of secretory activity within these cells is reflected by the presence of extensive granular endo-

plasmic reticulum (ER, Figs. 105-109) and numerous Golgi complexes (G, Fig. 107). Mitochondria (M, Figs. 107, 108) occur in groups dispersed throughout the cytoplasm. Two types of secretory products are produced by the uterine cells. The most obvious are large electron-dense globules (SG, Fig. 105) found within the uterine lumen. They are also observed within the cytoplasm (Fig. 109) near Golgi complexes and GER, which presumably are involved in their production. These globules, released through infoldings of the cytoplasm, accumulate in the lumen. A second type of secretion, apparently produced by the same organelles, consists of small membranous vesicles (FS, Fig. 107). Once in the lumen, these vesicles appear to break up and form a dense fibrous matrix.

The functions of these secretions are unknown, but either or both may be involved in (1) lubrication of the uterus for passage of eggs, (2) formation of additional egg shell layers, or (3) formation of polar egg filaments. Uterine involvement in secretion of an outer egg shell and in filament formation was described by Coil (1966) in a histochemical study of the notocotylid Ogmocotyle indica. Coil speculated that although the uterus was the site of filament formation, materials contributing to the filament originated in the vitellaria. In Quinqueserialis, filament formation first appears within the fourth uterine loop, quite some distance from the vitellaria, and development continues throughout the remainder

of the uterus. Because uterine cells are actively secreting materials in these regions, it is more probable to assume that filaments are produced from uterine secretions. Identification of the specific secretions involved and mechanisms of filament formation, however, must await further investigation.

Eggs

Long bipolar filaments (EF, Fig. 110) are characteristic of eggs of notocotylid trematodes. In measurements of twenty randomly selected eggs of Q. quinqueserialis, filaments vary in length from 306-560 μm ($\bar{x}$ 390). Rarely a double filament is observed on one pole. The ovoid egg capsules (EC, Fig. 110) measure 8-12 μm ($\bar{x}$ 9.5) in width by 16-20 μm ($\bar{x}$ 18) in length.

Viewed with the scanning electron microscope, the surface of the egg capsule (Fig. 111) is highly irregular containing many shallow pits. High magnification (Fig. 112) reveals a surface reminiscent of the lunar landscape with its many craters. Filaments (Fig. 111) have a smooth surface and are often twisted at the point of attachment to the egg capsule.

Observation of intrauterine eggs with the transmission microscope reveals the presence of two distinct layers within the egg capsule. The inner layer (IL, Figs. 113, 114) (0.6-

0.8 μm in thickness) forms the major portion of the egg shell. It stains uniformly with ultrastructural stains and is apparently produced from secretions of the vitellaria. The outer layer (OL, Figs. 113, 114) is thinner (0.3 μm) and appears as a membranous reticulum. Its outer edge (Fig. 113) is irregular but distinct pits, noted with the SEM, were not observed. This layer is most likely formed by secretions of the uterine epithelium, because eggs recently discharged from the ootype, when exposed by cryofracture techniques and examined with the SEM, have a smooth surface. Such eggs (Fig. 28) also lack polar filaments.

The occurrence of a reticulate outer egg shell layer has not been reported in previous ultrastructural studies on trematode egg shells. A smooth outer surface is characteristic of Fasciola egg shells (Wilson, 1967a), and microspines characterize egg shells of schistosomes (Hockley, 1968; Schnitzer et al., 1971). Krupa (1974), observing egg shells of Cryptocotyle lingua, noted villi-like protrusions and a thin filamentous coating along the outer layer. This filamentous coating is similar to the reticulate layer in Quinqueserialis but lacks membranous interconnections.

Lying within the egg capsule is the developing miracidium (Fig. 114). Observation of nuclear material of a spermatozoan (S) indicates that fertilization has occurred and mitosis is underway. Histochemical tests suggest that

developing miracidia (embryos) contain large amounts of carbohydrates (Fig. 11) and nucleic acids (Fig. 28). Carbohydrates, predominately glycogen, are demonstrated in embryos located only in the distal portions of the uterus. Burton (1962) observed a similar reaction for glycogen in embryos of Haematoloechus medioplexus and concluded that developing miracidia readily synthesize glycogen from exogenous glucose for use as a future food reserve.

MALE REPRODUCTIVE SYSTEM

Previous light and electron microscope studies on the male reproductive system of digenetic trematodes have dealt primarily with descriptions of spermatozoa and the processes of spermatogenesis and spermiogenesis (see reviews by Gresson (1965) and Burton (1972)). Although these topics have attracted much attention, few published reports are available on the fine structure of the terminal genitalia of trematodes. These include recent publications by Threadgold (1975a, b), who described the fine structure of components of the cirrus sac of Fasciola hepatica.

Much of the present investigation involves a detailed examination of components of the terminal male genitalia of Q. quinqueserialis. These structures, all lying within the cirrus sac, include the seminal vesicle, prostate gland, ejaculatory duct, and cirrus. Additional ultrastructural observations are presented on the spermatogonial cells of the testes, spermatozoa, and associated ducts.

Testes

The two conspicuous testes lie in the posterior end of the body. In whole mount specimens (Figs. 1, 2), the lateral surface of each testis is lobate (4-6 lobes per testis), whereas the medial surface is relatively smooth. Each testis

measures from 300-450 μm in width by 600-800 μm in length. In sectioned material, a number of cells in various stages of development are distributed throughout each testis. These cells include spermatogonia, spermatocytes, spermatids, and mature spermatozoa.

Morphological changes of these cells resulting in spermatogenesis (formation of spermatids) and spermiogenesis (formation of mature spermatozoa) have been reported for a number of trematode species. The major features of these processes have been described at the light level in Parorchis acanthus by Rees (1939), Fasciola hepatica by Yosufzai (1952), Haematoloechus medioplexes by Burton (1960), Halipegus eccentricus by Guilford (1961), and Philophthalmus megalurus by Khalil and Cable (1968). Most ultrastructural investigations have generally been restricted to descriptions of the mature spermatozoa (see review by Burton, 1972), and only recently have studies on the fine structure of early stages of spermatogenesis and of the maturation of spermatozoa (spermiogenesis) been published. These include reports by Sato, Oh, and Sakoda (1967) on Paragonimus miyazakii, Jansma (1971) on Fibricola cratera, Burton (1972) on H. medioplexus, Grant, Harkema, and Muse (1976) on Pharyngostomoides procyonis, and Halton and Hardcastle (1976) on Diclidophora merlangi.

Gresson (1965), in a review of spermatogenesis in the hermaphroditic Digenea, noted that this process conforms to a common pattern. Primary spermatogonia near the periphery of the testis divide mitotically to produce two secondary spermatogonia centrally connected by a narrow cytoplasmic bridge. These in turn divide to form a cluster of tertiary spermatogonia, whose division results in the formation of a rosette of eight spermatocytes. These undergo two meiotic divisions to give rise to a cluster of 32 spermatids. Subsequent spermiogenesis results in the formation of typical filamentous spermatozoa.

Unfortunately, there is no orderly arrangement of these developmental stages in the testes; thus, assignment of the proper stage to each germ cell is rather difficult. However, Halton and Hardcastle (1976), in an ultrastructural study of spermatogenesis in the monogenean Diclidophora merlangi, were able to characterize each developmental stage, and criteria for distinguishing these early stages in Q. quinqueserialis are based on their investigations.

Ovoid spermatogonia (Figs. 115, 116) are characterized by large, spherical nuclei (N, Fig. 115), each containing a granular nucleoplasm and scattered patches of heterochromatin. The reduced cytoplasmic volume is typical of these unspecialized, undifferentiated cells. The bulk of the cytoplasm consists of a ribosomal ground substance in which

a moderate number of small mitochondria (M, Fig. 116), occasional profiles of smooth endoplasmic reticulum (ER, Fig. 116), and a few Golgi complexes (G, Fig. 115) are observed.

Spermatocytes (Fig. 117), formed by mitotic division of tertiary spermatogonia, are the largest germ cells (15 μm in length) formed during spermatogenesis. Each spermatocyte is elongate and contains a large volume of cytoplasm. The centrally located nucleus (N) is similar in appearance to that of a spermatogonium but slightly smaller. The cytoplasmic ground substance contains free ribosomes, mitochondria (M), narrow cisternae of smooth endoplasmic reticulum (ER), and Golgi complexes (G), the latter apparently producing clusters of secretory vesicles (SG). The cytoplasm of some spermatocytes also contains filamentous chromosomes (CH, Fig. 118) undergoing division.

Groups of spermatocytes are centrally connected by narrow cytoplasmic bridges (Fig. 118) termed cytophores by Sato et al. (1967). Each cytophore is characterized by narrow cisternae of smooth endoplasmic reticulum lying within the outer plasma membrane.

After two meiotic divisions, each spermatocyte gives rise to a rosette of 32 spermatids, each of which undergoes spermiogenesis to form a single mature spermatozoan. The process of spermiogenesis, demonstrated at the light level in Fasciola hepatica and Dicrocoelium dendriticum by Hendel-

berg (1962) and at the EM level in Haematoloechus medioplexus by Burton (1972), may be summarized as follows: Initially, two cytoplasmic projections are formed near the apical end of the spermatid in a region termed the zone of differentiation by Burton. These projections extend outward from the spermatid and eventually give rise to two flagellar processes or axonemes. As axonemes become differentiated, a third cytoplasmic projection, the median process or mid-piece, arises from the zone of differentiation and extends between the axonemes. As these three cytoplasmic processes elongate, the spermatid nucleus becomes extended and migrates into the mid-piece. Condensation of chromatin into dense strands accompanies nuclear elongation. Eventually, the nucleus leaves the spermatid body and takes its place in the distal end of the mid-piece. Axonemes lying on each side of the mid-piece then fuse with the latter to form a monopartite spermatozoan. Each spermatozoan then detaches from the spermatid body which remains in the testis as a residual cytoplasmic body.

Spermiogenesis in Quinqueserialis appears to follow a similar course. Early spermatids (Figs. 119, 120) contain an elongate nucleus (N) coiled throughout the cytoplasm. The chromatin material has become condensed into thin electron-dense sheets or lamellae and gives the nucleus a scroll-

like appearance. Characteristic of the cytoplasm are thin cisternae of smooth endoplasmic reticulum (ER, Fig. 122) and extensive Golgi complexes (G, Fig. 120), the latter consisting of 10-12 elongate electron-lucid saccules. Function of the Golgi bodies is unclear, but Halton and Hardcastle (1976) speculate that may contribute membranous components to the plasma membrane as the cytoplasmic projections elongate.

Associated with the nucleus of the early spermatid is a centriole-like structure (Fig. 121) recently termed the microtubule-organizing center (MTC) by Grant et al. (1976). Lying on each side of the MTC are striated ciliary rootlets (RT) from which arise the two axonemes characteristic of trematode sperm. Apparently, the MTC is involved in the assembly of the nine peripheral doublets of microtubule (axial) units comprising each axoneme (Grant et al., 1976).

Axonemes extend outward from the MTC and form two cytoplasmic projections. Cross sections of axonemes (A, Figs. 123-129) illustrate the 9+1 arrangement of microtubule units. The 9+1 pattern, first observed in spermatozoa of Haematoloechus medioplexus by Shapiro, Hershenov, and Tulloch (1961), has been reported from all trematode sperm thus far examined and appears to be ubiquitous within the group. Each axoneme consists of nine sets of doublet microtubule or axial units (AU, Figs. 123, 125, 127) circularly arranged

around a single central axial core (CC). The central core is enclosed by a dense cortical sheath (CSH) from which spokes radiate outward to connect with each doublet unit. A thin translucent zone separates the central core and cortical sheath. The cortical sheath and radiating spokes have been interpreted by Burton (1967b) and Silveria (1969) as being composed of narrow tissue bands wrapped around the central core in a double helical pattern.

In addition to axonemal microtubules, a number of cortical microtubules (MT, Figs. 125, 127, 128) form a single row lying parallel to the outer membrane of developing and mature spermatozoa. These microtubules resist bending and are associated with maintenance of structural form (Lumsden, 1965b; Burton, 1966b).

As spermiogenesis in Q. quinqueserialis proceeds, three cytoplasmic processes (Fig. 123) extending from each spermatid become evident. These include two axonemes and a dumbbell-shaped mid-piece (MP) located between the axonemes. Numerous cortical microtubules (MT) are arranged in a single row along the expanded ends of each mid-piece. As reported by Burton (1972), the spermatid nucleus migrates into the distal end of the mid-piece, and eventually the three cytoplasmic extensions unite to form a single unit.

Examination of cross sections of spermatids after unification (Fig. 124) reveals two axonemes (A) separated

by a centrally located nucleus (N) containing dense chromatin. A few cortical microtubules lie in a finely granular cytoplasm. In sections posterior to the nuclear region (Fig. 125), one or two mitochondrial rods (M) replace the nucleus. These rods represent narrow, elongate acristate mitochondria lying in the center of the spermatid posterior to the nucleus. As in the nuclear region, two axonemes, cortical microtubules, and granular cytoplasm are observed in these sections.

In the last stage of spermatid development (Fig. 126), the nucleus (N) migrates from the central region of the unified spermatid and takes a peripheral position replacing one axoneme. A mitochondrial rod (M) appears just distal to the anterior end of the nucleus and is situated between the nucleus and single axoneme. The ultrastructure of this stage is very similar to that of the nuclear region of a mature spermatozoan (Fig. 127); however, cytoplasmic ground substance remains undifferentiated. At this stage, formation of the spermatozoan is near completion, and each is released from the spermatid body.

Mature spermatozoa of Q. quinqueserialis (Figs. 114, 127-129, 136) may be observed in the testes and uterus, and are stored in large numbers in the vas deferens, seminal vesicle, and receptaculum seminis uterinum. They are threadlike, small in diameter (0.7-1.0 μm), and extremely

long. Although the total length was not determined in this species, measurements of sperm of other trematodes indicates a common length of from 325 to 400 μm (Burton, 1972; Halton and Hardcastle, 1976). Three distinct regions are observed at the ultrastructural level. The head region (Fig. 127) contains a peripherally located circular nucleus (N) with dense chromatin, a central mitochondrial rod (M), and a single axonome situated opposite the nucleus. The cytoplasmic ground substance consists almost entirely of glycogen (GY). A few cortical microtubules (MT) are found along the plasma membrane between the axoneme and nucleus. In the mid-region of the mature spermatozoan (Fig. 128), the second axoneme appears and replaces the nucleus in position; otherwise, the ultrastructure is similar to that of the head region. In the tail region (Fig. 129), the spermatozoan is flattened, and its cytoplasmic volume is small. Two axonemes are separated by a small amount of glycogen.

In histochemical tests, mature spermatozoa from the seminal vesicle and receptaculum seminis uterinum stain with mercuric bromphenol blue for basic proteins (Figs. 20, 22) and azure B for DNA (Figs. 25, 27). Intense staining with P.A.S. (amylase and diastase labile) (Figs. 11, 13) and Best's carmine for glycogen (Figs. 15, 16) confirms the ultrastructural identification of this carbohydrate. Glycogen in the beta form has been demonstrated in the spermatozoa of both

trematodes and cestodes and is thought to represent a readily accessible carbohydrate source (Lumsden, 1965a).

These findings indicate a similarity in the ultrastructure of mature spermatozoa of Quinqueserialis with that reported for other trematode species. These reports are numerous and include observations on monogeneans (Tuzet and Ktari, 1971; MacDonald and Caley, 1975; Halton and Hardcastle, 1976), aspidobothreans (Rhode, 1971b; Bakker and Diegenbach, 1973) and digeneans(Shapiro et al., 1961; Hershenov et al., 1966; Tulloch and Hershenov, 1967; Sato et al., 1967; Morseth, 1969; Burton, 1972). Additionally, ultrastructural observations on the processes of spermatogenesis and spermiogenesis confirm the general patterns thus far established for the Trematoda.

Sperm Ducts

Little published information is available on the ultrastructure of ducts conducting spermatozoa from the testes to the exterior. In most digenetic trematodes, these ducts include vasa efferentia, a single vas deferens, and a seminal vesicle. Of these, only the seminal vesicle has been examined ultrastructurally. Such observations have recently been reported by Threadgold (1975b) in studies on Fasciola hepatica and by Grant et al. (1976), who investigated

the diplostomatid Pharyngostomoides procyonis.

In Q. quinqueserialis, mature spermatozoa move from the testes through two short vasa efferentia. These join at the level of the second uterine loop to form a single vas deferens, located dorsal to the uterus and extending the length of the uterus to enter the cirrus sac where it forms an internal seminal vesicle.

Each vas efferens, measuring 15 μm in diameter by 135-160 μm in length, extends anteriomesad from the anterior end of each testis. Ultrastructurally, this duct (Figs. 130-132) consists of a thick epithelium containing a few small scattered mitochondria, Golgi complexes, and various types of inclusion bodies. The highly convoluted lumenal surface contains numerous thin cytoplasmic projections extending into the lumen and commonly enclosing spermatozoa (Fig. 131). In addition to spermatozoa, the lumen occasionally contains spermatogonial cells which have migrated from the testes (Fig. 132).

The vas deferens, expanded to accommodate large numbers of spermatozoa, measures from 45-60 μm in diameter. Its wall (Fig. 134) is formed by a thin layer of epithelial cells, rich in granular endoplasmic reticulum (ER), Golgi complexes, and mitochondria (M). Desmosomes separate individual cells. Each cell nucleus (N) is irregular in

shape and characterized by a granular nucleoplasm containing dense peripheral heterochromatin. As in the vas efferens, the lumenal surface of the vas deferens is extended into short filiform cytoplasmic projections. Spermatozoa lying in the lumen are embedded in a dense, finely granular matrix.

The epithelium of the seminal vesicle (Figs. 133, 135) is similar to that of the vas deferens. The presence of mitochondria (M, Fig. 135), granular endoplasmic reticulum (ER), and Golgi complexes suggests this epithelium to be an active secretory structure. However, no distinct secretory bodies, other than the granular material (FS, Fig. 133) in which the spermatozoa lie, are evident. Numerous cytoplasmic projections (CE, Fig. 136) form the apical epithelial surface. These projections are frequently connected by septate desmosomes (D, Fig. 136).

In all sperm ducts, a thick layer of fibrous interstitial tissue (F, Fig. 130) containing bands of circular muscle (CM) lies below the epithelium. Musculature is poorly developed in the vasa efferentia and vas deferens, and individual bands are thin and widely separated. In the seminal vesicle, however, the musculature is quite extensive (Fig. 133). In all ducts, longitudinal muscle is lacking.

These findings suggest that sperm ducts are involved in a variety of functions in addition to simply providing a

conduit for the passage of spermatozoa. An obvious function is that of storage of spermatozoa until copulation, as the vas deferens and seminal vesicle are expanded to contain considerable numbers of sperm. Secondly, the epithelia of these ducts contain an extensive system of ER and Golgi complexes, indicative of secretory activity. The major secretory product appears to be the granular material within the lumen. This material is most likely involved in lubrication of the ducts. Threadgold (1975b) speculates that epithelial cells, particularly those of the seminal vesicle, may also secrete essential nutrients necessary for the maturation of spermatozoa. Additionally, Threadgold (loc. cit.) indicates that the epithelium may be involved in phagocytosis of abnormal or old spermatozoa, and states that the surface projections commonly enclose spermatozoa which may be sequestered into phagocytic vesicles. Although a variety of inclusion bodies were noted in Quinqueserialis, no hydrolytic enzyme activity could be demonstrated in these ducts. Thus, evidence for Threadgold's hypothesis is not demonstrable.

Prostate Gland

Detailed studies on the structure and function of the prostate gland of the male reproductive system of digenetic trematodes, other than observations made with the light

microscope in taxonomic descriptions, have largely been neglected. A single account was recently published by Threadgold (1975a), who described the fine structure of the prostate of Fasciola hepatica. As a result of this apparent lack of information on the prostate gland, a detailed histochemical and ultrastructural examination of its structure was undertaken during the present investigation.

The prostate gland of Q. quinqueserialis (P, Fig. 1) consists of numerous unicellular glands lying within the cirrus sac and grouped around the ejaculatory duct. Each cell (Fig. 137) is pyriform, measuring from 8-10 μm in width at the base by 20-40 μm in length, and tapers near the ejaculatory epithelium. Large numbers of secretory granules (SG, Figs. 6, 137, 139-141, 145, 148) are visible in these cells and within the ejaculatory duct where they accumulate. The prostatic complex, consisting of gland cells and secretory products in the ejaculatory lumen, may be divided into two distinct regions based on the affinity of secretory products for common histological stains such as paracarmine, hematoxylin, methylene blue, and P.A.S. Secretory products in the posterior regions of the prostatic complex stain intensely with these dyes, whereas little or no staining is evident in the anterior regions (Figs. 3, 6, 9).

The nucleus of each prostate gland cell is located

towards the cell base. In ultrastructural observations, the nucleus (N, Fig. 137) contains a large dense nucleolus (NU) and small areas of chromatin embedded in a granular nucleoplasm. The nuclear envelope (NM) is irregular in profile and is occasionally interrupted by pores.

Contained in the cytoplasm are occasional mitochondria, an extensive system of granular endoplasmic reticulum (GER), free ribosomes, and numerous Golgi complexes. Small oval to elongate mitochondria (M, Fig. 137), usually less than 1 μm in length, are randomly distributed throughout the cytoplasm. A few short cristae are generally oriented longitudinally within each mitochondrion. Wide cisternae of GER, appearing as lakes (EL, Fig. 142) containing a homogeneous, finely granular substance, commonly lie in the perinuclear cytoplasm. Ribosomes are liberally distributed along the membranes of the GER and throughout the cytoplasmic ground substance. Golgi complexes (G, Figs. 137-139) are the characteristic organelles of prostate gland cells. Each complex consists of 8-12 flattened, parallel saccules (GS, Fig. 138) with slightly expanded ends and numerous small vesicles which may represent primary lysosomes.

Golgi complexes and GER are apparently involved in the production of numerous large (1 μm in diameter) secretory products. These products take the form of granules in the

posterior prostate, but become vesicular in the anterior prostate. Two types of double membrane-bound, electron-dense granules are observed in the posterior region of the prostatic complex. The most common type (Figs. 137, 139), circular in outline, is moderately dense and contains smaller areas of greater density. The second type (Fig. 140), irregularly oval in appearance, contains a distinct central dense region. Cells in which these granules form are similar in fine structure, but rarely are both types of granules observed in a single cell. Secretory vesicles (Fig. 141), limited within the anterior region of the prostatic complex, are electron-lucent containing isolated granular regions which may represent phagocytized secretory granules.

Secretory granules and vesicles move from the prostate cells into the ejaculatory lumen via prostate ducts (PD, Fig. 148) passing through the muscle layers, interstitial tissue, and epithelium of the ejaculatory duct. Prostate ducts are supported and strengthened by large numbers of microtubules (MT, Fig. 149). Once in the lumen, groups of secretory products become enclosed by cytoplasmic projections of the ejaculatory epithelium. Granules become isolated in the posterior portion of the ejaculatory duct and vesicles are isolated in the anterior portion.

Careful examination of the cytoplasm of prostate gland cells reveals the presence of additional organelles previously

unreported in trematode reproductive structures. These organelles (AP, Figs. 143-145), termed autophagosomes (DeDuve and Wattiaux, 1966) or cytosegresomes (Ericsson, 1969), are double membrane-bound structures containing recognizable organelles such as granular ER (Fig. 143) and mitochondria (Fig. 144). Autophagosomes, part of the lysosomal system, serve an autophagic function encapsulating other cellular organelles, digesting them with lysosomal enzymes such as acid phosphatase, and ejecting undigested residues from the cell (Bogitsh, 1975b). Autophagosomes have been observed in the gastrodermis (Bogitsh, 1972, 1975b) and parenchymal cells (Threadgold and Arme, 1974) of digenetic trematodes exposed to stress conditions such as starvation. The reduction in food material available to the fluke possibly stimulates Golgi complexes to produce primary lysosomes rich in acid hydrolases. These fuse with autophagosomes, which now possess hydrolytic activity, and digestion of cellular organelles, no longer needed due to the diminished food supply, results (Bogitsh, 1975b). In parenchymal cells, autophagosomes appear to be involved in glycogenolysis providing much-needed glucose which is readily made available to other tissues (Threadgold and Arme, 1974).

The role of autophagosomes in the functioning of the prostate gland of Q. quinqueserialis is speculative, for such

cells are not involved in the digestion of food substances or in glycogen storage. In addition to the presence of remnants of GER and mitochondria, some autophagosomes in the posterior prostate contain secretory granules (Fig. 145). If an overproduction of secretory granules by these cells occurs, autophagosomes may function in removing the excess. Secretory vesicles of the anterior prostate contain a granular residue which may represent granules that have been phagocytized by these organelles and released into the ejaculatory lumen. Because both normal granules and phagocytized granules (=vesicles) are enclosed in cytoplasmic projections of the ejaculatory epithelium, epithelial cells apparently are unable to differentiate between them. Moreover, as in vertebrate tissues, there is probably a continual turnover of cellular components in the prostate cells, and the autophagosomes function in removing "worn out" organelles and recycling usable molecules.

Essentially, the fine structure of the prostate gland of Quinqueserialis is similar to that of Fasciola hepatica, as described by Threadgold (1975a). Although Threadgold did not observe autophagosomes, he reported vesicular secretory products and indicated that these vesicles, secreted directly by the GER-Golgi complex, contain a high level of carbohydrate or some type of fluid component.

Secretory granules in the posterior prostate of Q.

quinqueserialis stain intensely with P.A.S. (Fig. 9) and are resistant to amylase or diastase digestion (Fig. 10). Additionally, negative results with Best's carmine for glycogen indicate that these granules are composed of a complex carbohydrate. In tests for basic proteins, a slight positive reaction is demonstrated in some granules with mercuric bromphenol blue (Fig. 22) and naphthol yellow S (Fig. 24) suggesting that they contain a glycoprotein with a low level of protein. In all instances, secretory vesicles of the anterior prostate fail to react with histochemical stains. These negative results indicate the possibility of a fluid component, which could represent hydrolyzed cellular material, the end product of autophagy.

Histochemical evidence for autophagy in the prostate gland is demonstrated by an intense positive reaction for acid phosphatase (Fig. 34). Although specific sites of this hydrolytic enzyme cannot be determined at the light level, Bogitsh (1975b) reported that acid phosphatase is synthesized in endoplasmic reticulum and transported to Golgi complexes where the enzyme is packaged within primary lysosomes. These organelles empty the enzyme into autophagosomes where digestion of the enclosed cellular organelle occurs.

Histochemical tests confirm the secretory function of the prostate gland of Q. quinqueserialis. RNA, the major component of ribosomes and GER, is demonstrated in the gland

cells with azure B (Fig. 25). Positive reactions for proteins using mercuric bromphenol blue (Fig. 22) and naphthol yellow S (Fig. 24) in prostate cells indicate a high level of protein synthesis resulting in enzyme formation. The major group of enzymes associated with the prostate gland are the phosphatases. In addition to production of acid phosphatase, prostate cells contain a large amount of alkaline phosphatase (Fig. 35). This enzyme is thought to play a role in the phosphorylated active transport of metabolites and secretory products into and out of cells, usually against a concentration gradient (Halton, 1967b).

Functions of the prostate gland secretions are not known, but several hypotheses have been proposed. Threadgold (1975a) speculates that these secretions may (1) stimulate the spermatozoa which are stored in a quiescent stage in the seminal vesicle, (2) provide an additional energy source for spermatozoa in addition to intraspermatozoan glycogen, or (3) stimulate or somehow influence the female reproductive ducts. Coil (1966) suggests that secretions of the prostate may (4) contribute part of the trematode egg shell. Evidence for the latter two hypotheses is sparse, as ultrastructural examination of the female reproductive ducts of Quinqueserialis, reported in a previous section of this dissertation, reveals no discernable prostate secretory products. These products have a characteristic structure,

and if present in the uterus, could easily be distinguished. It is most plausible, then, to assume that these secretions directly affect spermatozoa, either by stimulating them during copulation or by providing an additional nutritive source. Unfortunately, our knowledge of events taking place during copulation is meager. Ultrastructural and cytochemical studies on terminal genitalia of trematodes *in copula* are necessary to elucidate the functions of specialized structures such as the prostate gland.

Ejaculatory Duct

The short ejaculatory duct within the cirrus sac extends from the seminal vesicle to the cirrus. It is closely associated with prostate gland cells, whose ducts extend through the wall of the ejaculatory duct and release secretory products into the lumen.

The wall of the ejaculatory duct (Figs. 146-149) consists of a thin epithelium lying upon a dense basal lamina (B, Figs. 147-149). Underlying the lamina are large bands of circular muscle (CM, Figs. 146, 148, 149) and a thick layer of longitudinal muscle (LM, Fig. 146) embedded in a fibrous interstitial tissue.

The epithelium consists of distinct cells separated from one another by plasma membranes occurring in junctional complexes (J, Fig. 147). Each cell contains a large,

irregularly oval nucleus (N, Fig. 146) containing a granular nucleoplasm. No nucleolus or large amounts of chromatin material are observed within the nucleus. The cytoplasm (Figs. 147-149) contains a moderately extensive system of granular endoplasmic reticulum, elongate mitochondria (M) with longitudinal cristae, and occasional Golgi complexes. The ER and Golgi complexes may be involved in the secretion of a fibrous material (FS, Fig. 148) lying in the ejaculatory lumen along the epithelial surface. Other types of secretory bodies were not noted.

The apical surface of each epithelial cell is characterized by numerous filiform cytoplasmic projections (CE, Fig. 148) extending into the ejaculatory lumen. These projections commonly enclose prostate ducts which are expanded to contain groups of prostate secretory products. Eventually, these projections, enclosing groups of secretory products, separate from the epithelium and enter the lumen.

The muscle layers, fibrous tissue, and epithelium of the ejaculatory duct are frequently interrupted by prostate ducts (PD, Fig. 148). Such ducts extend between epithelial cells and not through the cytoplasm, as evidenced by the presence of infoldings of the basal plasma membrane of the epithelium running along each duct. This plasma membrane and that of the prostate duct are apparently attached by a basal lamina originating from the epithelium. Although no

septate desmosomes or tight junctions support this attachment, the entire area is made rigid by a peripheral ring of microtubules (MT, Fig. 149) lying within the prostate duct.

In the anterior region of the cirrus sac, the ejaculatory duct suddenly narrows and the epithelium gives way to a thin, highly convoluted syntegument (ST, Fig. 150) containing a dense ground substance and a few poorly developed mitochondria. Its basal membrane, anchored by numerous hemidesmosomes, and lamina (B) extend downward into the fibrous interstitial tissue, almost surrounding the underlying bands of circular muscle (CM).

This region apparently represents a transitional zone between the epithelium of the posterior ejaculatory duct and the tegument of the cirrus. A junction between the epithelium and tegument was not observed, but one is probably formed by a septate desmosome. Such a connection has been noted in other trematode systems where the tegument and an epithelium meet (Morris and Threadgold, 1968).

In histochemical tests, the muscular wall and epithelium of the ejaculatory duct stain intensely with mercuric bromphenol blue for basic proteins (Fig. 22) and slightly with P.A.S. (diastase labile) for carbohydrates (Fig. 9). These regions also give a positive reaction for nonspecific esterase (Fig. 36). This enzyme has been demonstrated in the ejaculatory duct of Fasciola hepatica by Halton (1967c), but

its functional role is unknown.

Generally, the structure of the ejaculatory duct of Quinqueserialis and of Fasciola, as described by Threadgold (1975b), is similar. Threadgold, however, was unable to find plasma membranes to distinguish individual epithelial cells and concluded that the ejaculatory lining of Fasciola is a syncytium. In Quinqueserialis, distinct plasma membranes observed in junctional complexes, as indicated above, do occur.

Functionally, the ultrastructure and histochemistry of the ejaculatory epithelium of Q. quinqueserialis is indicative of secretory activity. The major type of secretory product is the fibrous material evident in the ejaculatory lumen. This material, apparently secreted by GER and Golgi complexes, may serve as a lubricant during copulation. Additionally, the presence of nonspecific esterase suggests a high degree of enzymatic activity within the epithelium. Such activity, apparently related to the intimate association of ejaculatory duct and prostate gland, its ducts and secretory products, may be involved in the general metabolism of these tissues.

Cirrus

The terminal portion of the male reproductive system of Q. quinqueserialis is formed by the cirrus (C, Fig. 1) which extends through the common genital opening (GO) to the exterior. This copulatory structure is eversible and may reach a length of 1.4 mm when fully extended.

The surface of the cirrus, when viewed with the scanning electron microscope, consists of numerous spinelike protuberances, 8-10 μm in length, directed posteriad (Fig. 151). High magnification of these protuberances reveals many small surface evaginations (Fig. 152). In observations with the transmission microscope, such protuberances appear as a modified syntegument (ST, Fig. 153) containing many membrane-bound vesicles in the apical regions and a small number of poorly developed mitochondria (M) in the central region. Paracrystalline spines are absent. The convoluted basal membrane rests upon a thin, dense basal lamina (B). Tubular invaginations of the basal membrane form hemidesmosomes and serve as points of attachment between the membrane and lamina. Underlying the lamina is a layer of fibrous interstitial connective tissue (F) containing bands of circular muscle (CM) and a thick layer of longitudinal muscle (LM). Internuncial processes (IP) of the cytotegument commonly interrupt the longitudinal muscle layer.

The cytoplasm of the cytotegument (CT, Fig. 153) is limited in amount within an extensive system of thin cisternae arranged in parallel rows lying below the muscle layers. Cytoplasmic elements contained within these cisternae are occasional mitochondria, glycogen, and dark-staining inclusions. No distinct tegumental cytons were observed. The muscular wall of the cirrus sac lies below the cytotegument.

In histochemical tests, the cirrus syntegument stains uniformly with P.A.S. (Fig. 12) and is resistant to diastase digestion. An intense reaction also occurs with the mercuric bromphenol blue test for proteins (Fig. 21), suggesting that the major component of the syntegument is a glycoprotein. Similar histochemical results have been demonstrated in the general body teguments of numerous trematodes including Q. quinqueserialis, as reported in a previous section of this dissertation. Although no hydrolytic enzyme activity is detected in the syntegument, nonspecific esterase is demonstrated along the muscular wall of the cirrus sac (Fig. 38). This enzyme is commonly associated with various components of the cirrus sac of Fasciola including the cirrus lining, ejaculatory epithelium, and cirrus sac musculature (Halton, 1967c). Its role, however, in the metabolic activities of these structures is unknown.

Many helminth morphologists have suspected that the

covering of the cirrus is merely an extension of the general body tegument. A second hypothesis, as indicated by Hyman (1951), considers the cirrus to be a temporary projection formed by eversion of the ejaculatory duct. Results of ultrastructural studies on the cirrus and ejaculatory duct of Fasciola, as provided by Threadgold (1975b), and of Quinqueserialis (present study) indicate that the cirrus is indeed a tegumental structure, whereas the ejaculatory duct is an epithelium composed of distinct cells. These findings lend support to the former hypothesis.

The surface of platyhelminth cirri are commonly armed with spines, bristles, or hooks (Hyman, 1951). The origin of these armaments, however, varies. In Fasciola, the cirrus armament is formed by paracrystalline spines lying in the syntegument (Threadgold, 1975b). Such spines are absent in the cirrus of Quinqueserialis, whose spinose surface results from convolutions of the syntegument forming sharp protuberances. Otherwise, the structure of the cirrus teguments of these two trematodes is similar.

The cirrus syntegument of Quinqueserialis most closely resembles that of the dorsal body surface. Both teguments consist of a dense ground substance containing numerous inclusions and few mitochondria.

Threadgold (1975b) reported that the cirrus sac of Fasciola is covered by a syncytial tegument similar to that

of the cirrus but lacking spines. In Quinqueserialis, the wall of the cirrus sac is formed by two layers of muscle (circular and longitudinal) lying within a thick layer of fibrous interstitial tissue. No tegumental structures are observed in association with the cirrus sac. These observations suggest that in this species the cirrus sac arises from parenchymatous musculature, whereas the cirrus is formed by invagination of the body tegument. Support for this hypothesis is most clearly shown within the acoel turbellarians, as indicated by Beklemishev (1964), where the simplest copulatory organs are formed by tubular invaginations of the body surface into the parenchyma. Spermatozoa accumulate at the open ends of these tubes. Eventually, a sac is formed around each tube and accumulated spermatozoa from musculature arising within the parenchyma. Contraction of these muscles forces the eversion of the tube (cirrus) to the exterior and the outflow of spermatozoa during copulation.

SUMMARY AND CONCLUSIONS

1. Histochemical and ultrastructural studies were conducted on the tegument, ventral papillae, musculature, parenchyma, caecum, and female and male reproductive systems of the notocotylid caecal trematode Quinqueserialis quinqueserialis (Barker and Laughlin, 1911).
2. A total of 123 rodents (representing 11 species) collected from areas near the Iowa Lakeside Laboratory and Iowa State University were examined for Q. quinqueserialis. Infected hosts included muskrats (Ondatra zibethicus) and meadow voles (Microtus pennsylvanicus).
3. The dorsal tegument of Q. quinqueserialis, functioning primarily as a protective covering, is composed of a syncytial confluent layer (syntegument) and underlying nucleated cells (cytotegument). The thick syntegument, composed of glycoproteins, contains a dense ground substance formed by two types of tegumental inclusions. The cytotegument, characterized by an extensive granular endoplasmic reticulum and numerous ribosomes, is involved in the production of these inclusions.
4. Detailed studies were undertaken to determine the structure and chemical composition of the ventral papillae, structures characterizing members of the Notocotylidae. Specific components of a papilla include a thin outer

syntegument, large pyriform cells underlying the syntegument and forming the bulk of the papilla, and osmoregulatory ducts connected to pyriform cells by means of junctional complexes. The syntegument is highly convoluted in the apical region of the papilla but becomes spinose marginally. Its cytoplasm is characterized by mitochondria, tegumental inclusions, and two types of presumed sensory receptors. Pyriform cells contain large numbers of elongate, cristate mitochondria, but lack secretory organelles. Cytoplasmic projections from each cell are connected to the overlying syntegument by junctional complexes. Extending into each papilla are osmoregulatory ducts formed by epithelial cells possessing numerous lamellae which form a continuous border along the lumenal surface.

5. Histochemical tests reveal the presence of glycoproteins in the ventral syntegument. The pyriform cells stain intensely for basic proteins and protein-bound lipids, but tests for carbohydrates, mucosubstances, lipids, RNA, and hydrolytic enzymes are negative.
6. Evaluation of ultrastructural observations and histochemical tests indicates that the ventral papillae of Q. quinqueserialis are nonglandular and the term "ventral gland" should be discarded. It is suggested

that these structures may function in absorption of nutrients or in osmoregulation.

7. Bands of muscle fibers occur throughout the body of Q. quinqueserialis, but are primarily concentrated in the oral sucker and parenchyma, beneath the syntegument, and surrounding the reproductive structures. Each myofiber is nonstriated and contains numerous thick and thin myofilaments.
8. Two types of parenchymal cells (designated A and B) are observed in Q. quinqueserialis. Type A cells contain numerous secretory organelles and appear to be involved in protein synthesis and lipid metabolism. Paracrystalline inclusions are common in these cells. Type B cells are extremely large and primarily involved in carbohydrate metabolism. Histochemical tests reveal large deposits of glycogen throughout the parenchyma.
9. The caecum is comprised of a gastrodermis characterized by numerous microvilli extending into the gut lumen. The cytoplasm contains extensive granular endoplasmic reticulum, Golgi complexes, mitochondria, and lipid inclusions. In histochemical tests, the gastrodermis stains for mucosubstances, proteins, and acid phosphatase, providing evidence for concomitant functions of secretion, digestion, and absorption.

10. The ovary is composed of gonial cells occurring in varying stages of maturation. Two types of secretory cells are found in the Mehlis' gland, one producing a dense secretory product; the other, a membranous product. Laterally situated vitellaria, composed of vitelline cells occurring in four developmental states, produces protein globules eventually forming most of the egg shell. Observations of an extensive granular endoplasmic reticulum and Golgi complexes in the epithelial cells forming the uterus is indicative of a high degree of secretory activity which may be associated with the formation of additional egg shell layers or polar egg filaments. The egg capsule includes a thick inner proteinaceous layer and a thin outer reticulate layer.
11. Extensive studies on components of the male reproductive system were conducted with emphasis on the ultrastructure of the terminal genitalia. The eversible cirrus is covered by spinelike protuberances formed by a modified syntegument. The prostate gland consists of numerous unicellular glands grouped around the ejaculatory duct. Each gland cell contains numerous free ribosomes and Golgi complexes, an extensive system of granular endoplasmic reticulum, and occasional autophagosomes. Secretory products produced by the prostate

migrate into the ejaculatory lumen where they accumulate. It is suggested that these secretions affect the spermatozoa, either by stimulating them during copulation or by providing an additional nutritive source.

12. The processes of spermatogenesis and spermiogenesis in Q. quinqueserialis are apparently similar to those described in other trematodes. Each mature spermatozoan possesses two axonemes containing a 9+1 microtubule arrangement, a dense, elongate nucleus, and extensive glycogen stores.

LITERATURE CITED

Abram, J. B. 1969. Some gastrointestinal helminths of Ondatra zibethicus Linnaeus, the muskrat in Maryland. Proc. Helminthol. Soc. Wash. 36: 93-95.

Anderson, D. R., and R. L. Beaudoin. 1966. Host habitat and age as factors in the prevalence of intestinal parasites of the muskrat. Bull. Wildlife Dis. Ass. 2: 70-77.

Arata, A. A. 1959. Ecology of muskrats in strip-mine pools in southern Illinois. J. Wildlife Manage. 23: 177-186.

Axmann, M. C. 1947. Morphological studies on glycogen deposition in schistosomes and other flukes. J. Morphol. 80: 321-334.

Bailey, H. H., and S. J. Tompkins. 1971. Ultrastructure of the integument of Aspidogaster conchicola. J. Parasitol. 57: 848-854.

Bakker, K. E., and P. C. Diegenbach. 1973. The ultrastructure of spermatozoa of Aspidogaster conchicola Baer, 1826 (Aspidogastridae, Trematoda). Neth. J. Zool. 23: 345-346.

Ball, L. 1952. Notes on the helminth parasites of muskrats from western Colorado. J. Parasitol. 38: 83-84.

Bancroft, J. D. 1967. An introduction to histochemical technique. Butterworths & Co., Ltd., London. 268 pp.

Barker, F. D. 1915. Parasites of the American muskrat (Fiber zibethicus). J. Parasitol. 1: 184-197.

Barker, F. D. 1916. A new monostome trematode parasitic in the muskrat with a key to the parasites of the American muskrat. Trans. Am. Microsc. Soc. 35: 175-184.

Barker, F. D., and J. W. Laughlin. 1911. A new species of trematode from the muskrat, Fiber zibethicus. Trans. Am. Microsc. Soc. 30: 261-274.

Beckett, J. V., and V. Gallicchio. 1967. A survey of helminths of the muskrat, Ondatra z. zibethica Miller, 1912, in Portage County, Ohio. J. Parasitol. 53: 1169-1172.

Behnke, O. 1964. A preliminary report on "microtubules" in undifferentiated and differentiated vertebrate cells. J. Ultrastruct. Res. 11: 139-146.

Beklemishev, W. N. 1964. Principles of comparative anatomy of invertebrates, Vol. 2, Organology. The University of Chicago Press, Chicago. 529 pp.

Beverly-Burton, M. 1958. A new notocotylid trematode, Uniserialis gippyensis gen. et sp. nov., from the mallard, Anas platyrhyncha platyrhyncha L. J. Parasitol. 44: 412-415.

Beverly-Burton, M., and V. H. Logan. 1976. The ventral papillae of notocotylid trematodes. J. Parasitol. 62: 148-151.

Beverly-Burton, M., and P. R. Sweeny. 1972. Intranuclear, paracrystalline inclusions in various cells of Quinqueserialis quinqueserialis and Notocotylus urbanensis (Trematoda: Notocotylidae). Can. J. Zool. 59: 345-348.

Bhatti, I., and A. D. Johnson. 1971. In vitro uptake of tritiated glucose, tyrosine, and leucine by adult Alaria marcianae (LaRue) (Trematoda). Comp. Biochem. Physiol. 40A: 987-997.

Bibby, M. C., and G. Rees. 1971. The uptake of radioactive glucose in vivo and in vitro by the metacercaria of Diplostomum phoxini (Faust) and its conversion to glycogen. Z. Parasitenkd. 37: 187-197.

Bils, R. F., and W. E. Martin. 1966. Fine structure and development of the trematode integument. Trans. Am. Microsc. Soc. 85: 78-88.

Björkman, N., and W. Thorsell. 1962. The fine morphology of the mitochondria from parenchymal cells in the liver fluke (Fasciola hepatica, L.). Exp. Cell Res. 27: 342-346.

Björkman, N., and W. Thorsell. 1963. On the fine morphology of the formation of egg-shell globules in the vitelline glands of the liver fluke (Fasciola hepatica, L.). Exp. Cell Res. 32: 153-156.

Björkman, N., and W. Thorsell. 1964a. On the fine structure and resorptive function of the cuticle on the liver fluke, Fasciola hepatica L. Exp. Cell Res. 33: 319-329.

Björkman, N., and W. Thorsell. 1964b. On the ultrastructure of the ovary of the liver fluke (Fasciola hepatica L.). Z. Zellforsch. 63: 538-549.

Bogitsh, B. J. 1968. Cytochemical and ultrastructural observations on the tegument of the trematode Megalodiscus temperatus. Trans. Am. Microsc. Soc. 87: 477-487.

Bogitsh, B. J. 1970. Observations on the cytochemistry of the Mehlis' gland cells of Haematoloechus medioplexus. J. Parasitol. 56: 1084-1094.

Bogitsh, B. J. 1972. Cytochemical and biochemical observations on the digestive tracts of digenetic trematodes. IX. Megalodiscus temperatus. Exp. Parasitol. 32: 244-266.

Bogitsh, B. J. 1973. Cytochemical and biochemical observations on the digestive tracts of digenetic trematodes. X. Starvation effects on Megalodiscus temperatus. J. Parasitol. 59: 94-100.

Bogitsh, B. J. 1975a. Cytochemical observations on the gastrodermis of digenetic trematodes. Trans. Am. Microsc. Soc. 94: 524-528.

Bogitsh, B. J. 1975b. Cytochemistry of gastrodermal autophagy following starvation in Schistosoma mansoni. J. Parasitol. 61: 237-248.

Bogitsh, B. J., and F. P. Aldridge. 1967. Histochemical observations on Posthodiplostomum minimum. IV. Electron microscopy of tegument and associated structures. Exp. Parasitol. 21: 1-8.

Bogitsh, B. J., and W. A. Shannon. 1971. Cytochemical and biochemical observations on the digestive tracts of digenetic trematodes. VIII. Acid phosphatase activity in Schistosoma mansoni and Schistosomatium douthitti. Exp. Parasitol. 29: 337-347.

Bogitsh, B. J., D. A. Davis, and D. A. Nunnally. 1968. Cytochemical and biochemical observations on the digestive tracts of digenetic trematodes. II. Ultrastructural localization of acid phosphatase in Haematoloechus medioplexus. Exp. Parasitol. 23: 303-308.

Burnett, M. P. 1956. A preliminary report on the helminth parasites from muskrats collected in the vicinity of Fort Collins, Colorado. J. Colo.-Wyo. Acad. Sci. 4: 45.

Burton, P. R. 1960. Gametogenesis and fertilization in the frog lung fluke, Haematoloechus medioplexus (Trematoda: Plagiorchiidae). J. Morphol. 107: 93-122.

Burton, P. R. 1962. In vitro uptake of radioglucose by a frog lung-fluke and correlation with the histochemical identification of glycogen. J. Parasitol. 48: 874-882.

Burton, P. R. 1963. A histochemical study of vitelline cells, egg capsules, and Mehlis' gland in the frog lung-fluke, Haematoloechus medioplexus. J. Exp. Zool. 154: 247-258.

Burton, P. R. 1964. The ultrastructure of the integument of the frog lung-fluke, Haematoloechus medioplexus (Trematoda: Plagiorchiidae). J. Morphol. 115: 305-318.

Burton, P. R. 1966a. The ultrastructure of the integument of the frog bladder fluke, Gorgoderina sp. J. Parasitol. 52: 926-934.

Burton, P. R. 1966b. Substructure of certain cytoplasmic microtubules: An electron microscopic study. Science 154: 903-905.

Burton, P. R. 1967a. Fine structure of the reproductive system of a frog lung fluke. I. Mehlis' gland and associated ducts. J. Parasitol. 53: 540-555.

Burton, P. R. 1967b. Fine structure of the unique central region of the axial unit of lung-fluke spermatozoa. J. Ultrastruct. Res. 19: 166-172.

Burton, P. R. 1972. Fine structure of the reproductive system of a frog lung fluke. III. The spermatozoon and its differentiation. J. Parasitol. 58: 68-83.

Byram, J. E., S. C. Ernst, R. D. Lumsden, and F. Sogandares-Bernal. 1975. Viruslike inclusions in the cecal epithelial cells of Paragonimus kellicotti (Digenea, Troglotermatidae). J. Parasitol. 61: 253-264.

Cameron, M. L., and J. E. Steele. 1959. Simplified aldehyde-fuchsin staining of neurosecretory cells. Stain Technol. 34: 265-266.

Cardell, R. R., and D. E. Philpott. 1960. The ultrastructure of the tail of the cercaria of Himasthla quissentensis (Miller and Northup, 1926). Trans. Am. Microsc. Soc. 79: 442-450.

Chapman, H. D. 1973. The functional organization and fine structure of the tail musculature of the cercariae of Cryptocotyle lingua and Himasthla secunda. Parasitology 66: 487-497.

Chayen, J., L. Bitensky, and R. Butcher. 1973. Practical histochemistry. John Wiley & Sons, London. 271 pp.

Clegg, J. A. 1965. Secretion of lipoprotein by Mehlis' gland in Fasciola hepatica. Ann. N.Y. Acad. Sci. 118: 969-986.

Coil, W. H. 1966. Egg shell formatin in the notocotylid trematode, Ogmocotyle indica (Bhalerao, 1942) Ruiz, 1946. Z. Parasitenkd. 27: 205-209.

Davis, D. A., and B. J. Bogitsh. 1971a. Gorgoderina attenuata: Cytochemical and biochemical observations on the digestive tracts of digenetic trematodes. Exp. Parasitol. 29: 320-329.

Davis, D. A., and B. J. Bogitsh. 1971b. Cytochemical localization of the gastrodermal glycocalyx of Gorgoderina attenuata and Haematoloechus medioplexus. Acta Histochem. Cytochem. 4: 65-68.

Davis, D. A., B. J. Bogitsh, and D. A. Nunnally. 1968. Cytochemical and biochemical observations on the digestive tracts of digenetic trematodes. I. Ultrastructure of Haematoloechus medioplexus gut. Exp. Parasitol. 22: 96-106.

Davis, D. A., B. J. Bogitsh, and D. A. Nunnally. 1969. Cytochemical and biochemical observations on the digestive tracts of digenetic trematodes. III. Nonspecific esterase in Haematoloechus medioplexus. Exp. Parasitol. 24: 121-129.

Dawes, B. 1940. Notes on the formation of egg capsule in the monogenetic trematode, Hexacotyle extensicauda, Dawes, 1940. Parasitology 32: 287-295.

Dawes, B. 1954. Maintenance in vitro of Fasciola hepatica. Nature 174: 654-655.

Dawes, B. 1962. A histological study of the cecal epithelium of Fasciola hepatica L. Parasitology 52: 483-493.

DeDuve, C., and R. Wattaiux. 1966. Functions of lysosomes. Annu. Rev. Physiol. 28: 435-495.

Diesing, K. M. 1839. Neue Gattungen von Binnenwürmern. Ann. Wiener Mus. Naturgesch. 2: 219-242.

Dike, S. C. 1967. Ultrastructure of the ceca of the digenetic trematodes Gorgodera amplicava and Haematoloechus medioplexus. J. Parasitol. 53: 1173-1185.

Dike, S. C. 1969. Acid phosphatase activity and ferritin incorporation in the ceca of digenetic trematodes. J. Parasitol. 55: 111-123.

Dike, S. C. 1971. Ultrastructure of the esophageal region in Schistosoma mansoni. Am. J. Trop. Med. Hyg. 20: 552-568.

Dorsey, C. H., and M. A. Stirewalt. 1971. Schistosoma mansoni: Fine structure of cercarial acetabular glands. Exp. Parasitol. 30: 199-214.

Dunagan, T. T. 1957. Helminth parasites of Alaskan muskrats. Trans. Am. Microsc. Soc. 76: 318-320.

Edwards, R. L. 1949. Internal parasites of central New York muskrats. J. Parasitol. 35: 547-548.

Erasmus, D. A. 1967a. The host-parasite interface of Cyathocotyle bushiensis Khan, 1962 (Trematoda: Strigeoidea). II. Electron microscope studies of the tegument. J. Parasitol. 53: 703-714.

Erasmus, D. A. 1967b. Ultrastructural observations on the reserve bladder system of Cyathocotyle bushiensis Khan, 1962 (Trematoda: Strigeoidea) with special reference to lipid excretion. J. Parasitol. 53: 525-536.

Erasmus, D. A. 1969. Studies on the host-parasite interface of strigeoid trematodes. V. Regional differentiation of the adhesive organ of Apatemon gracilis minor Yamaguti, 1933. Parasitology 59: 245-256.

Erasmus, D. A. 1970. The host-parasite interface of strigeoid trematodes. VII. Ultrastructural observations on the adhesive organ of Diplostomum phoxini Faust, 1918. Z. Parasitenkd. 33: 211-224.

Erasmus, D. A. 1973. A comparative study of the reproductive system of mature, immature and 'unisexual' female Schistosoma mansoni. Parasitology 67: 165-183.

Erasmus, D. A. 1975a. Schistosoma mansoni: Development of the vitelline cells, its role in drug sequestration, and changes induced by Astiban. Exp. Parasitol. 38: 240-256.

Erasmus, D. A. 1975b. The subcellular localization of labelled tyrosine in the vitelline cells of Schistosoma mansoni. Z. Parasitenkd. 46: 75-81.

Erasmus, D. A., and C. Öhman. 1963. The structure and function of the adhesive organ in strigeid trematodes. Ann. N.Y. Acad. Sci. 113: 7-35.

Erasmus, D. A., and C. Öhman. 1965. Electron microscope studies of gland cells and host-parasite interface of the adhesive organ of Cyathocotyle bushiensis Khan, 1962. J. Parasitol. 51: 761-769.

Erhardova, B. 1958. Parasiticti cervi hlodavcu Cesklovenska. Cesk. Parasitol. 1: 27-92.

Erickson, A. B. 1938. Parasites of some Minnesota Cricetidae and Zapodidae, and a host catalogue of helminth parasites of native American mice. Am. Midl. Nat. 20: 575-589.

Ericsson, J. L. E. 1969. Mechanism of cellular autophagy. Pages 345-394 in J. T. Dingle and H. B. Fell, eds. Lysosomes in biology and pathology, Vol. 2. North Holland Publishing, Amsterdam.

Ernst, S. C. 1975. Biochemical and cytochemical studies of digestive-absorptive functions of esophagus, cecum, and tegument in Schistosoma mansoni: Acid phosphatase and tracer studies. J. Parasitol. 61: 633-647.

Fried, B., and B. E. Stromberg. 1971. Egg-shell precursors in trematodes. Proc. Helminthol. Soc. Wash. 38: 262-264.

Führmann, O. 1928. Zweite Klasse des Cladus Plathelminthes: Trematoda. Hand. Zool. 2: 1-140.

Gallagher, S. S. E., and L. T. Threadgold. 1967. Electron-microscope studies of Fasciola hepatica. II. The interrelationship of the parenchyma with other organ systems. Parasitology 57: 627-632.

Gilford, J. H. 1954. A survey of muskrat helminths in Illinois. J. Parasitol. 40: 702-703.

Gönnert, R. 1962. Histologische Untersuchungen über die Feinbau der Eibildungsstätte Oogenotop von Fasciola hepatica. Z. Parasitenkd. 21: 475-492.

Govaert, J. 1960. Étude cytologique et cytochimique des cellules de la lignée germinative chez Fasciola hepatica. Exp. Parasitol. 9: 141-158.

Grant, W. C., R. Harkema, and K. E. Muse. 1976. Ultrastructure of Pharyngostomoides procyonis Harkema 1942 (Diplostomatidae). I. Observations on the male reproductive system. J. Parasitol. 62: 39-49.

Gresson, R. A. R. 1962. The membrane system of the oocyte of Fasciola hepatica L. Exp. Cell Res. 26: 212-216.

Gresson, R. A. R. 1964. Electron microscopy of the ovary of Fasciola hepatica. Q. J. Microsc. Sci. 105: 213-218.

Gresson, R. A. R. 1965. Spermatogenesis in the hermaphroditic Digenea (Trematoda). Parasitology 55: 117-125.

Gresson, R. A. R., and L. T. Threadgold. 1959. Light and electron microscopic studies of the epithelial cells of the gut of Fasciola hepatica L. J. Biophys. Biochem. Cytol. 6: 157-162.

Grundmann, A. W., and Y. Tsai. 1967. Some parasites of the muskrat, Ondatra zibethicus osoyoosensis (Lord, 1863) Miller, 1912 from the Salt Lake Valley, Utah. Trans. Am. Microsc. Soc. 86: 139-144.

Guilford, H. G. 1961. Gametogenesis, egg-capsule formation, and early miracidial development in the digenetic trematode Halipegus eccentricus Thomas. J. Parasitol. 47: 757-764.

Gupta, S. P. 1962. On a new trematode, Quinqueserialis zibethicai sp. nov., of the sub-family Notocotylinae from the duodenum of muskrat (Ondatra zibethica) from Canada. Indian J. Helminthol. 14: 66-70.

Halton, D. W. 1966. The occurrence of microvilli-like structures in the gut of digenetic trematodes. Experientia (Basel) 22: 828-829.

Halton, D. W. 1967a. Studies on glycogen deposition in Trematoda. Comp. Biochem. Physiol. 23: 113-120.

Halton, D. W. 1967b. Studies on phosphatase activity in Trematoda. J. Parasitol. 53: 46-54.

Halton, D. W. 1967c. Histochemical studies of carboxylic esterase activity in Fasciola hepatica. J. Parasitol. 53: 1210-1216.

Halton, D. W. 1967d. Observations on the nutrition of digenetic trematodes. Parasitology 57: 639-660.

Halton, D. W., and E. Dermott. 1967. Electron microscopy of certain gland cells in two digenetic trematodes. J. Parasitol. 53: 1186-1191.

Halton, D. W., and A. Hardcastle. 1976. Spermatogenesis in a monogenean, Diclidophora merlangi. Int. J. Parasitol. 6: 43-53.

Halton, D. W., and R. A. W. Lyness. 1971. Ultrastructure of the tegument and associated structures of Aspidogaster conchicola (Trematoda: Aspidogastrea). J. Parasitol. 57: 1198-1210.

Halton, D. W., S. D. Stranock, and A. Hardcastle. 1974. Vitelline cell development in monogenean parasites. Z. Parasitenkd. 45: 45-61.

Hanna, R. E. B. 1976. Fasciola hepatica: A light and electron autoradiographic study of shell-protein and glycogen synthesis by vitelline follicles in tissue slices. Exp. Parasitol. 39: 18-28.

Harrah, E. C. 1922. North American monostomes primarily from fresh water hosts. Ill. Biol. Monogr. 7: 225-324.

Harris, K. R., T. C. Cheng, and A. Cali. 1974. An electron microscope study of the tegument of the matacercaria and adult of Leucochloridiomorpha constantiae (Trematoda: Brachylaemidae). Parasitology 68: 57-67.

Harwood, P. D. 1939. Notes on Tennessee helminths. IV. North American trematodes of the subfamily Notocotylinae. J. Tenn. Acad. Sci. 14: 332-340, 421-437.

Hendelberg, J. 1962. Paired flagella and nucleus migration in the spermiogenesis of Dicrocoelium and Fasciola (Digenea, Trematoda). Zool. Bidr. Upps. 35: 569-587.

Herber, E. C. 1962. Life history studies of two trematodes of the subfamily Notocotylinae. J. Parasitol. 28: 179-196.

Hershenov, B. R., G. S. Tulloch, and A. D. Johnson. 1966. The fine structure of trematode sperm-tails. Trans. Am. Microsc. Soc. 85: 480-483.

Hockley, D. J. 1968. Small spines on the egg shells of Schistosoma. Parasitology 58: 367-370.

Hockley, D. J. 1973. Ultrastructure of the tegument of Schistosoma. Adv. Parasitol. 11: 233-305.

Holmes, J. C. 1961. Effects of concurrent infections on Hymenolepis diminuta (Cestoda) and Moniliformis dubius (Acanthocephala). I. General effects and comparison with crowding. J. Parasitol. 47: 209-216.

Huxley, H. E. 1960. Muscle cells. Pages 365-481 in J. Brachet and A. Mirsky, eds. The cell, vol. 4. Academic Press, New York.

Hyman, L. H. 1951. The invertebrates: Platyhelminthes and Rhynchocoela. Volume II. McGraw-Hill Book Company, New York. 550 pp.

Irwin, S. W. B., and L. T. Threadgold. 1970. Electron-microscope studies on Fasciola hepatica. VIII. The development of the vitelline cells. Exp. Parasitol. 28: 399-411.

Irwin, S. W. B., and L. T. Threadgold. 1972. Electron microscope studies of Fasciola hepatica. X. Egg formation. Exp. Parasitol. 31: 321-331.

Isseroff, H., and C. P. Read. 1969. Studies on membrane transport. VI. Absorption of amino acids by fascioliid trematodes. Comp. Biochem. Physiol. 30: 1153-1159.

Jansma, W. B. 1971. Ultrastructure and histochemistry of Fibricola cratera (Trematoda: Diplostomatidae). Ph.D. dissertation. Iowa State University, Ames.

Johnson, A. D., I. Bhatti, and N. Kanemoto. 1971. Structure and function of the holdfast organ and lappets of Alaria marcianae (LaRue, 1917) (Trematoda: Diplostomatidae). J. Parasitol. 57: 235-243.

Khalil, G. M., and R. M. Cable. 1968. Germinal development in Philophthalmus megalurus (Cort, 1914) (Trematoda: Digenea). Z. Parasitenkd. 31: 211-231.

Kilejian, A. 1970. The formation of the L-proline pool in Hymenolepis diminuta. Pages 62-65 in A. J. MacInnis and M. Voge, eds. Experiments and techniques in parasitology. W. H. Freeman and Co., San Francisco.

King, J. W., and R. D. Lumsden. 1969. Cytological aspects of lipid assimilation by cestodes. Incorporation of linoleic acid into the parenchyma and eggs of Hymenolepis diminuta. J. Parasitol. 55: 250-260.

Kinsella, J. M. 1967. Helminths of Microtinae in western Montana. Can. J. Zool. 45: 269-274.

Kinsella, J. M. 1971. Growth, development, and intraspecific variation of Quinqueserialis quinqueserialis (Trematoda: Notocotylidae) in rodent hosts. J. Parasitol. 57: 62-70.

Knight, I. M. 1951. Diseases and parasites of the muskrat (Ondatra zibethica) in British Columbia. Can. J. Zool. 29: 184-215.

Knox, B. E., and E. M. Pantelouris. 1966. Osmotic behaviour of Fasciola hepatica L. in modified Hedon-Fleig media. Comp. Biochem. Physiol. 18: 609-615.

Kossack, W. 1911. Über Monostomiden. Zool. Jahrb. Abt. Syst. Geogr. Biol. Tiere 31: 493-590.

Kritsky, D. C., and F. J. Kruidenier. 1976. Fine structure and development of the body wall in the monogenean, Gyrodactylus eucaliae Ikezaki and Hoffman, 1957. Proc. Helminthol. Soc. Wash. 43: 47-58.

Kruidenier, F., and A. Vatter. 1958. Microstructure of muscles in cercariae of the digenetic trematodes Schistosoma mansoni and Tetrapapillatrema concavocorpa. Proc. 4th Int. Congr. Electron Microscopy 2: 332-335.

Krupa, P. L. 1974. Ultrastructural topography of a trematode eggshell. Exp. Parasitol. 35: 244-247.

Krupa, P. L., G. H. Cousineau, and A. K. Bal. 1969. Electron microscopy of the excretory vesicle of a trematode cercaria. J. Parasitol. 55: 985-992.

Kümmel, G. 1959. Feinstruktur der Wimperflamme in den Protonephridien. Protoplasma 51: 371-376.

Kuns, M. L., and R. Rausch. 1950. An ecological study of helminths of some Wyoming voles (Microtus spp.) with a description of a new species of Nematospiroides (Heligmosomidae: Nematoda). Zoologica 35: 181-188.

Kuntz, R. E., G. S. Tulloch, D. L. Davidson, and T. Huang. 1976. Scanning electron microscopy of the integumental surfaces of Schistosoma haematobium. J. Parasitol. 62: 63-69.

Lal, M. B., and S. C. Shrivastava. 1960. Some histochemical observations on the cuticle of Fasciola indica Verma, 1953. Experientia (Basal) 16: 185-186.

Lavrov, N. P. 1953. Endo- and ectoparasites of muskrats (in Russian). Trudy Vsesoiuz. Nauchno-Issled. Inst. Okhot. Promys. No. 12.

Law, R. G., and A. H. Kennedy. 1932. Parasites of fur-bearing animals. Bull. Dept. Game and Fisheries, Ontario 4: 1-30.

Lee, C., and J. H. Miller. 1967. Fine structure of Dirofilaria immitis body-wall musculature. Exp. Parasitol. 20: 334-344.

Lee, D. L. 1966. The structure and composition of the helminth cuticle. Adv. Parasitol. 4: 187-254.

Llewellyn, J. 1965. The evolution of parasitic platyhelminths. Pages 47-78 in A. E. R. Taylor, ed. Evolution of parasites. Blackwell Scientific Publications, Oxford.

Loewenstein, W. R., and Y. Kanno. 1964. Studies on an epithelial (gland) cell junction. J. Cell Biol. 22: 565-586.

Lumsden, R. D. 1965a. Macromolecular structure of glycogen in some cyclophyllidean and trypanorhynch cestodes. J. Parasitol. 51: 501-515.

Lumsden, R. D. 1965b. Microtubules in the peripheral cytoplasm of cestode spermatozoa. J. Parasitol. 51: 929-931.

Lumsden, R. D. 1966. Fine structure of the medullary parenchymal cells of a trypanorhynch cestode, Lacistorhynchus tenuis (V. Beneden, 1858), with emphasis on specializations for glycogen metabolism. J. Parasitol. 52: 417-427.

Lumsden, R. D. 1970. Preparatory technique for electron microscopy. Pages 217-228 in A. J. MacInnis and M. Voge, eds. Experiments and techniques in parasitology. W. H. Freeman and Co., San Francisco.

Lumsden, R. D. 1975. Surface ultrastructure and cytochemistry of parasitic helminths. Exp. Parasitol. 37: 267-339.

Lumsden, R. D., and J. Byram. 1967. The ultrastructure of cestode muscle. J. Parasitol. 53: 326-342.

Lumsden, R. D., and W. E. Foor. 1968. Electron microscopy of schistosome cercarial muscle. J. Parasitol. 54: 780-794.

Lumsden, R. D., and G. W. Harrington. 1966. Incorporation of linoleic acid by the cestode Hymenolepis diminuta (Rudolphi, 1819). J. Parasitol. 52: 695-700.

Lyons, K. M. 1970a. The fine structure and function of the adult epidermis of two skin parasitic monogeneans, Entobdella soleae and Acanthocotyle elegans. Parasitology 60: 39-52.

Lyons, K. M. 1970b. Fine structure of the outer epidermis of the viviparous monogenean Gyrodactylus sp. from the skin of Gasterosteus aculeatus. J. Parasitol. 56: 1110-1117.

Lyons, K. M. 1971. Comparative electron microscope studies on the epidermis of the blood living juvenile and gill living adult stages of Amphibdella flavolineata (Monogenea) from the electric ray Torpedo nobiliana. Parasitology 63: 181-190.

Lyons, K. M. 1972. Ultrastructural observations on the epidermis of the polyopisthocotylinean monogeneans Rajonchocotyle emarginata and Plectanocotyle gurnardi. Z. Parasitenkd. 40: 87-100.

MacDonald, S., and J. Caley. 1975. Sexual reproduction in the monogenean Diclidophora merlangi: tissue penetration by sperms. Z. Parasitenkd. 45: 323-334.

Machulskii, S. N. 1959. The helminth fauna of rodents in the Buryat ASSR (in Russian). Papers on helminthology presented to academician K. I. Skrjabin on his 80th birthday. Moscow: Izdatelstvo Akad. Nauk SSSR.

MacRae, E. K. 1963. Observations on the fine structure of pharyngeal muscle in the planarian Dugesia tigrina. J. Cell Biol. 18: 657-662.

MacRae, E. K. 1965. The fine structure of muscle in a marine turbellarian. Z. Zellforsch. 68: 348-362.

McCracken, R. O. 1972. Glucose absorption and metabolism in Haematoloechus medioplexus (Trematoda: Haematoloechiidae). Ph.D. dissertation. Iowa State University, Ames.

McIntosh, A., and G. E. McIntosh. 1934. A new trematode, Notocotylus hassalli, n. sp. (Notocotylidae), from a meadow mouse. Proc. Helminthol. Soc. Wash. 1: 36-37.

Meyer, M. C., and J. R. Reilly. 1950. Parasites of muskrats in Maine. Am. Midl. Nat. 44: 467-477.

Miller, F. H., G. S. Tulloch, and R. E. Kuntz. 1972. Scanning electron microscopy of integumental surface of Schistosoma mansoni. J. Parasitol. 58: 693-698.

Morita, M. 1965. Electron microscopic studies on planaria. I. Fine structure of muscle fiber in the head of the planarian Dugesia dorotocephala. J. Ultrastruct. Res. 13: 383-395.

Morris, G. P. 1968. Fine structure of the gut epithelium of Schistosoma mansoni. Experientia (Basel) 24: 480-482.

Morris, G. P. 1973. The fine structure of the caecal epithelium of Megalodiscus temperatus. Can. J. Zool. 51: 457-460.

Morris, G. P., and D. W. Halton. 1971. Electron microscope studies of Diclidophora merlangi (Monogenea: Polyopisthocotylea). II. Ultrastructure of the tegument. J. Parasitol. 57: 49-61.

Morris, G. P., and L. T. Threadgold. 1968. Ultrastructure of the tegument of adult Schistosoma mansoni. J. Parasitol. 54: 15-27.

Morseth, D. J. 1969. Spermtail fine structure of Echinococcus granulosus and Dicrocoelium dendriticum. Exp. Parasitol. 24: 47-53.

Moseley, C., and P. M. Nollen. 1973. Autoradiographic studies on the reproductive system of Philophthalmus hegeneri Penner and Fried, 1963. J. Parasitol. 59: 650-654.

Nollen, P. M. 1968a. Uptake and incorporation of glucose, tyrosine, leucine, and thymidine by adult Philophthalmus megalurus (Cort, 1914) (Trematoda), as determined by autoradiography. J. Parasitol. 54: 295-304.

Nollen, P. M. 1968b. Autoradiographic studies on reproduction in Philophthalmus megalurus (Cort, 1914) (Trematoda). J. Parasitol. 54: 43-48.

Nollen, P. M. 1971. Digenetic trematodes: Quinone tanning system in eggshells. Exp. Parasitol. 30: 64-72.

Nollen, P. M., and M. J. Nadakavukaren. 1974. Megalodiscus temperatus: Scanning electron microscopy of the tegumental surfaces. Exp. Parasitol. 36: 123-130.

Odlaug, T. O. 1948. The finer structure of the body wall and parenchyma of three species of digenetic trematodes. Trans. Am. Microsc. Soc. 67: 236-253.

Öhman, C. 1966. The structure and function of the adhesive organ in strigeid trematodes. III. Apatemon gracilis minor Yamaguti, 1933. Parasitology 56: 209-226.

Pantelouris, E. M., and L. T. Threadgold. 1963. The excretory system of the adult Fasciola hepatica L. Cellule 64: 63-67.

Parkening, T. A., and A. D. Johnson. 1969. Glucose uptake in Haematoloechus medioplexus and Gorgoderina trematodes. Exp. Parasitol. 25: 358-367.

Pappas, P. W. 1971. Haematoloechus medioplexus: Uptake, localization, and fate of tritiated arginine. Exp. Parasitol. 30: 102-119.

Pearse, A. G. E. 1960. Histochemistry theoretical and applied. Second edition. J. and A. Church., Ltd., London. 998 pp.

Phifer, K. 1960a. Permeation and membrane transport in animal parasites: The absorption of glucose by Hymenolepis diminuta. J. Parasitol. 46: 51-62.

Phifer, K. 1960b. Permeation and membrane transport in animal parasites: Further observations on the uptake of glucose by Hymenolepis diminuta. J. Parasitol. 46: 137-144.

Politoff, A., S. J. Socolar, and W. R. Loewenstein. 1967. Metabolism and the permeability of cell membrane functions. Biochim. Biophys. Acta 135: 791-793.

Prichard, R. C. and P. J. Schofield. 1968. The glycolytic pathway in adult liver fluke, Fasciola hepatica. Comp. Biochem. Physiol. 24: 697-710.

Prichard, R. C., and P. J. Schofield. 1969. The glycoxylate cycle, fructose-1,6-diphosphatase and glyconeogenesis in Fasciola hepatica. Comp. Biochem. Physiol. 29: 581-590.

Rausch, R. 1952. Studies on the helminth fauna of Alaska. XI. Helminth parasites of microtine rodents - taxonomic considerations. J. Parasitol. 38: 415-426.

Rausch, R., and J. D. Tiner. 1948. Studies on the parasitic helminths of the North Central States. I. Helminths of Sciuridae. Am. Midl. Nat. 39: 728-747.

Rausch, R., and J. D. Tiner. 1949. Studies on the parasitic helminths of the North Central States. II. Helminths of voles (Microtus spp.) Preliminary report. Am. Midl. Nat. 41: 665-694.

Read, C. P. 1951. The "crowding effect" in tapeworm infections. J. Parasitol. 37: 174-178.

Read, C. P., A. H. Rothman, and J. E. Simmons. 1963. Studies on membrane transport, with special reference to parasite-host integration. Ann. N.Y. Acad. Sci. 113: 154-205.

Rees, G. 1939. Studies on the germ cell cycle of the digenetic trematode Parorchis acanthus Nicoll. I. Anatomy of the genitalia and gametogenesis in the adult. Parasitology 31: 417-433.

Rees, G. 1974. The ultrastructure of the body wall and associated structures of the cercaria of Cryptocotyle lingua (Creplin) (Digenea: Heterophyidae) from Littorina littorea (L.). Z. Parasitenkd. 44: 239-265.

Rhode, K. 1971a. Untersuchungen an Multicotyle purvisi Dawes, 1941 (Trematoda: Aspidogastrea). IV. Ultrastruktur des Integuments der geschlechtsreifen Form und der freien Larve. Zool. Jahrb. Anat. 88: 365-386.

Rhode, K. 1971b. Untersuchungen an Multicotyle purvisi Dawes, 1941 (Trematoda: Aspidogastrea). VI. Ultrastruktur des Spermatozoons. Zool. Jahrb. Anat. 88: 399-405.

Rhode, K. 1975. Fine structure of the Monogenea, especially Polystomoides Ward. Adv. Parasitol. 13: 1-33.

Robinson, G., and L. T. Threadgold. 1975. Electron microscope studies of Fasciola hepatica. XII. The fine structure of the gastrodermis. Exp. Parasitol. 37: 20-36.

Rosenbluth, J. 1965. Ultrastructural organization of obliquely striated muscle fibers in Ascaris lumbricoides. J. Cell Biol. 25: 495-515.

Rothschild, M. 1938. Notes on the classification of cercariae of the superfamily Notocotyloidea (Trematoda), with special reference to the excretory system. Novit. Zool. 41: 75-83.

Rudolphi, C. A. 1819. Entozoorum synopsis cui accedunt mantissa duplex et indiced locupletissimi. Berolini. 811 pp.

Sato, M., M. Oh, and K. Sakoda. 1967. Electron microscope study of spermatogenesis in the lung fluke (Paragonimus miyazakii). Z. Zellforsch. Mikrosk. Anat. 77: 232-243.

Schad, G. A. 1954. Helminth parasites of mice in northeastern Quebec and the coast of Labrador. Can. J. Zool. 32: 215-224.

Schnitzer, R., T. Sodeman, W. A. Sodeman, J. and T. Durkee. 1971. Microspines on Schistosoma japonicum and S. haematobium egg shells. Parasitology 62: 385-387.

Senft, A. W., D. E. Philpott, and A. H. Pelofsky. 1961. Electron microscope observations of the integument, flame cells, and gut of Schistosoma mansoni. J. Parasitol. 47: 217-229.

Senger, C. M., and J. W. Bates. 1957. The occurrence of Hymenolepis evaginata and H. ondatrae in Utah muskrats. Proc. Helminthol. Soc. Wash. 24: 141-142.

Senger, C. M., and K. A. Neiland. 1955. Helminth parasites of some fur bearers of Oregon. J. Parasitol. 41: 637-638.

Shannon, W. A., and B. J. Bogitsh. 1969. Cytochemical and biochemical observations on the digestive tracts of digenetic trematodes. V. Ultrastructure of Schistosomatium douthitti gut. Exp. Parasitol. 26: 344-353.

Shannon, W. A., and B. J. Bogitsh. 1971. Megalodiscus temperatus: Comparative radioautography of glucose-3H and galactose-3H incorporation. Exp. Parasitol. 29: 309-319.

Shapiro, J. E., B. R. Hershenov, and G. S. Tulloch. 1961. The fine structure of Haematoloechus spermatozoan. J. Biophys. Biochem. Cytol. 9: 211-217.

Short, R. B., and H. T. Gagné. 1975. Fine structure of a possible photoreceptor in cercariae of Schistosoma mansoni. J. Parasitol. 61: 69-74.

Silk, M. H., and I. M. Spence. 1969. Ultrastructural studies of the blood fluke - Schistosoma mansoni. II. The musculature. S. Afr. J. Med. Sci. 34: 11-20.

Silk, M. H., I. M. Spence, and J. H. S. Gear. 1969. Ultrastructural studies of the blood fluke - Schistosoma mansoni. I. The integument. S. Afr. J. Med. Sci. 34: 1-10.

Silveria, M. 1969. Ultrastructural studies on a "nine-plus-one" flagellum. J. Ultrastruct. Res. 26: 274-288.

Skvortsov, A. A. 1934. Zur Kenntniss der Helminthenfauna der Wasserratten (Arvicola terrestris L.) (in Russian, German summary). Vestn. Mikrobiol. Epidemiol. Parazitol. 13: 317-326.

Smith, C. F. 1954. Studies on Quinqueserialis hassalli and taxonomic considerations of the species of Quinqueserialis (Trematoda: Notocotylidae). J. Parasitol. 40: 209-215.

Smith, J. H., E. S. Reynolds, and F. von Lichtenberg. 1969. The integument of Schistosoma mansoni. Am. J. Trop. Med. Hyg. 18: 28-49.

Smyth, J. D., and J. A. Clegg. 1959. Egg-shell formation in trematodes and cestodes. Exp. Parasitol. 8: 286-323.

Sodeman, T. M., W. A. Sodeman, and B. Schnitzer. 1972. Lamellar structures in the gut of Schistosoma haematobium. Ann. Trop. Med. Parasitol. 66: 475-478.

Spence, I. M., and M. H. Silk. 1970. Ultrastructural studies of the blood fluke Schistosoma mansoni. IV. The digestive system. S. Afr. J. Med. Sci. 35: 93-112.

Spence, I. M., and M. H. Silk. 1971. Ultrastructural studies on the blood fluke - Schistosoma mansoni. V. The female reproductive system - a preliminary report. S. Afr. J. Med. Sci. 36: 41-50.

Stephenson, W. 1947. Physiological and histochemical observations on the adult liver fluke, Fasciola hepatica L. III. Egg shell formation. Parasitology 38: 128-139.

Stiles, C. W., and A. Hassall. 1894. A preliminary catalogue of the parasites contained in the collections of the United States Bureau of Animal Industry, United States Army Medical Museum, Biological Department of the University of Pennsylvania (coll. Leidy) and in coll. Stiles and Hassall. Vet. Mag. 1: 245-253; 331-354.

Stirewalt, M. A. 1965. Mucus in schistosome cercariae. Ann. N.Y. Acad. Sci. 118: 966-968.

Sweatman, G. K. 1952. Endoparasites of muskrats in the vicinity of Hamilton, Ontario. J. Mammalogy 33: 248-250.

Tenora, F. 1956. Prispevek k poznani helmintofauny ondatry pozmove (Ondatra zibethica L.) v CSR. Sborn. Vysoke Zemed. a Lesnicke Fak. Brne, Rada A, Spis. Fak Agron. a Zootech. 1: 37-50.

Thorsell, W., and N. Björkman. 1965a. Morphological and biochemical studies on absorption and secretion in the alimentary tract of Fasciola hepatica L. J. Parasitol. 51: 217-223.

Thorsell, W., and N. Björkman. 1965b. On the fine structure of the Mehlis gland cells in the liver fluke, Fasciola hepatica L. Z. Parasitenkd. 26: 63-70.

Thorsell, W., N. Björkman, and L. E. Applegren. 1966. Radioautographic studies on the ovary and vitelline glands of the liver fluke, Fasciola hepatica L. after short in vitro incubation with some amino acids. Z. Parasitenkd. 28: 108-115.

Threadgold, L. T. 1963. The tegument and associated structures of Fasciola hepatica. Q. J. Microsc. Sci. 104: 505-512.

Threadgold, L. T. 1967a. The ultrastructure of the animal cell. Pergamon Press, Oxford. 313 pp.

Threadgold, L. T. 1967b. Electron-microscope studies of Fasciola hepatica. III. Further observations on the tegument and associated structures. Parasitology 57: 633-637.

Threadgold, L. T. 1968a. The tegument and associated structures of Haplometra cylindracea. Parasitology 58: 1-7.

Threadgold, L. T. 1968b. Electron microscope studies of Fasciola hepatica. VI. The ultrastructural localization of phosphatases. Exp. Parasitol. 23: 264-276.

Threadgold, L. T. 1975a. Electron microscope studies of Fasciola hepatica. III. Fine structure of the prostate gland. Exp. Parasitol. 37: 117-124.

Threadgold, L. T. 1975b. Fasciola hepatica: the ultrastructure of the epithelium of the seminal vesicle, the ejaculatory duct and the cirrus. Parasitology 71: 437-443.

Threadgold, L. T., and C. Arme. 1974. Electron microscope studies of Fasciola hepatica. XI. Autophagy and parenchymal cell function. Exp. Parasitol. 35: 389-405.

Threadgold, L. T., and S. S. E. Gallagher. 1966. Electron microscope studies of Fasciola hepatica. I. The ultrastructure and interrelationship of the parenchymal cells. Parasitology 56: 299-304.

Threadgold, L. T., and S. W. B. Irwin. 1970. Electron microscope studies of Fasciola hepatica. IX. The fine structure of Mehlis' gland. Z. Parasitenkd. 35: 16-30.

Threadgold, L. T., and C. P. Read. 1970. Cell relationships in Hymenolepis diminuta. Parasitology 60: 181-184.

Toner, P. G., and K. E. Carr. 1971. Cell structure. An introduction to biological electron microscopy. Churchill Livingstone, Edinburgh and London. 256 pp.

Tulloch, G. S., and B. R. Hershenov. 1967. Fine structure of platyhelminth sperm tails. Nature 213: 299-300.

Tulloch, G. S., and J. E. Shapiro. 1957. The ultrastructure of the vitelline cells of Haematoloechus. J. Parasitol. 43: 628-632.

Tuzet, O., and M. H. Ktari. 1971. Récherchés sur l'ultrastructure du spermatozoide de quelques monogènes. Bull. Soc. Zool. Fr. 96: 535-540.

von Brand, T. 1952. Chemical physiology of endoparasitic animals. Academic Press, New York. 339 pp.

von Brand, T., and T. I. Mercado. 1961. Histochemical glycogen studies on Fasciola hepatica. J. Parasitol. 47: 459-464.

Waitz, J. A. 1963. Histochemical studies of the cestode Hydatigera taeniaeformis Batsch, 1786. J. Parasitol. 49: 73-80.

Waitz, J. A., and J. L. Schardein. 1964. Histochemical studies of four cyclophyllidean cestodes. J. Parasitol. 50: 271-277.

Watertor, J. L., and S. B. Van Landingham. 1976. Host-induced histochemical variations in Telorchis bonnerensis (Trematoda: Telorchiidae). J. Parasitol. 62: 152-153.

Wheater, P. R., and R. A. Wilson. 1976. The tegument of Schistosoma mansoni: A histochemical investigation. Parasitology 72: 99-109.

Wilson, R. A. 1967a. The structure and permeability of the shell and vitelline membrane of the egg of Fasciola hepatica. Parasitology 57: 47-58.

Wilson, R. A. 1967b. The protonephridial system in the miracidium of the liver fluke, Fasciola hepatica L. Comp. Biochem. Physiol. 20: 337-342.

Wilson, R. A. 1969a. The fine structure of the protonephridial system in the miracidium of Fasciola hepatica. Parasitology 59: 461-467.

Wilson, R. A. 1969b. Fine structure and organization of the musculature in the miracidium of Fasciola hepatica. J. Parasitol. 55: 1153-1161.

Wilson, R. A. 1970. Fine structure of the nervous system and specialized nerve endings in the miracidium of Fasciola hepatica. Parasitology 60: 399-410.

Wilson, R. A., and P. E. Barnes. 1974. The tegument of Schistosoma mansoni: Observations on the formation, structure and composition of cytoplasmic inclusions in relation to tegument function. Parasitology 68: 239-258.

Yosufzai, H. K. 1952. Cytological studies on the spermatogenesis of Fasciola hepatica L. Cellule 55: 5-21.

Zeder, J. G. H. 1800. Erster Nachtrag zur Naturgeschichte der Eingeweiderwürmer, mit Zufässen und Anmerkungen herausgegeben. Leipzig. 320 pp.

ACKNOWLEDGMENTS

The author wishes to extend his sincere appreciation to Dr. Martin J. Ulmer for his supervision and guidance during this investigation. His able advice, kind encouragement, and personal friendship will always be remembered.

Thanks are also due to Dr. Harry T. Horner, Jr. for providing excellent training in electron microscopy and generous use of facilities. Appreciation is also expressed to Dr. Edwin C. Powell for his assistance in interpreting electron micrographs.

Thanks are expressed to my fellow graduate students, Larry Lightner, Dave Fredericksen, Jim Palmieri, Ed Reedholm, Sam Loker, Gary Hendrickson, and Bill McGeachin, for their contributions to this study. I also wish to extend my appreciation to the staff of the Iowa Lakeside Laboratory, particularly Bob and Tanya Benson, for providing research facilities during collecting trips.

A special note of appreciation is extended to my parents for their understanding and encouragement throughout my educational career.

Grateful acknowledgment is expressed to the Graduate College for its generous generous financial support of this research.

PLATES

Abbreviations

A - axoneme

AP - autophagosome

AU - axial (microtubule) unit

B - basal lamina

BS - bulbous sensory receptor

C - cirrus

CA - caecum

CC - central core

CE - cytoplasmic extension

CG - cortical granule

CH - chromosome

CM - circular muscle

CP - cirrus pouch

CR - crista

CS - ciliated sensory receptor

CSH - cortical sheath

CT - cytotegument

D - desmosome

DB - dense tegumental inclusion

DP - myofibrilar dense patch

E - egg

EC - egg capsule

EF - egg filament

EJ - ejaculatory duct

EL - endoplasmic lakes

ER - endoplasmic reticulum

F - fibrous interstitial connective tissue

FS - fibrous secretory material

G - Golgi complex

GC - glycocalyx

GD - gastrodermis

GN - gonial cell

GO - genital opening

GS - Golgi saccule

GV - Golgi vesicle

GY - glycogen

H - heterochromatin

HD - hemidesmosome

I - osmiophilic inclusion

IL - inner egg capsule layer

IP - internuncial process

L - lipid inclusion

LA - lamella

LM - longitudinal muscle

LM - longitudinal muscle

LU - lumen

M - mitochondrion

ME - metraterm

MG - Mehlis' gland

MP - mid-piece

MS - membranous secretory product

MT - microtubule

MTC- microtubule-organizing center

MU - muscle

MV - microvilli

MW - membranous whorl

N - nucleus

NM - nuclear membrane

NP - nuclear pore

NU - nucleolus

O - ovary

OD - osmoregulatory duct

OL - outer egg capsule layer

OS - oral sucker

OV - oviduct

P - prostate gland

PA - parenchyma

PC - pyriform cell

PD - prostate duct

PG - vitelline protein granule

PI - paracrystalline inclusion

PM - plasma membrane

PS - perinuclear space

R - ribosome

RC - cytoplasmic rod

RS - receptaculum seminis uterinum

RT - ciliated rootlet

S - spermatozoan

SG - secretory granule

SL - sarcolemma

SP - paracrystalline spine

SR - sarcoplasmic reticulum

ST - syntegument

SV - seminal vesicle

T - testis

TI - tegumental infolding

TK - thick myofilament

TN - thin myofilament

U - uterus

V - vitellaria

VA - vacuole

VB - vesicular tegumental inclusion

VD - vas deferens

VE - vas efferens

VS - synaptic vesicle

VT - vitelline duct

Y - yolk droplet

Plate I

Fig. 1. Diagram of adult Quinqueserialis quinqueserialis from meadow vole (Microtus pennsylvanicus) depicting major internal organs.

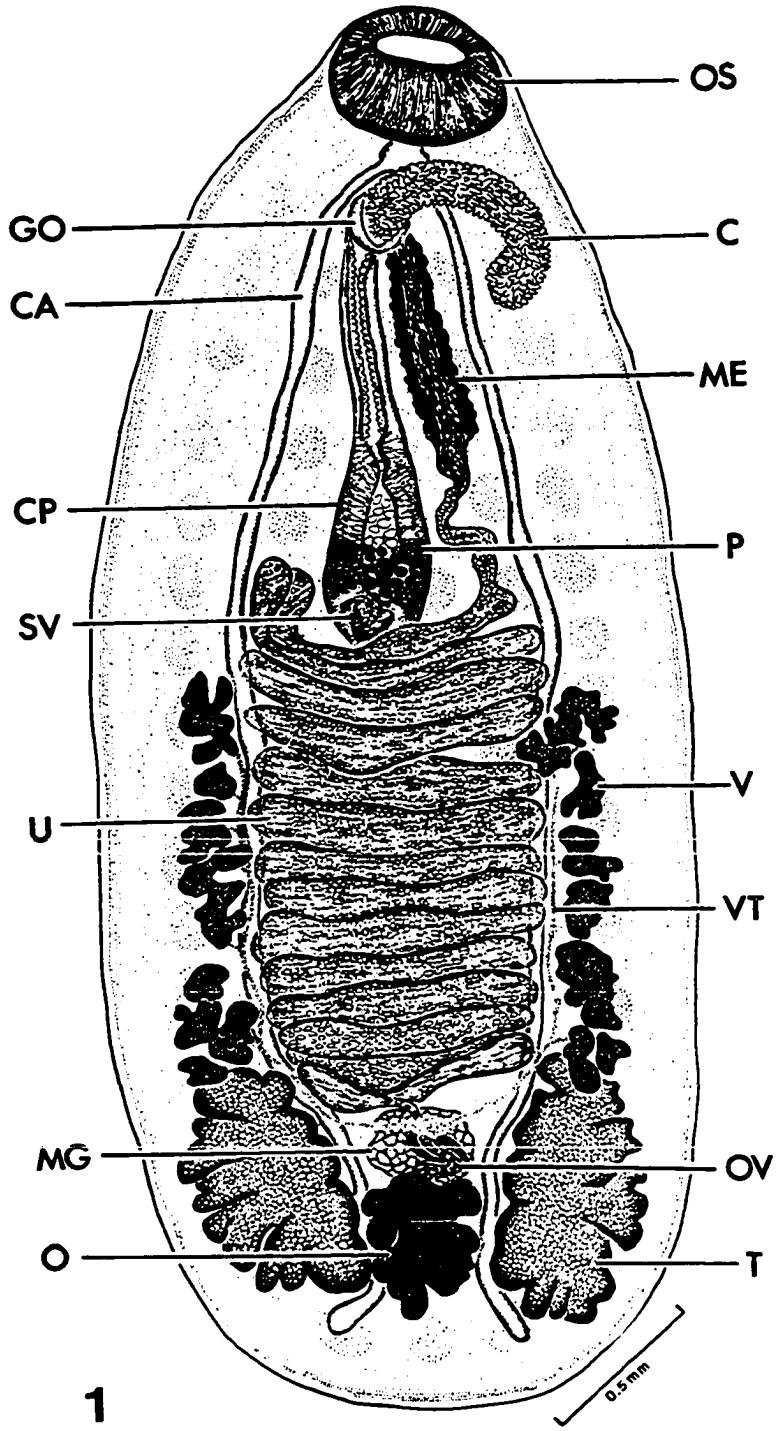

1

Plate II

Figs. 2-8. General staining of *Q. quinqueserialis*.

Fig. 2. Whole mount specimen stained with Mayer's paracarmine and fast green. Note intense paracarmine staining of reproductive structures. (X 16)

Fig. 3. Paracarmine staining of terminal reproductive structures. Note intense staining of posterior prostate gland (P), vas deferens (VD), and metraterm (ME). (X 50)

Fig. 4. One micrometer-thick epon section of ventral papillae stained with methylene blue-azure II. Components of each papilla include outer syntegument (ST), underlying pyriform cells (PC), and osmoregulatory ducts (OD). (X 380)

Fig. 5. Sagittal section through row of ventral papillae stained with hematoxylin and eosin. Note eosinophilic pyriform cells (PC) containing numerous nuclei. (X 80)

Fig. 6. Epon section of cirrus pouch. Components include seminal vesicle (SV), prostate gland (P), ejaculatory duct (EJ) containing prostate secretory granules (SG), and cirrus. Note differential staining of prostate and secretory granules. (X 200)

Fig. 7. Epon section of caecum (CA). Note lightly-staining lumen and unstained inclusions within gastrodermis. Caecum lies dorsal to uterus (U). (X 380)

Fig. 8. Epon section through ventral papillae at level of vitellaria (V). Osmoregulatory ducts (OD) are evident within each papilla. (X 380)

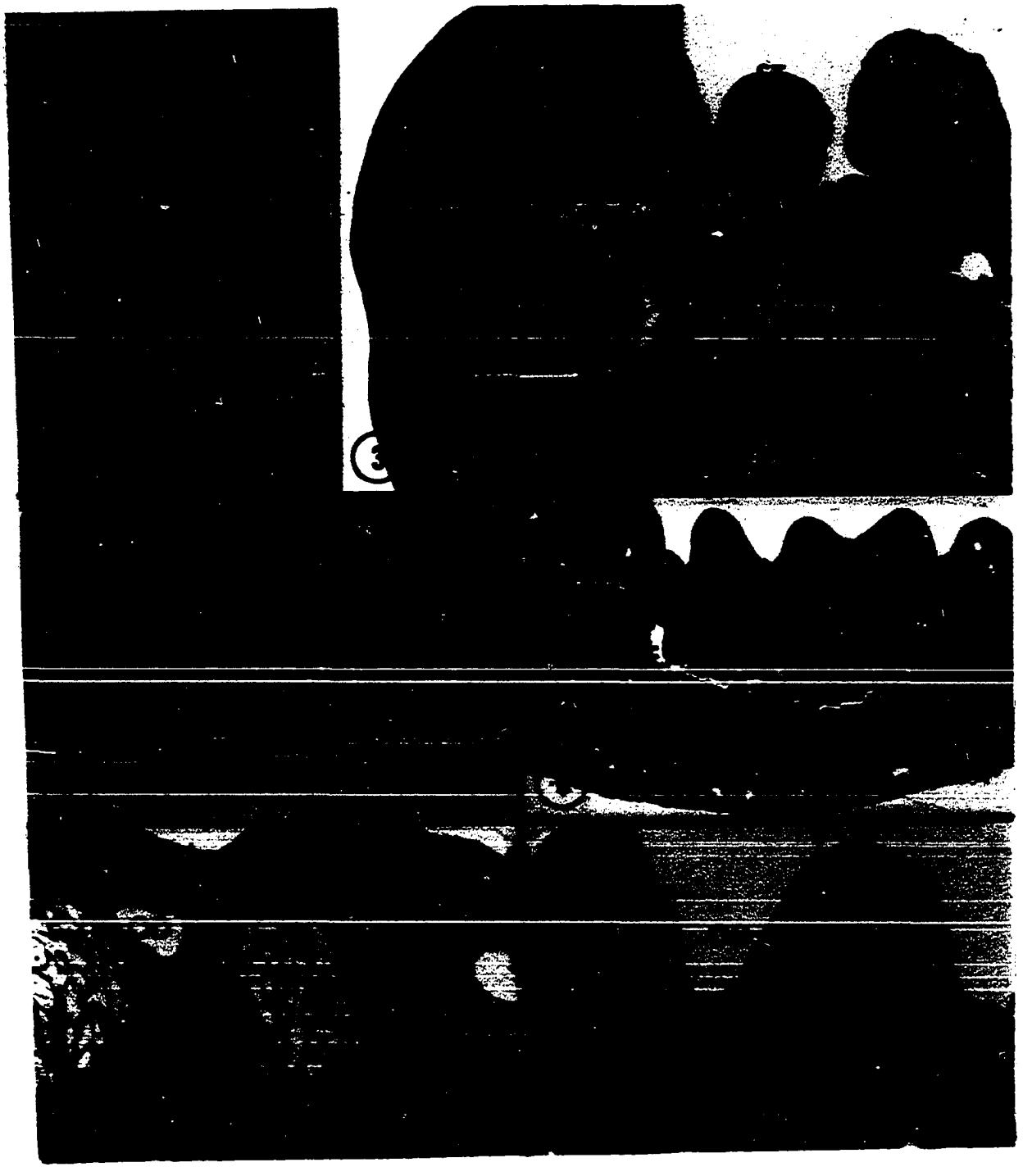

Plate III

Figs. 9-16. Carbohydrate histochemistry of Q. quinqueserialis. (X 170)

Fig. 9. P.A.S. staining of cirrus pouch. Note strong reactions in spermatozoa of seminal vesicle (SV) and in posterior portions of prostate gland (P) and secretory granules (SG).

Fig. 10. P.A.S. staining of cirrus pouch after diastase digestion. Only posterior secretory granules (SG) and cirrus syntegument (C) stain. Postive reaction is also elicited by dorsal syntegument (ST).

Fig. 11. P.A.S. staining of ventral papillae. Positive reaction occurs only in syntegument (ST); pyriform cells (PC) are negative. Note other positive reactions in eggs (E) and spermatozoa in vas deferens (VD).

Fig. 12. P.A.S.-positive reactions of synteguments of cirrus (C) and dorsal body surface (ST). Note concentrations of polysaccharides (glycogen) throughout parenchyma (PA).

Fig. 13. P.A.S. staining of caecum (CA). Note concentration of dye along lumenal surface of gastrodermis.

Fig. 14. Alcian blue staining of caecum (CA) for acid mucopolysaccharides. Note intense reaction in gastrodermis and lumen.

Fig. 15. Best's carmine staining for glycogen. Note positive reactions in spermatozoa stored in seminal vesicle (SV) and in eggs (E) of distal uterus.

Fig. 16. Best's carmine staining for glycogen. Note concentrations in spermatozoa of receptaculum seminis uterinum (RS) and in parenchyma (PA).

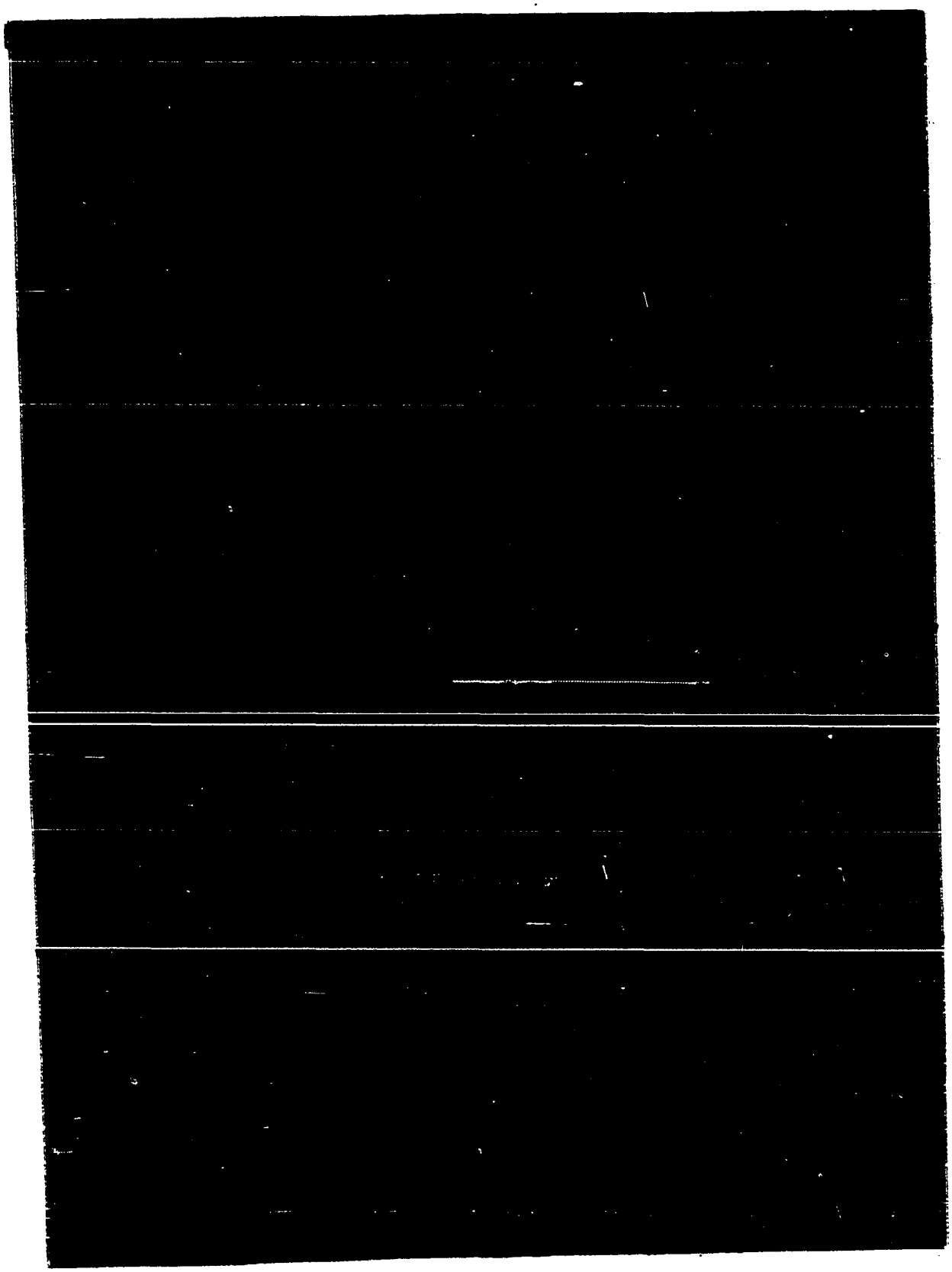

Plate IV

Figs. 17-24. Protein histochemistry of *Q. quinqueserialis*.

Fig. 17. Mercuric bromphenol blue (HgBPB) staining of ventral papillae. Note strong positive reactions for basic proteins in syntegument (ST) and pyriform cells (PC).

Fig. 18. Positive HgBPB reaction in gastrodermis of caecum (CA). Note positive reaction in dorsal cytotegument (CT).

Fig. 19. Positive HgBPB reaction for proteins in vitellaria (V). Components of dorsal tegument are also stained.

Fig. 20. HgBPB staining of female reproductive structures. Note strong reactions in ovary (O) and receptaculum seminis uterinum (RS) and slight reaction in Mehlis' gland (MG).

Fig. 21. Intense reaction of cirrus syntegument (C) with HgBPB for basic proteins.

Fig. 22. HgBPB staining of cirrus pouch. Note positive reactions in spermatozoa of seminal vesicle (SV), wall of ejaculatory duct (EJ), and prostate gland cells (P). A slight reaction is elicited by secretory granules (SG).

Fig. 23. Ninhydrin-Schiff test for basic proteins. A strong positive reaction occurs in syntegument (ST) and a slight reaction is demonstrated in pyriform cells (PC) of ventral papillae. Uterine wall (U) also stains for proteins.

Fig. 24. Naphthol yellow S staining of cirrus pouch. Positive reactions for proteins are shown in seminal vesicle (SV), prostate (P), secretory granules (SG), ejaculatory duct (EJ), and cirrus (C).

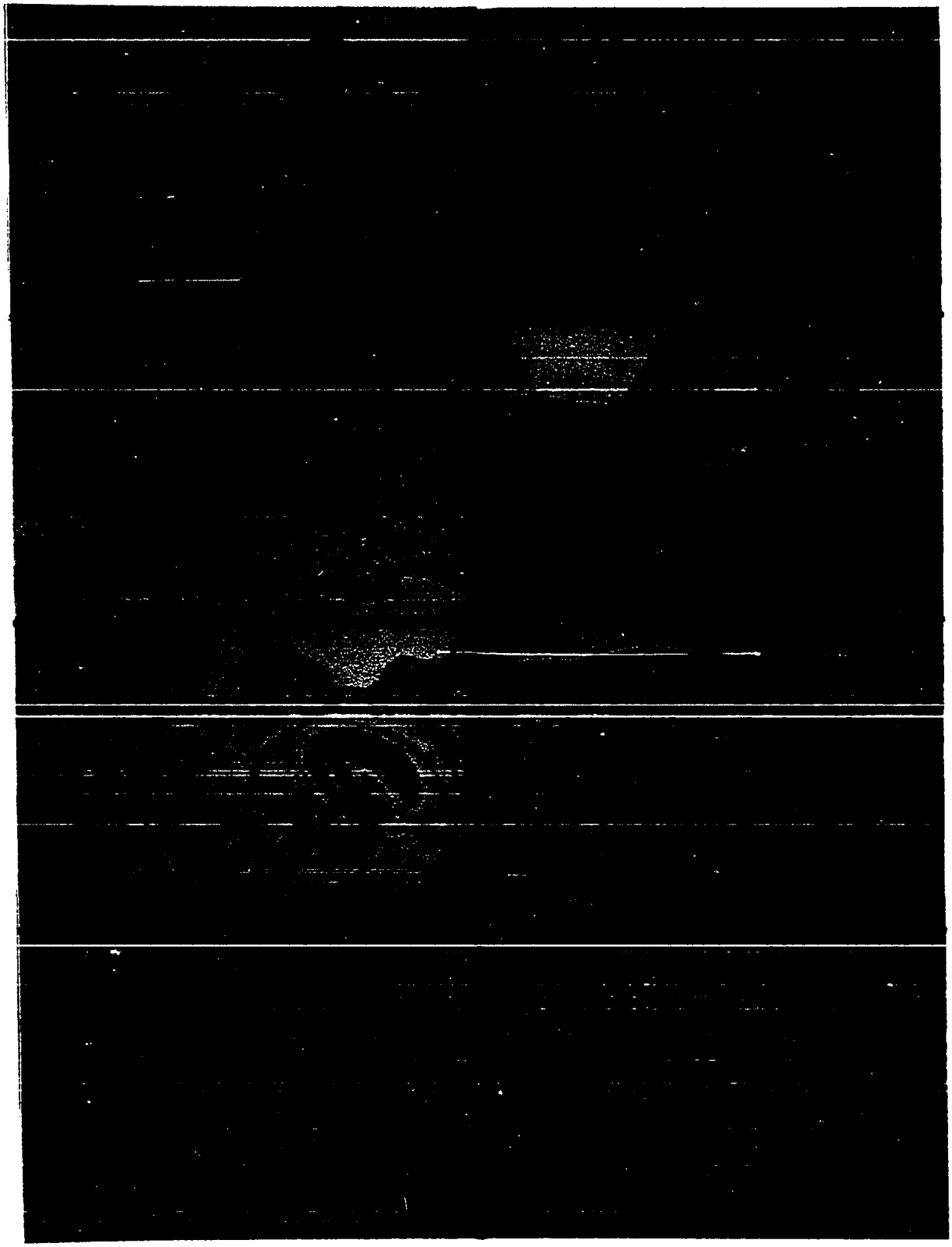

Plate V

Figs. 25-28. Nucleic acid histochemistry of Q. quinqueserialis. (X 170)

Fig. 25. Azure B staining of cirrus pouch. RNA is demonstrated in prostate gland (P), and DNA occurs in spermatozoa stored in seminal vesicle (SV). Positive reaction for RNA is also shown in dorsal cytotegument (CT).

Fig. 26. Intense staining of vitellaria (V) with azure B for RNA. A slight reaction for DNA occurs within eggs (E).

Fig. 27. Azure B staining of female reproductive structures. Note positive reactions for RNA in ovary (O) and Mehlis' gland (MG). DNA is demonstrated in spermatozoa stored in receptaculum seminis uterinum (RS).

Fig. 28. Positive reactions for both RNA and DNA occur in testis (T) with azure B. A slight reaction occurs in the basal gastrodermis of the caecum (CA). Note the absence of filaments in newly formed eggs (E).

Figs. 29-32. Lipid histochemistry of Q. quinqueserialis.

Fig. 29. Demonstration of lipids in caecum (CA) using oil red O staining of frozen sections. (X 170)

Fig. 30. Staining of lipid inclusions (L) with oil red O. (X 380)

Fig. 31. Sudan black B staining of lipids of caecum. Note intense reactions in inclusions. (X 170)

Fig. 32. Acetone-Sudan black B test for protein-bound lipids. Note positive reactions in syntegument (ST) and pyriform cells (PC) of ventral papillae. (X 170)

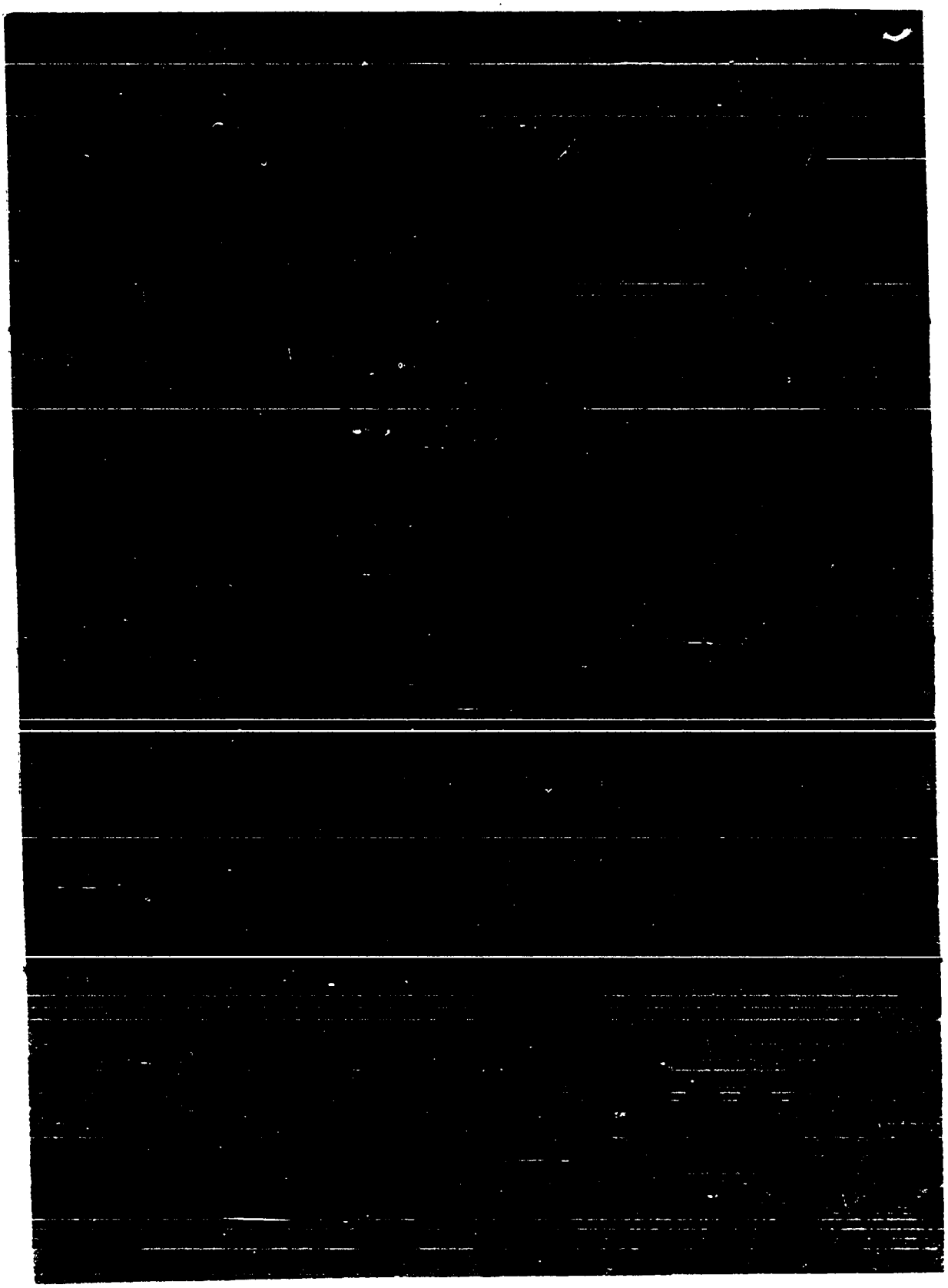

Plate VI

Figs. 33-38. Enzyme histochemistry of Q. quinqueserialis.

Fig. 33. Demonstration of acid phosphatase activity in caecum (CA) using modified azo dye coupling technique. (X 170)

Fig. 34. Intense reaction for acid phosphatase in prostate gland. (X 170)

Fig. 35. Alkaline phosphatase activity in prostate gland (P). (X 170)

Fig. 36. Demonstration of nonspecific esterase in ejaculatory duct (EJ) using α-naphthol acetate technique. (X 170)

Fig. 37. Nonspecific esterase activity in Mehlis' gland (MG). (X 170)

Fig. 38. Nonspecific esterase activity in basal portions of cirrus (C) and metraterm (ME). (X 360)

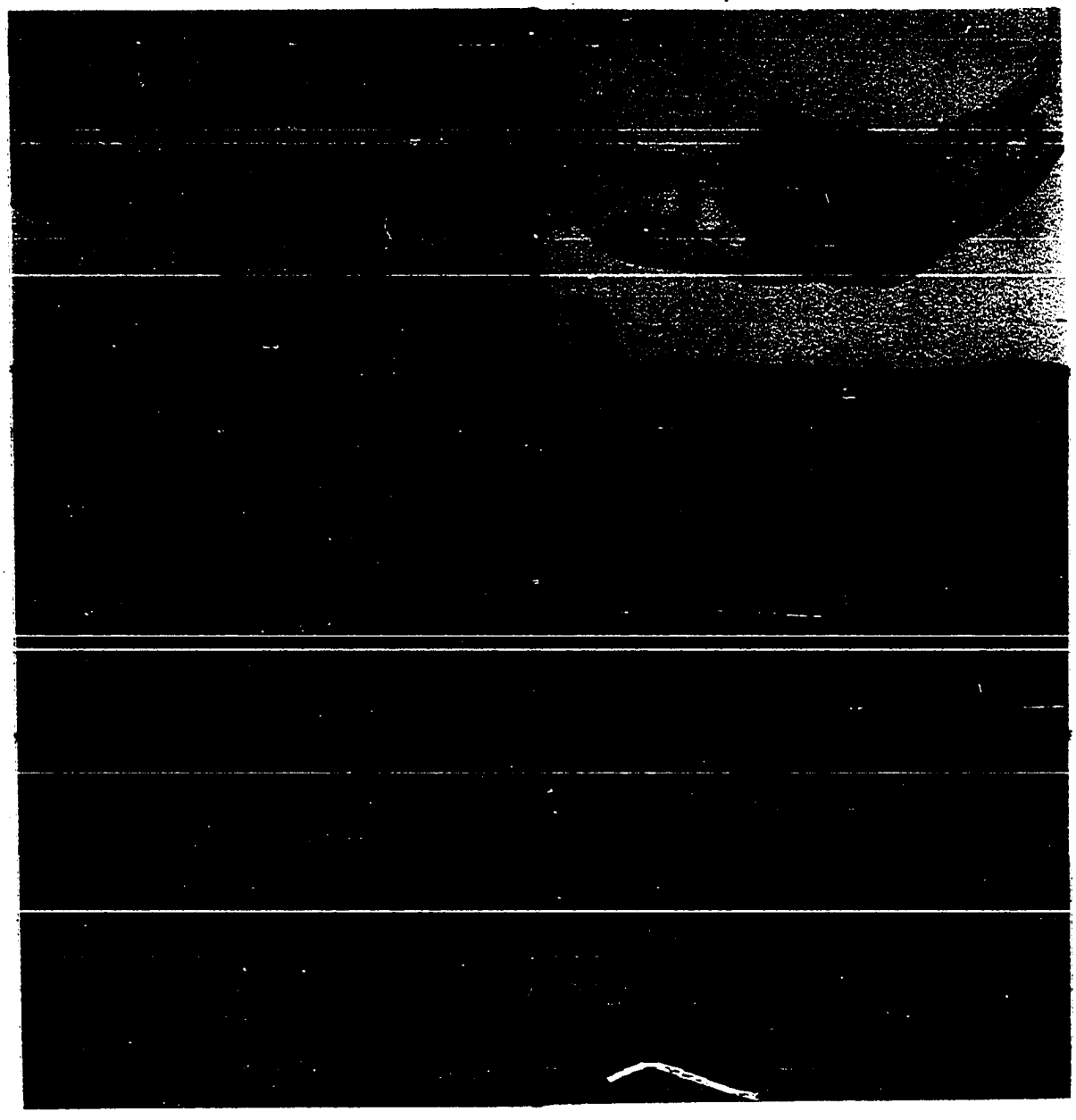

Plate VII

Fig. 39. Dorsal tegument of Q. quinqueserialis. Note shallow infoldings of external surface of thick syntegument (ST). Elements of cytotegument (CT) lie below tegumental musculature. (X 10,600)


IP
F
G
C

Plate VIII

Fig. 40. Scanning electron micrograph of surface of dorsal syntegument. (X 8,000)

Fig. 41. Basal portion of dorsal syntegument. Note the numerous hemidesmosomes (HD) which secure the basal membrane to basal lamina (B). Mitochondria (M) with poorly developed cristae and vesicular tegumental inclusions (VB) occur in this region. (X 35,150)

Fig. 42. Ciliated rootlet (RT) of presumed sensory receptor lies in basal syntegument. Note thick layer of fibrous interstitial connective tissue (F) underlying basal lamina (B) of syntegument. (X 19,320)

Fig. 43. Internuncial process (IP) from underlying cytotegument extends through tegumental muscles and connects with syntegument. (X 35,900)

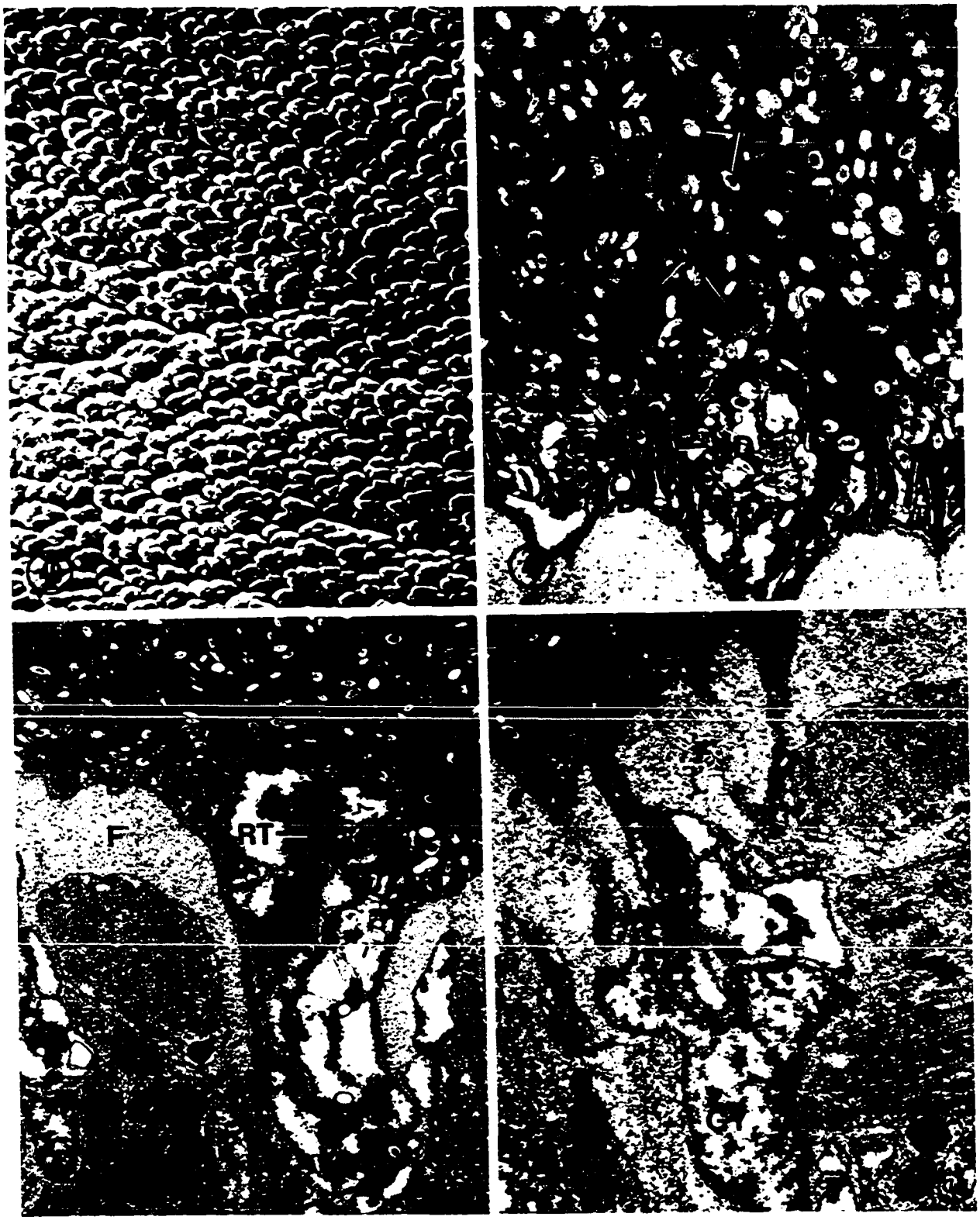
F
RT

Plate IX

Fig. 44. Nucleated cell of dorsal cytotegument. Note irregular nucleus (N) containing central nucleolus (NU) and peripheral heterochromatin (H). (X 29,500)

Fig. 45. Cytoplasm of cytotegument. Note cluster of tegumental inclusions and extensive system of granular endoplasmic reticulum (ER). (X 37,000)

Fig. 46. Cytoplasm of cytotegument. Note cluster containing stacks of dense tegumental inclusions (DB) and numerous free ribosomes (R). (X 47,600)

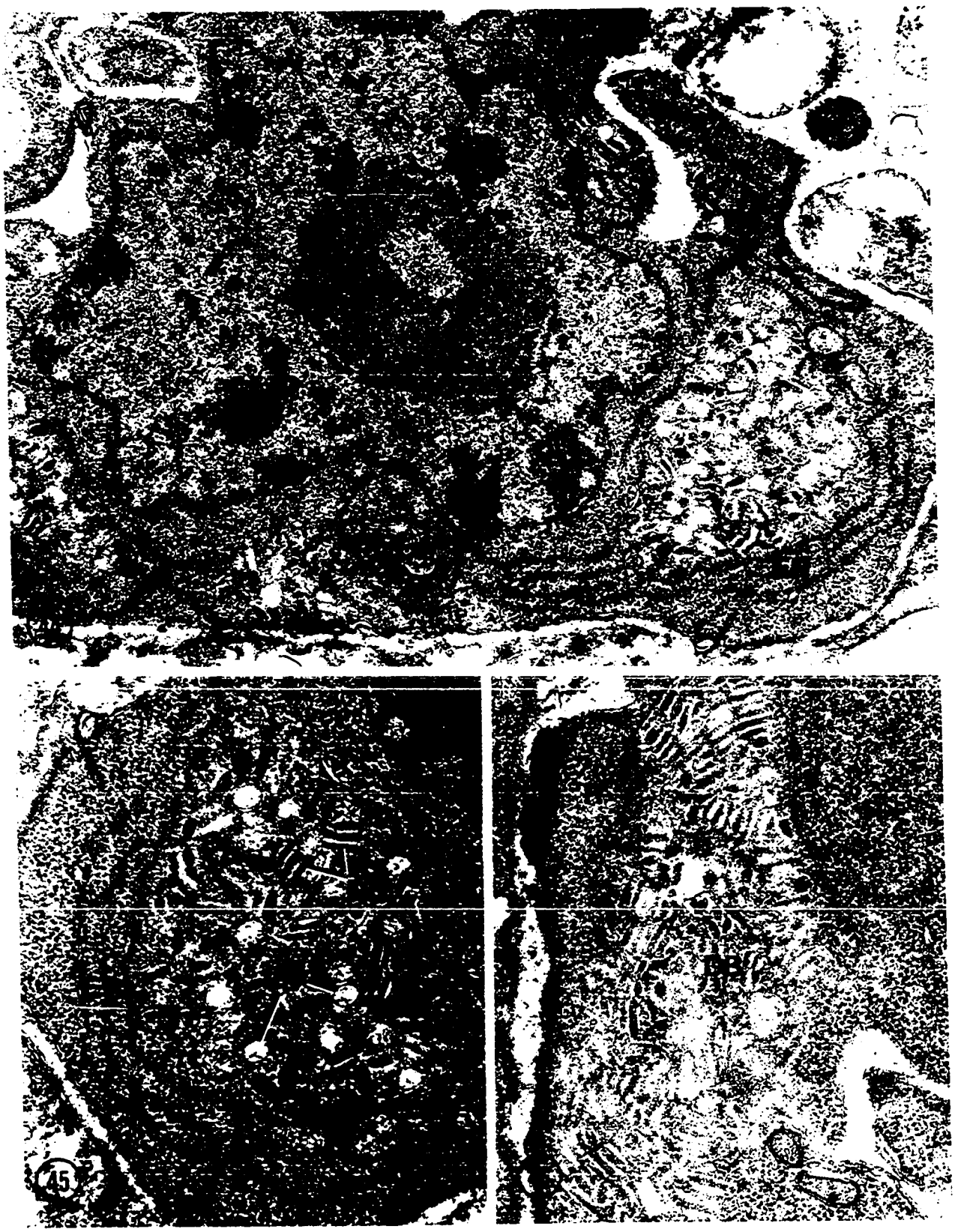
45

Plate X

Figs. 47-50. Scanning electron micrographs of ventral papillae of Q. quinqueserialis.

Fig. 47. Low magnification of whole mount specimen. Note five distinct rows of ventral papillae. (X 40)

Fig. 48. Anterior end of specimen showing well-developed oral sucker (OS) and five rows of papillae. (X 175)

Fig. 49. Ventral papilla. Note two distinct tegumental infoldings (TI) near apex. Rectangle indicates area depicted in Figure 50. (X 2,500)

Fig. 50. High magnification of syntegument of ventral papilla. Apical region is highly convoluted and devoid of spines. Ciliated sensory receptors (CS) are rarely observed in this region. Numerous spines (SP) characterize marginal regions. (X 17,500)

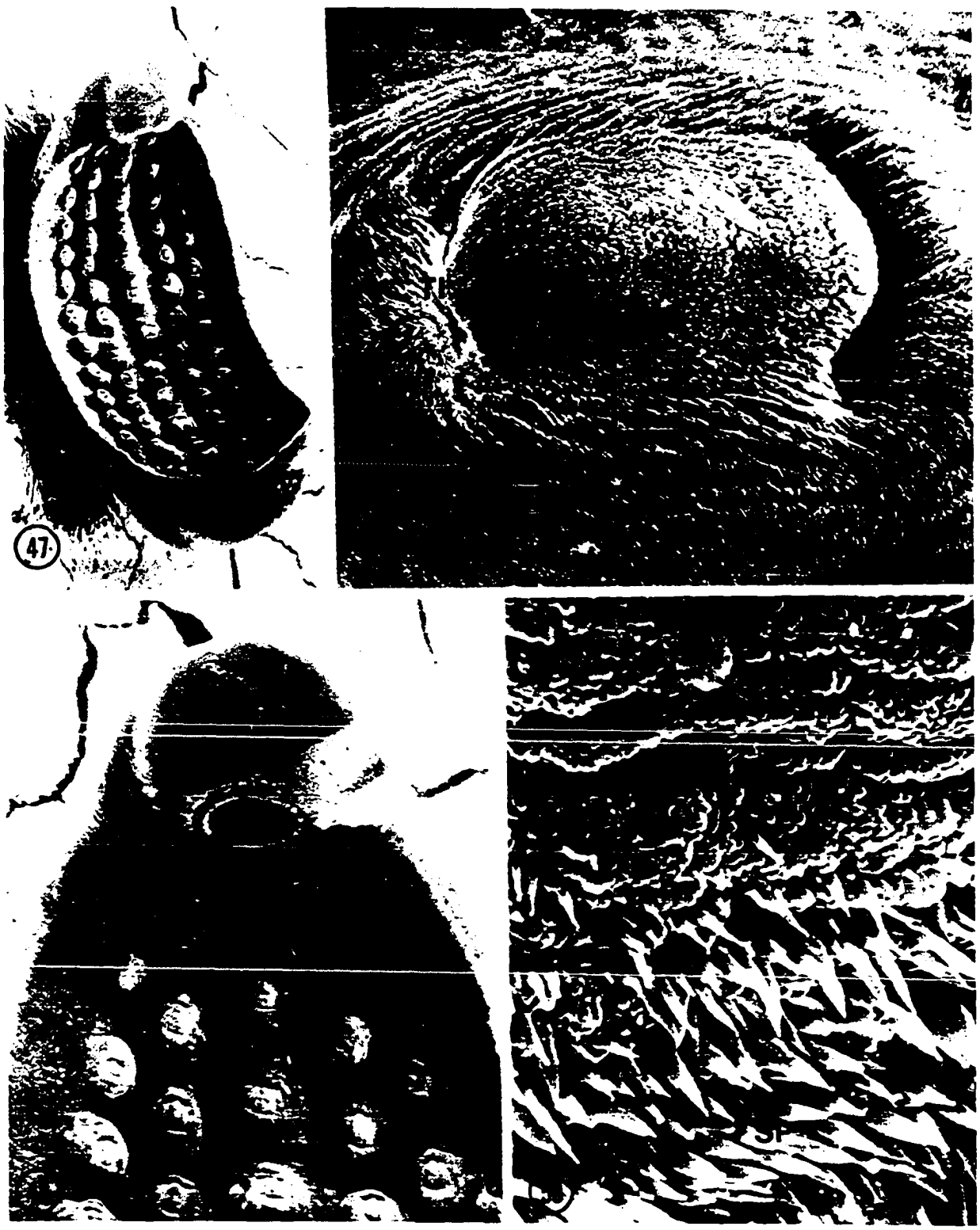
47

Plate XI

Fig. 51. Survey transmission electron micrograph of ventral papilla. Note outer syntegument (ST), tegumental musculature (MU), and underlying pyriform cells (PC). Nuclei of parenchymal cells (PA) are interspersed between pyriform cells. (X 4,800)

Fig. 52. Syntegument of ventral papilla. Note paracrystalline spines (SP), vesicular tegumental inclusions (VB), and mitochondria (M) in syntegument. Cytoplasmic extensions (CE) of pyriform cells are connected to syntegument via junctional complexes (J). (X 53,000)

Fig. 53. Cytoplasmic projection (CE) of pyriform cell extending through tegumental musculature. Note cytoplasmic rods (RC) which support this process. (X 35,600)

Fig. 54. Bulbous sensory receptor in ventral syntegument. Note numerous synaptic vesicles (VS) within receptor. (X 44,800)

Fig. 55. Ciliated sensory receptor in ventral syntegument. Cilium contains nine peripheral doublets of microtubules (MT) and nine single microtubules. (X 68,000)

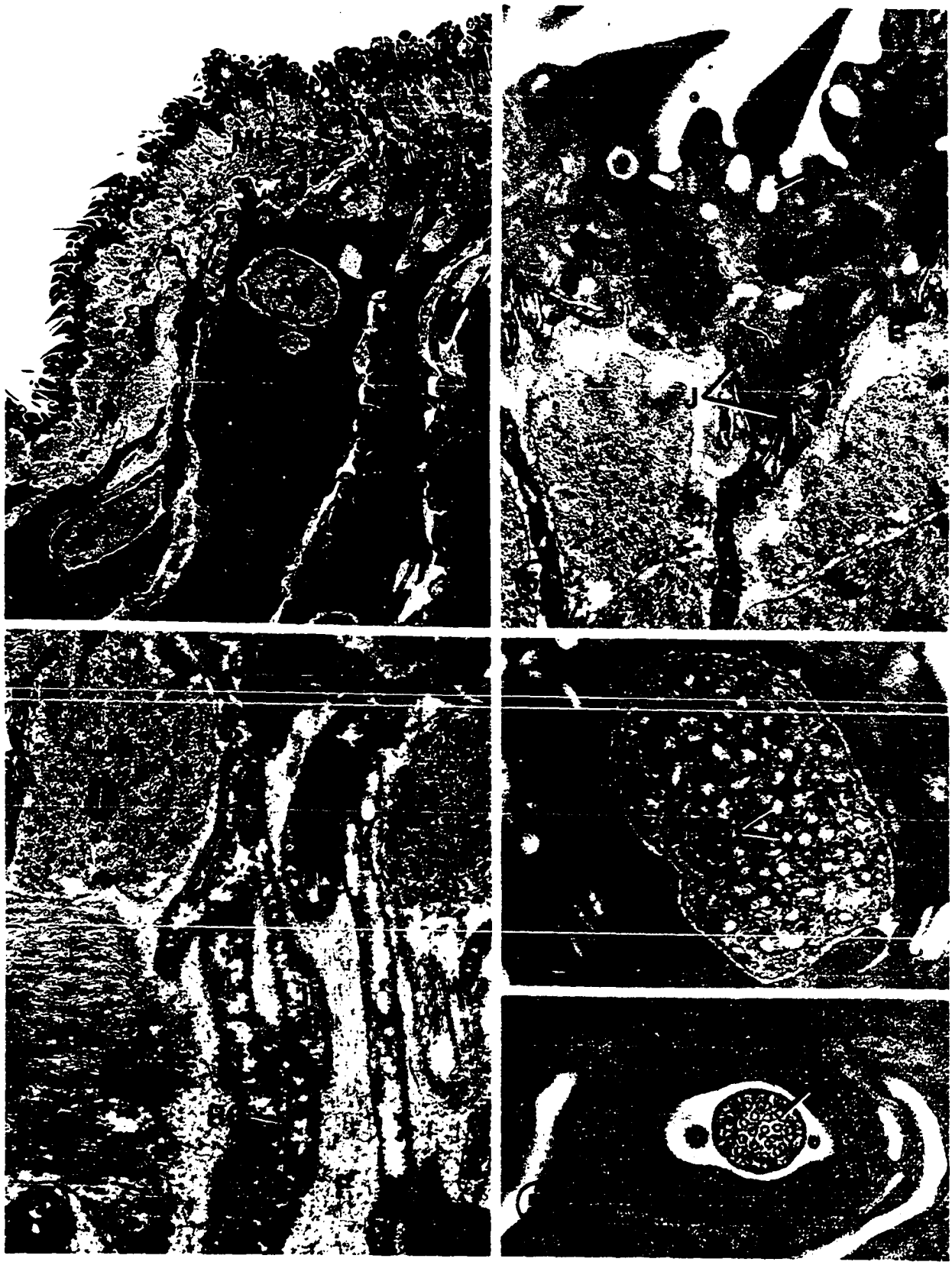

Plate XII

Fig. 56. Apical tegument of ventral papilla. Convoluted syntegument (ST) is limited by basal lamina (B). Bands of circular muscle (CM) and thick layer of longitudinal muscle (LM) lie within fibrous interstitial tissue (F) beneath syntegument. Cytoplasmic extensions (CE) of pyriform cells (PC) project through musculature and join with syntegument. (X 35,000)


F
GM

Plate XIII

Fig. 57. Apical syntegument of ventral papilla. Note numerous convolutions of external surface. Bulbous sensory receptor (BS), vesicular tegumental inclusions (VB), and mitochondria (M) are common in cytoplasm. (X 36,425)

Fig. 58. Marginal syntegument of ventral papilla containing numerous paracrystalline spines (SP), dense tegumental inclusions (DB), and mitochondria (M). Internally, syntegument is limited by basal lamina (B) and fibrous interstitial tissue (F). Cytoplasmic projections (CE) of pyriform cells extend into syntegument. (X 25,800)

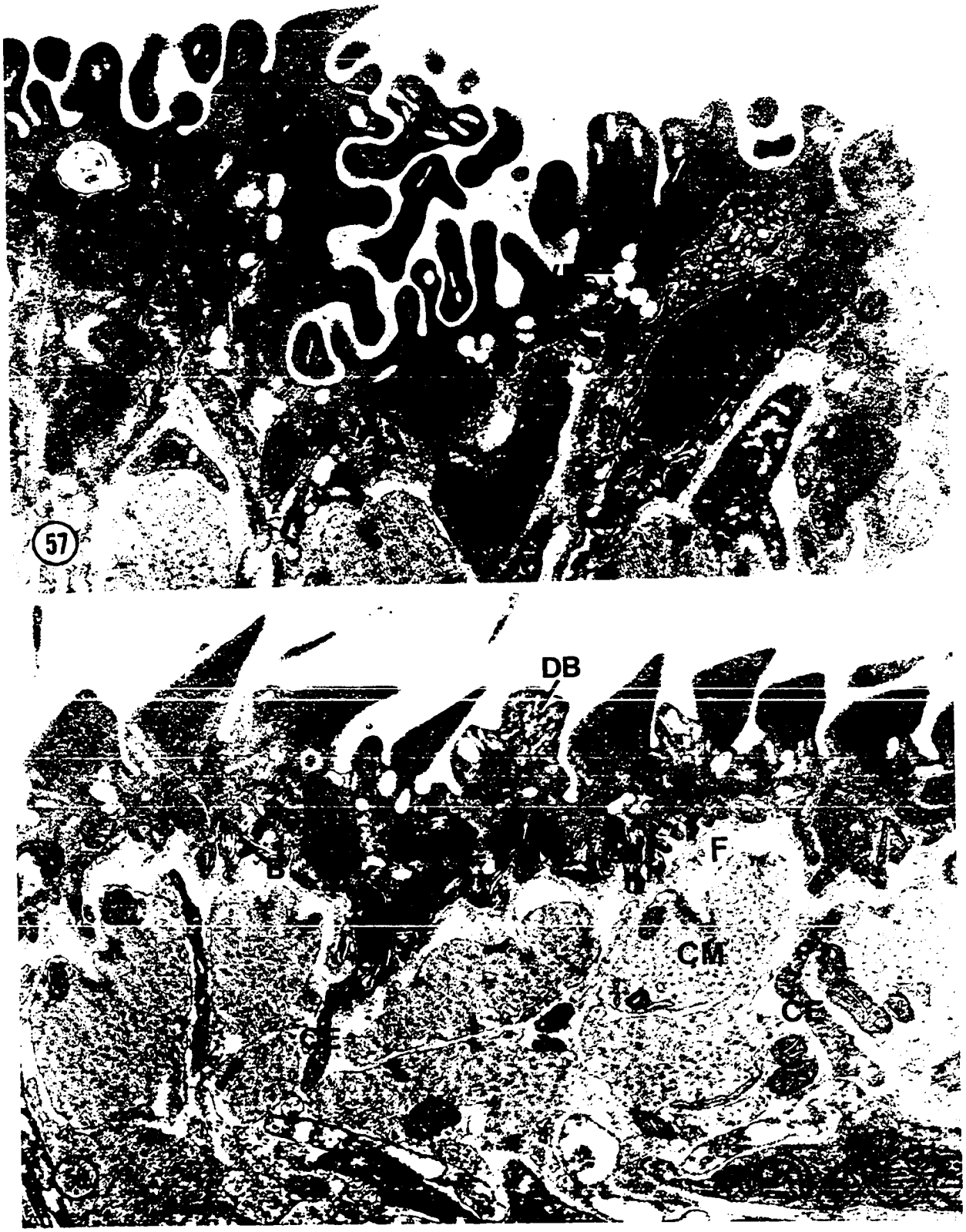
57
DB
F
CM

Plate XIV

Fig. 59. Pyriform cell of ventral papilla. Note numerous large mitochondria (M) with extensive cristae (CR), sparse granular endoplasmic reticulum (ER), and elongate nucleus (N). (X 34,400)


CH
ER
P

Plate XV

Fig. 60. Cytoplasm of pyriform cell. Cytoplasmic elements include large mitochondria (M), small amount of endoplasmic reticulum (ER), and large osmiophilic inclusions (I). (X 33,000)

Fig. 61. Cytoplasm of pyriform cell. Note well-developed cristae (CR) within mitochondria. Peripheral cytoplasm contains long cytoplasmic rods (RC). (X 34,000)

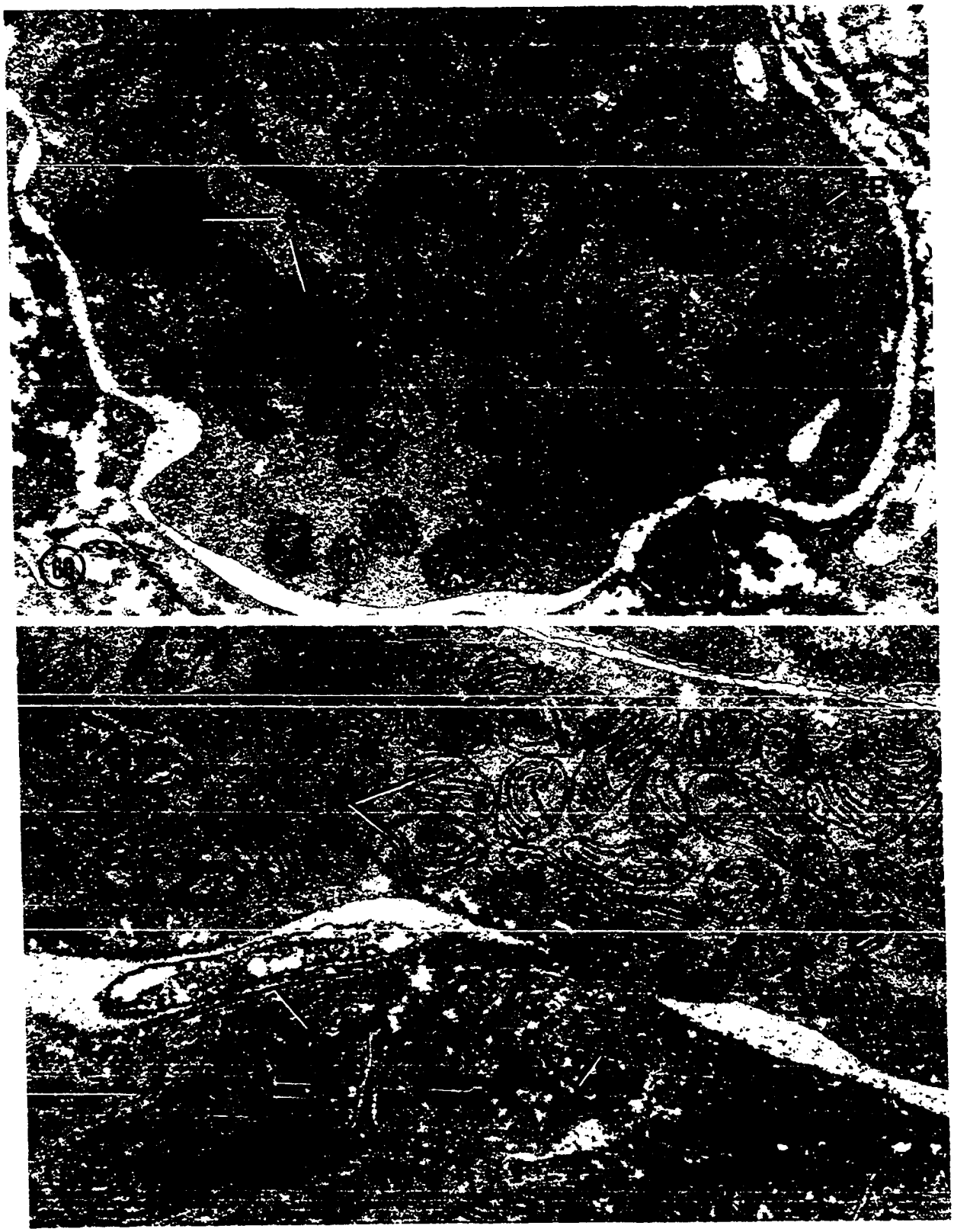

Plate XVI

Fig. 62. Pyriform cell associated with osmoregulatory duct (OD). Note junctional complexes (J) connecting adjacent pyriform cells and pyriform cells to osmoregulatory ducts. Extensive fibrous interstitial tissue (F) surrounds osmoregulatory duct. (X 21,500)

Fig. 63. Osmoregulatory duct. Cytoplasm contains free ribosomes (R), mitochondria (M), and numerous lamellae (LA) along lumenal surface. Junctional complexes (J) connect osmoregulatory duct with pyriform cell. (X 41,200)

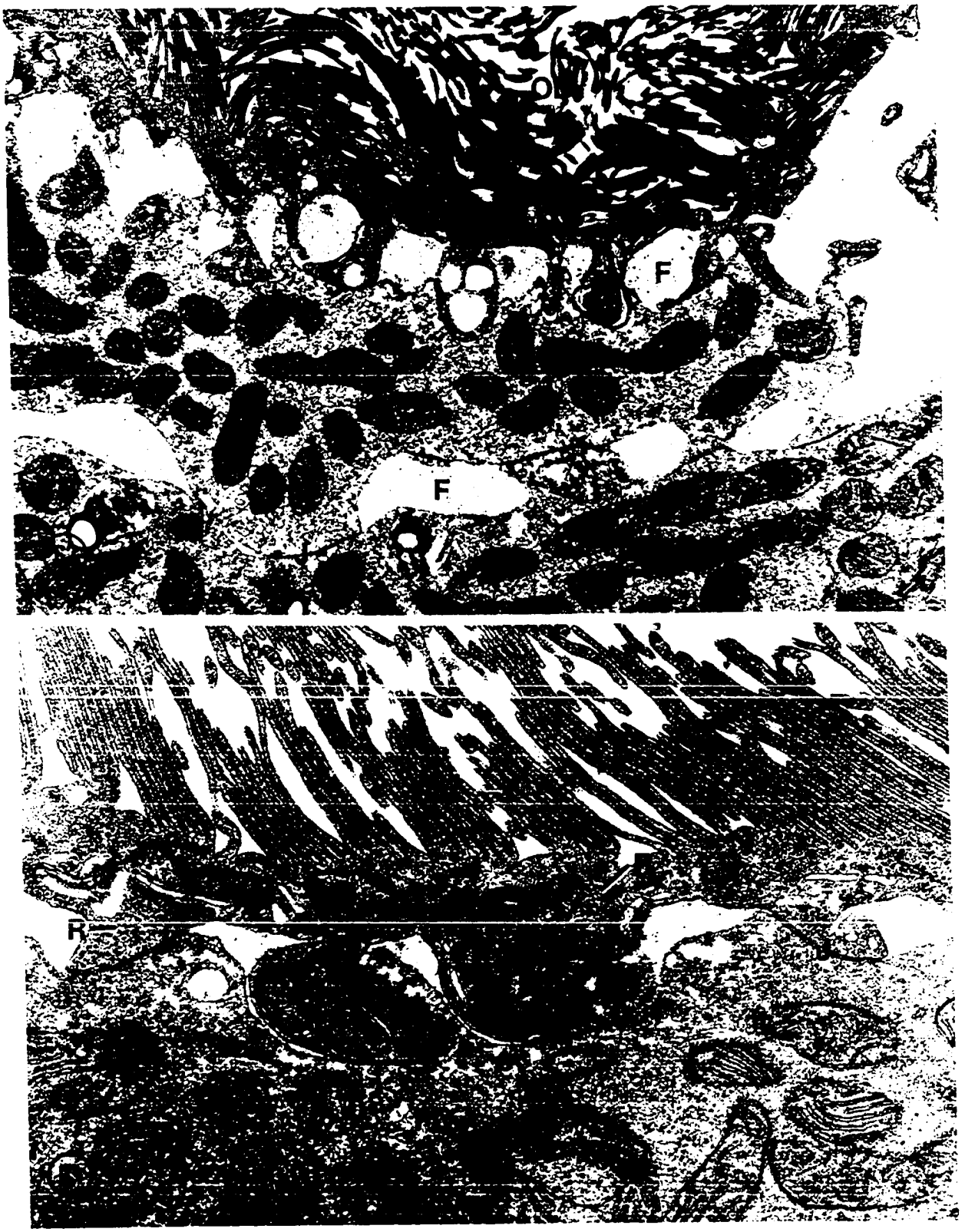
F
F
R

Plate XVII

Figs. 64-67. Osmoregulatory ducts of Q. quinqueserialis.

Fig. 64. Epithelial cells separated by septate desmosome (D). (X 27,250)

Fig. 65. Nucleus (N) of epithelial cell. Note distension of cytoplasmic layer to accommodate large nucleus. (X 13,900)

Fig. 66. Lamellae of osmoregulatory duct. These (LA) often occur in stacks. Note junctional complex (J) between duct and parenchyma. (X 64,000)

Fig. 67. Cytoplasm of epithelial cell containing Golgi complex (G) and group of mitochondria (M). (X 48,000)

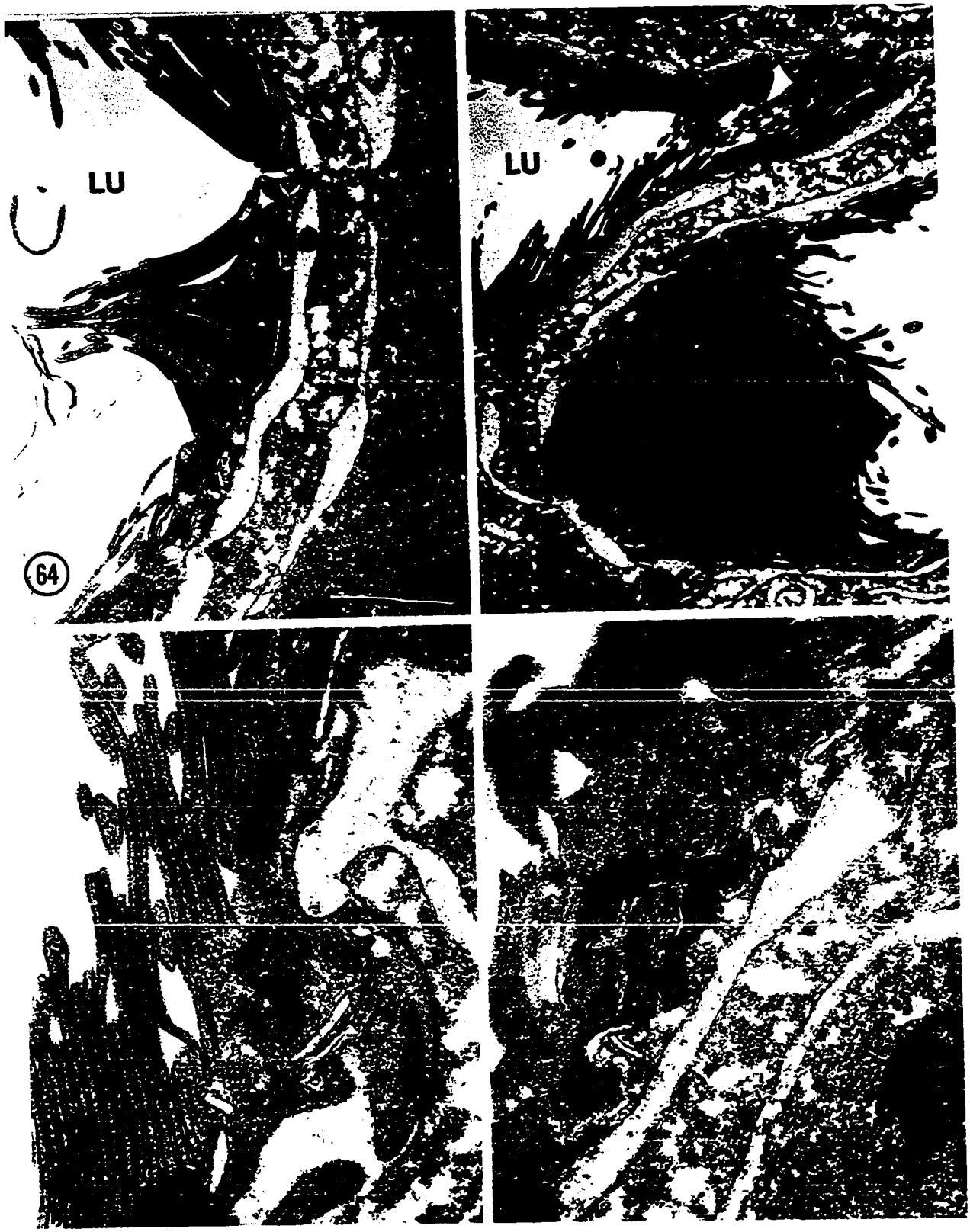
LU
LU
64

Plate XVIII

Figs. 68-72. Musculature of Q. quinqueserialis.

Fig. 68. Tegumental musculature. Bands of circular muscle (CM) and a thick layer of longitudinal muscle (LM) lie within fibrous interstitial tissue (F) below syntegument. (X 16,500)

Fig. 69. Circular muscle of seminal vesicle. Each myofiber is enclosed by sarcolemma (SL). Mitochondria (M) containing a single crista lie in periphery of myofiber. Desmosomes (D) attach sarcolemma to myofilaments. (X 38,300)

Fig. 70. Components of myofiber include numerous thick (TK) and thin (TN) myofilaments. Note sac-like cisternae of sarcoplasmic reticulum (SR) near sarcolemma. (X 48,325)

Fig. 71. Dense patches or bodies (DP) are scattered throughout sarcoplasm. (X 56,900)

Fig. 72. Groups of microtubules (MT), oriented parallel to myofilaments, lie in periphery of myofiber. (X 38,300)

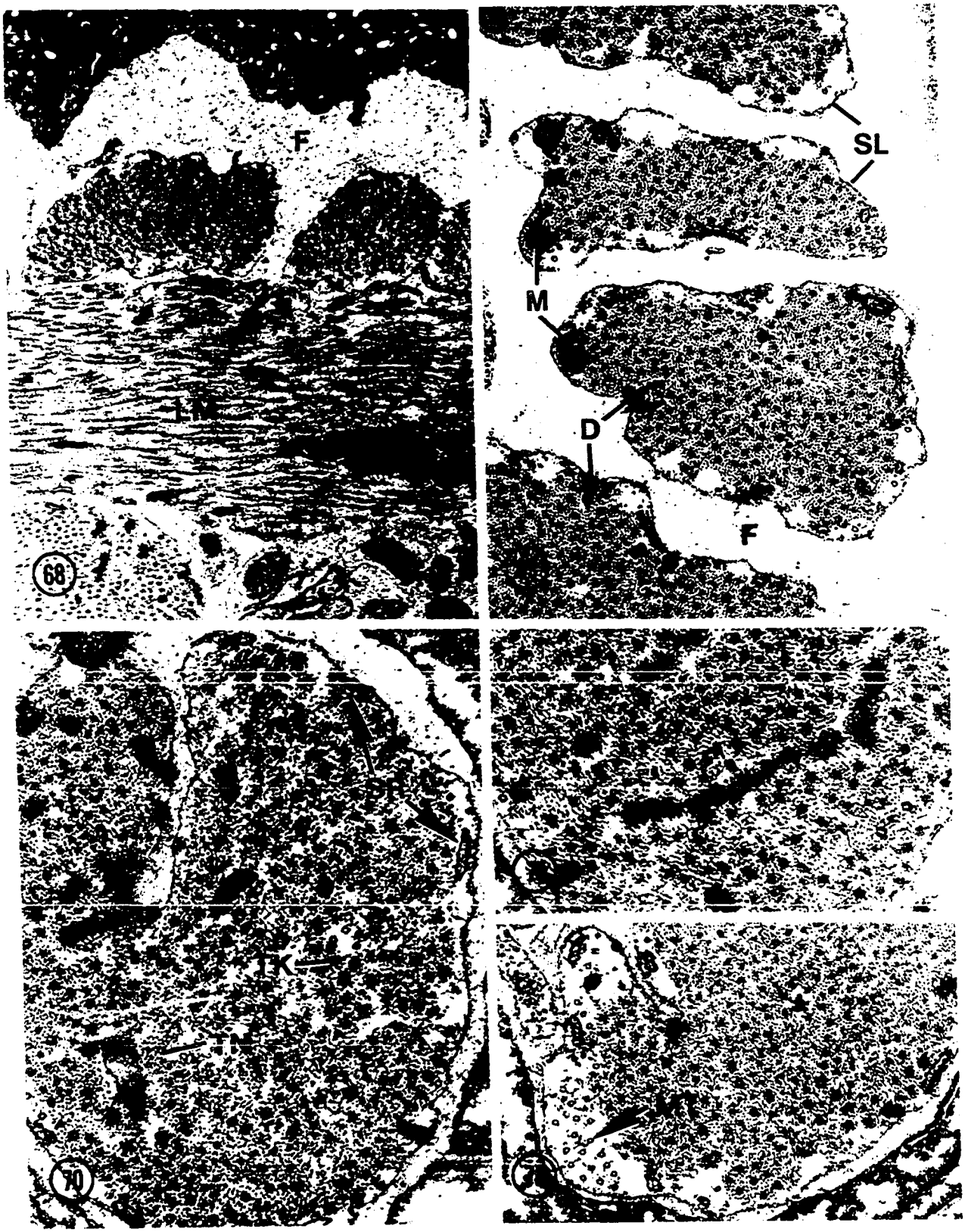
F
LM
68
SL
M
D
F
TK
TN
70

Plate XIX

Fig. 73. Longitudinal section of muscle. Aggregations of microtubules (MT) lie perpendicular to myofilaments. Fibrous interstitial tissue (F) separates individual myofibers. (X 58,000)


SMLT.

Plate XX

Fig. 74. Type A parenchymal cell. Note large nucleus (N) containing distinct nucleolus (NU). Cytoplasmic elements include Golgi complexes (G), mitochondria (M), and granular endoplasmic reticulum (ER). (X 20,200)

Fig. 75. Type A parenchymal cell. Elongate nucleus (N) contains large amounts of heterochromatin (H). Golgi complex consists of elongate saccules (GS) and ovoid vesicles (GV). Quantity of fibrous interstitial tissue (F) lies near Golgi. There is no evidence of membrane between cytoplasm and fibrous tissue (arrow). (X 35,200)

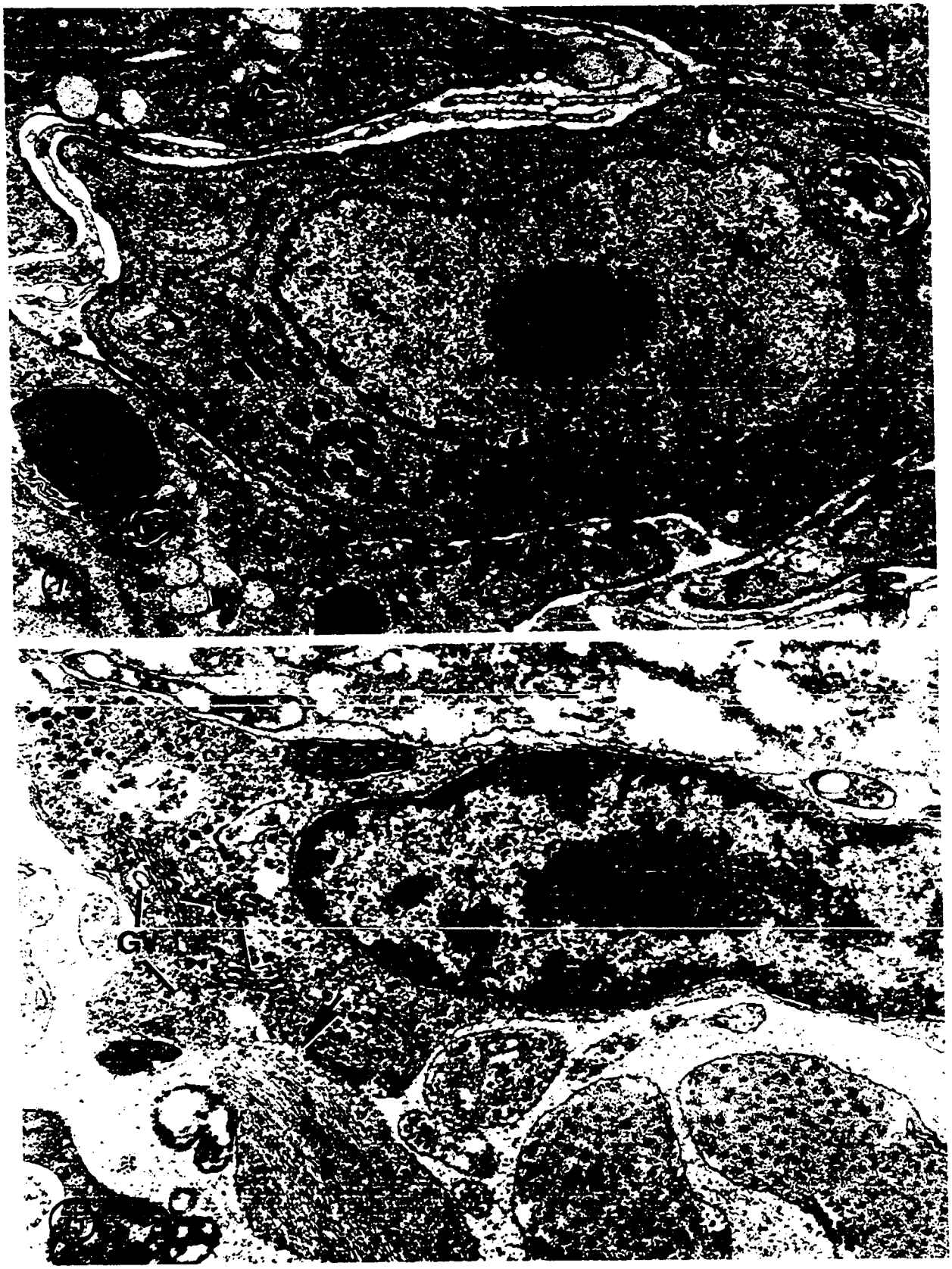
G

Plate XXI

Figs. 76-80. Type A parenchymal cells of Q. quinqueserialis.

Fig. 76. Lipid inclusion (L) and associated membranous whorl (MW). Numerous free ribosomes (R) and granular endoplasmic reticulum (ER) lie in surrounding cytoplasm. (X 32,200)

Fig. 77. Junctional complexes (J) attach adjacent parenchymal cells. (X 77,400)

Fig. 78. Paracrystalline inclusion (PI) lies in perinuclear cytoplasm. (X 42,600)

Fig. 79. High magnification of paracrystalline inclusion. Hexagonal, electron-dense granules appear in honeycomb-like pattern. Note absence of enclosing membrane. (X 71,700)

Fig. 80. Sagittal section of paracrystalline inclusion. Note wavelike pattern of parallel, electron-lucid lines. (X 29,250)

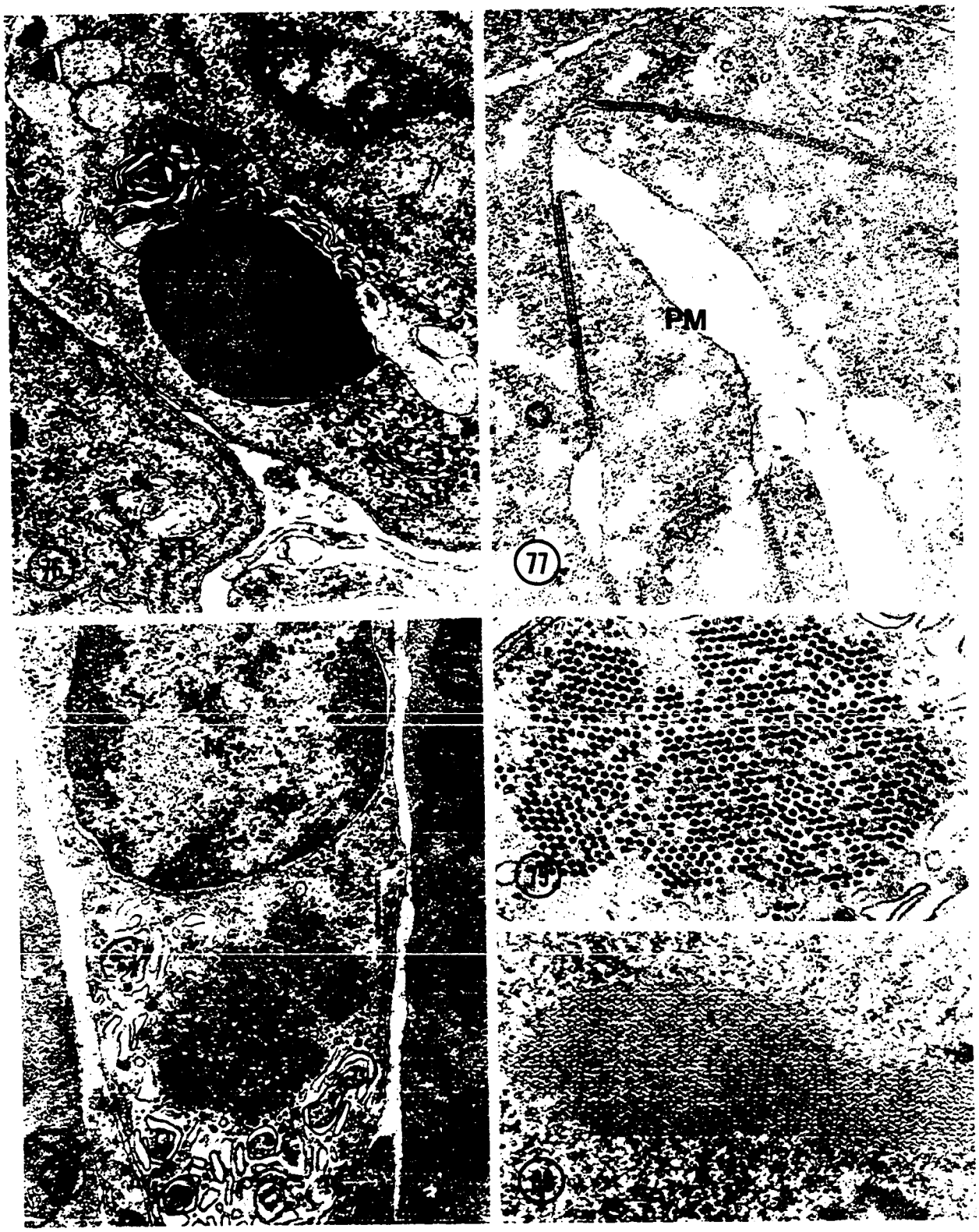
PM
77

Plate XXII

Fig. 81. Type B parenchymal cell. Note large, circular nucleus (N) lying in cell center. Golgi complexes (G), smooth endoplasmic reticulum (ER), and lakes of granular endoplasmic reticulum (EL) occur in cytoplasm. (X 13,625)

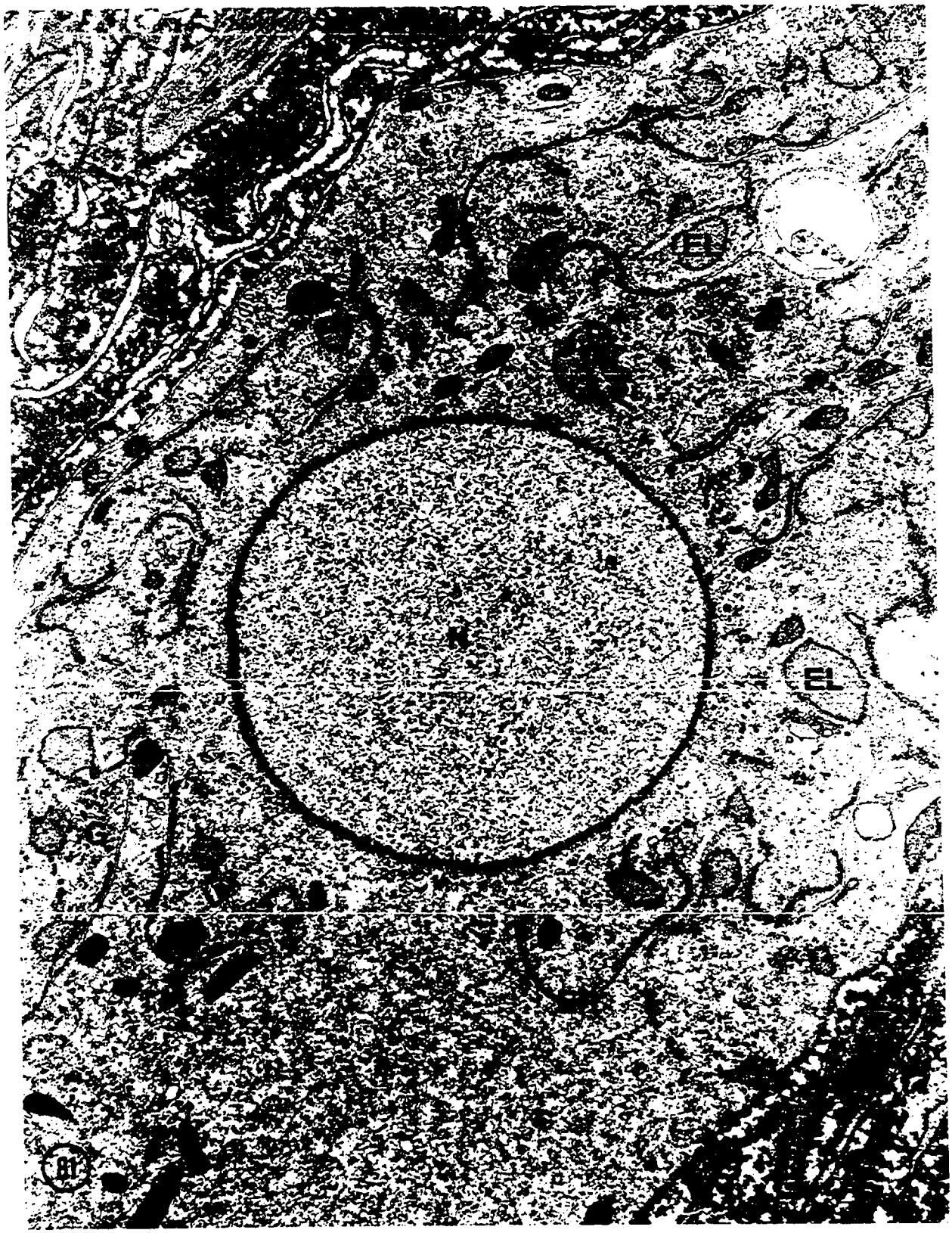
EL
EL
M

Plate XXIII

Figs. 82-84. Type B parenchymal cells of Q. quinqueserialis.

Fig. 82. Nucleus (N) containing distinct nucleolus (NU). Note numerous endoplasmic lakes (EL) lying in perinuclear cytoplasm. (X 13,300)

Fig. 83. Golgi complexes (G) consist of numerous ovoid vesicles. (X 18,400)

Fig. 84. Cytoplasm of type B cell. Note large lakes of endoplasmic reticulum (EL), numerous free ribosomes (R), and few mitochondria (M). Cytoplasmic ground substance appears to be extracted in many areas. (X 39,500)

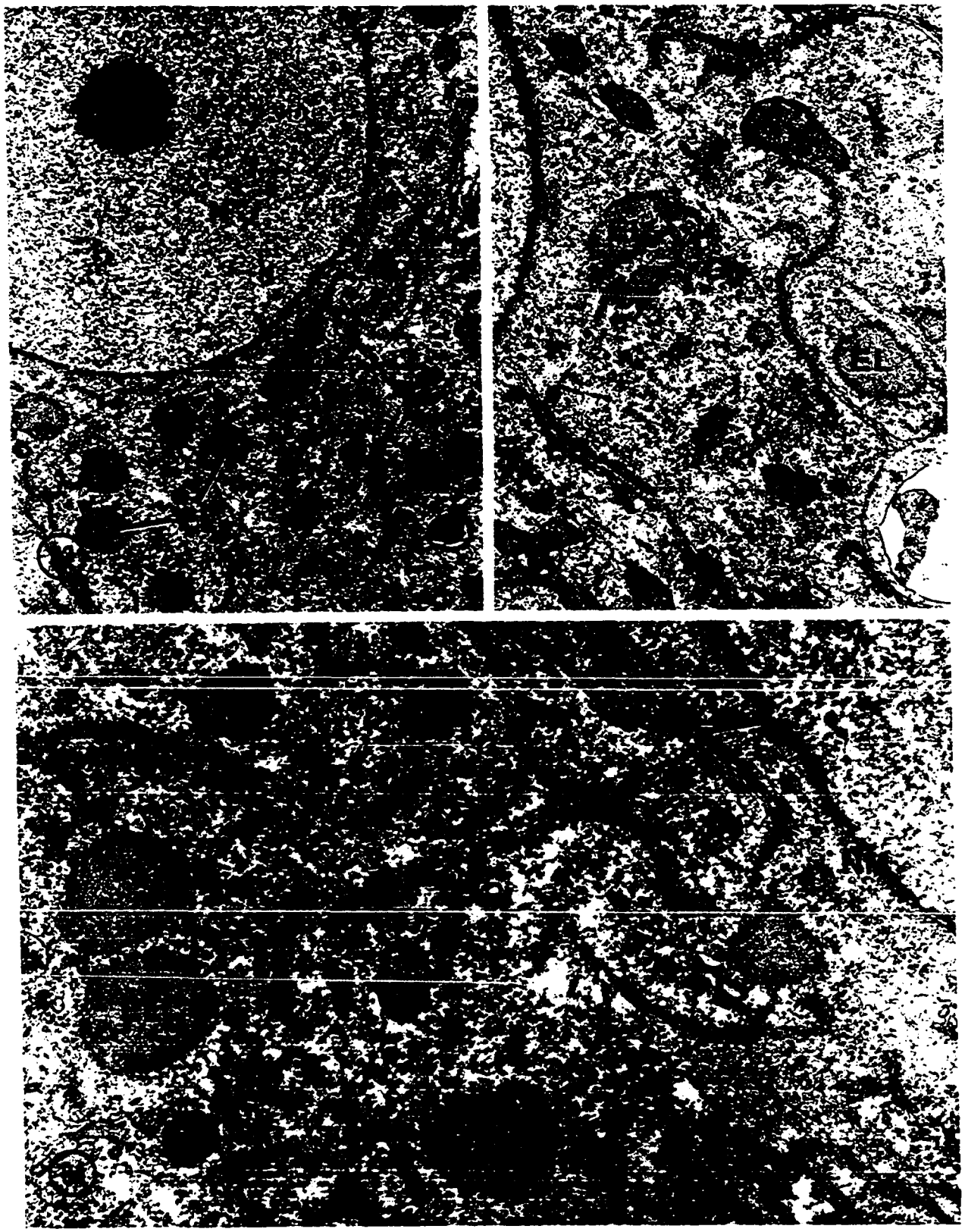

Plate XXIV

Fig. 85. Caecum of Q. quinqueserialis. Numerous microvilli (MV) extend from lumenal surface of gastrodermis (GD). Occasional muscle bands (MU) and thick layer of fibrous interstitital tissue (F) surround gastrodermis. (X 12,800)

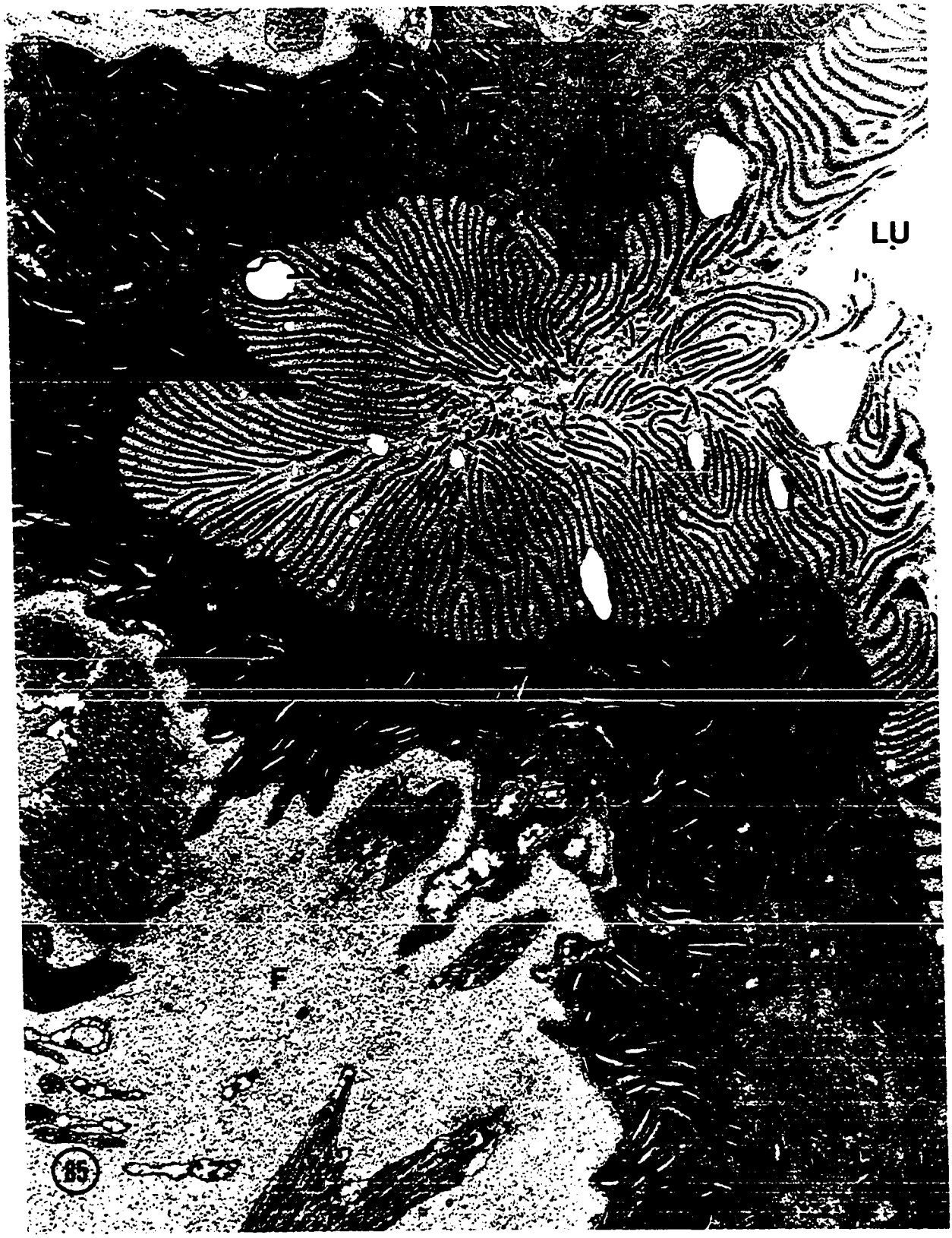
LU
F
85

Plate XXV

Figs. 86-89. Caecum of Q. quinqueserialis.

Fig. 86. Lipid inclusions (L) lying in gastrodermis. (X 12,000)

Fig. 87. Basal gastrodermis. Cytoplasm contains mitochondria (M) and granular endoplasmic reticulum (ER). Note thick basal lamina (B) and lamellar structures (LA) which may represent infoldings of basal membrane. (X 22,500)

Fig. 88. Microvilli (MV) extending into gastrodermal lumen. Note superficial vacuoles (VA) lying between microvilli. (X 18,600)

Fig. 89. Cytoplasm of gastrodermis. Note large desmosome (D) separating adjacent cells and thick particulate coating or glycocalyx (GC) associated with microvilli. Mitochondria (M) lacking cristae and Golgi complexes (G) occur in this region. Junctional complexes (J) form connections with adjacent parenchymal cells. (X 44,000)

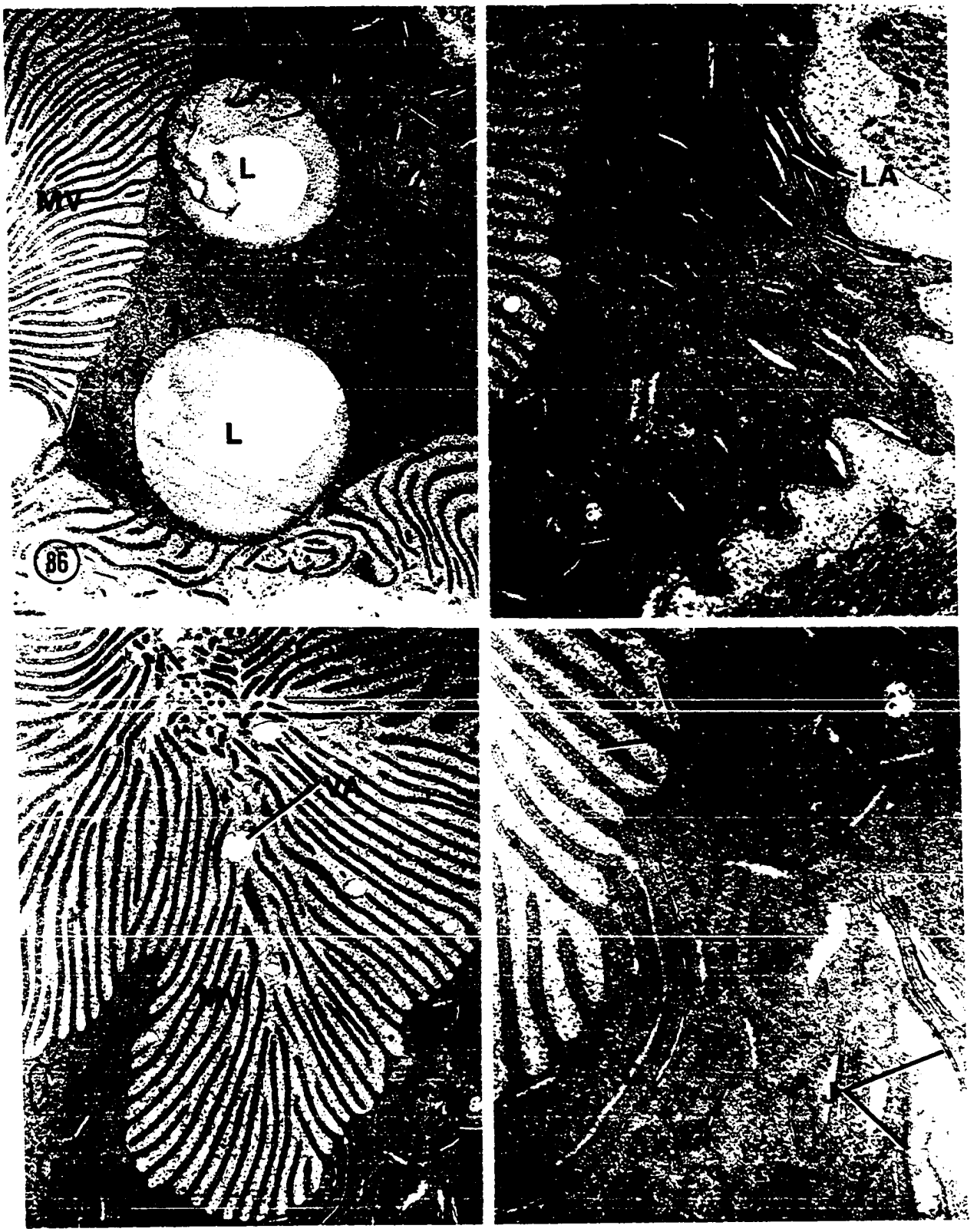
MV
L
L
86
LA

Plate XXVI

Fig. 90. Ovary of Q. quinqueserialis contains numerous gonial cells (GN). Ovarian wall is formed by basal lamina (B) and supported by occasional muscle bands (MU). (X 12,500)

Fig. 91. Gonial cell nucleus (N). Note distinct nucleolus (NU) and scattered patches of heterochromatin (H). Numerous mitochondria (M) lie in perinuclear cytoplasm. (X 15,500)

Fig. 92. Gonial cell cytoplasm. Note cortical granules (CG), mitochondria (M), and endoplasmic reticulum (ER). Narrow perinuclear spaces (PS) are associated with nuclear membrane (NM). (X 40,200)

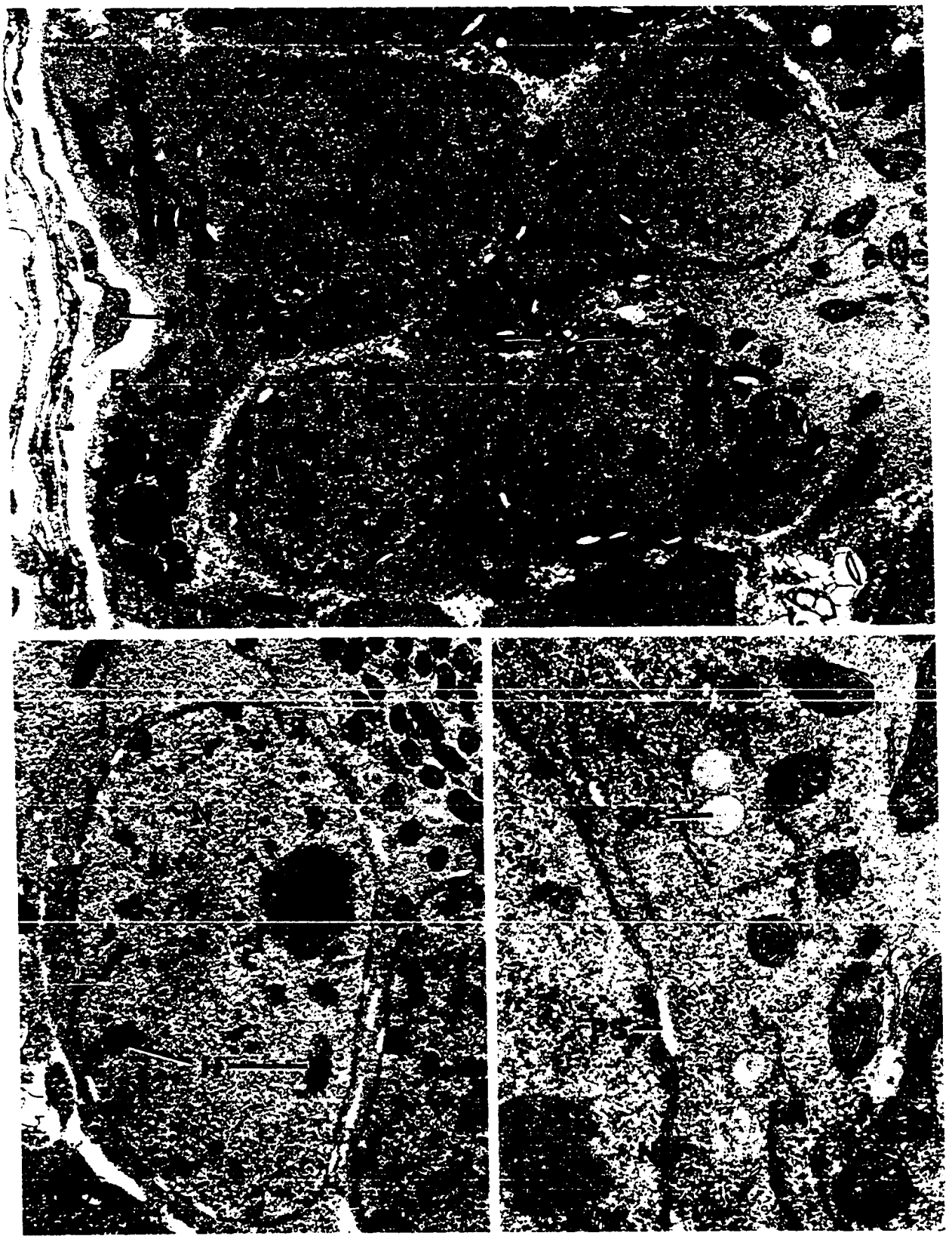

Plate XXVII

Figs. 93-96. Mehlis' gland of *Q. quinqueserialis*.

Fig. 93. DB-cell containing numerous dense secretory granules (SG). (X 23,650)

Fig. 94. MB-cell nucleus (N) containing large nucleolus (NU). Note Golgi complexes (G) and mitochondria (M) lying in perinuclear cytoplasm. (X 13,000)

Fig. 95. Perinuclear cytoplasm of MB-cell. Note large vacuoles containing membranous secretory bodies (MS). Golgi complexes (G) and endoplasmic reticulum (ER) are closely associated with secretory bodies. Paracrystalline inclusion (PI) occurs within nucleus. (X 24,000)

Fig. 96. Membranous secretory bodies (MS). Note thin cisternae of endoplasmic reticulum (ER) near nuclear membrane (NM). (X 20,000)

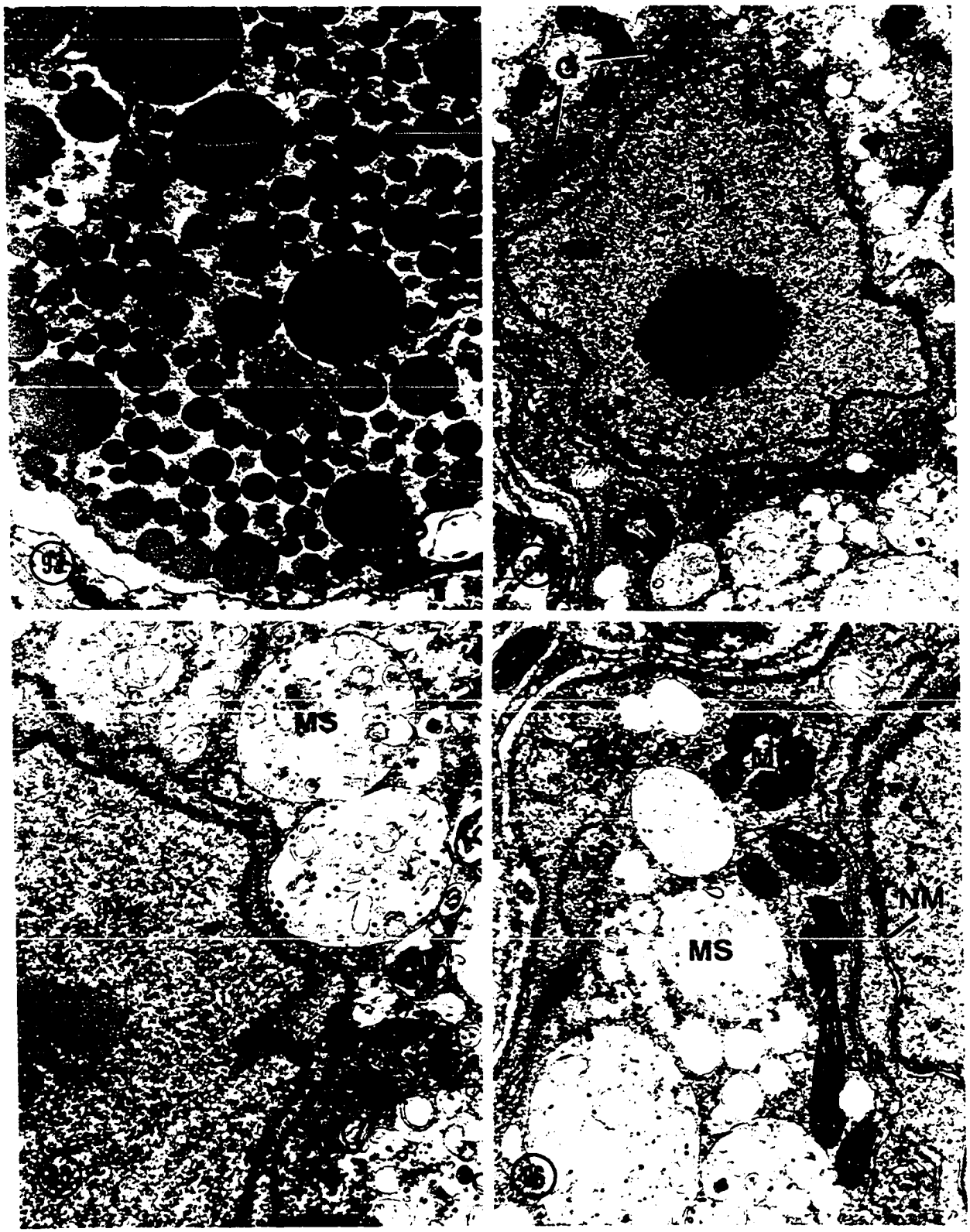
MS
M
NM
MS

Plate XXVIII

Figs. 97-99. Vitellaria of *Q. quinqueserialis*.

Fig. 97. Immature (stage 1) vitelline cell. Cytoplasm contains numerous free ribosomes (R) and sparse endoplasmic reticulum (ER). Note extensive chromatin material in nucleus (N). (X 23,150)

Fig. 98. Nurse cell. Note large nucleus (N) and cytoplasmic extension (CE) between vitelline cells. (X 23,800)

Fig. 99. Cytoplasm of stage 2 vitelline cells. Note extensive granular endoplasmic reticulum (ER), free ribosomes (R), and small globules of shell protein (PG). Large yolk droplets (Y) occur commonly in these cells. (X 38,400)

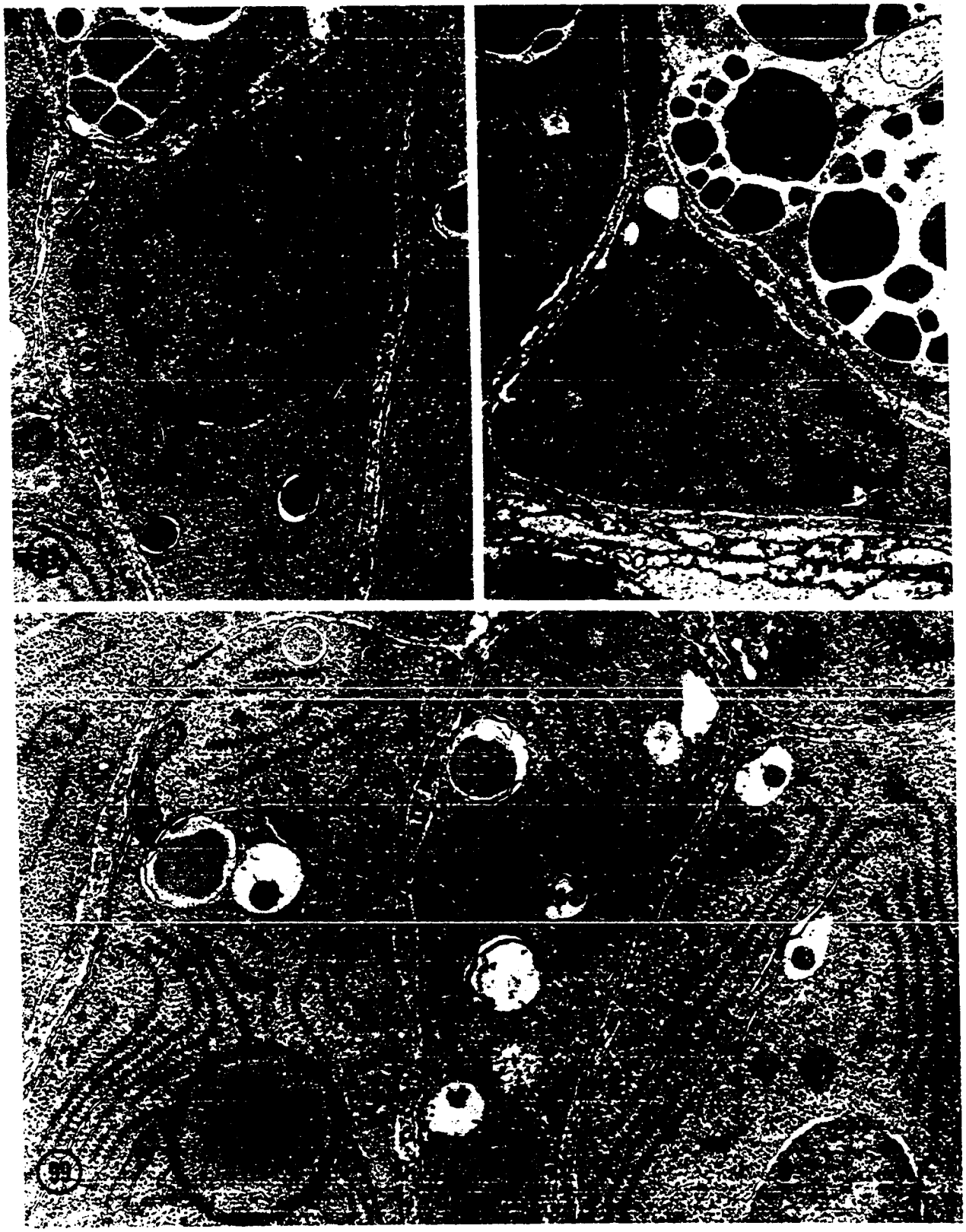

Plate XXIX

Figs. 100-101. Vitellaria of Q. quinqueserialis.

Fig. 100. Stage 3 vitelline cell. Note aggregation of protein globules (PG). Cytoplasm contains numerous ribosomes (R) and an extensive endoplasmic reticulum (ER). (X 21,000)

Fig. 101. Granular endoplasmic reticulum (ER) of stage 3 cell. Note parallel arrangement around nucleus. (X 44,000)

Fig. 102. Mature (stage 4) vitelline cell. Note large clusters of protein globules (PG). Cytoplasm containing endoplasmic reticulum (ER) is displaced to periphery of cell. (X 26,250)

Fig. 103. Cytoplasm of mature (stage 4) vitelline cell. Small amounts of glycogen (GY) occur near clusters of protein globules (PG). Note displacement of endoplasmic reticulum (ER) to cell periphery. (X 29,000)

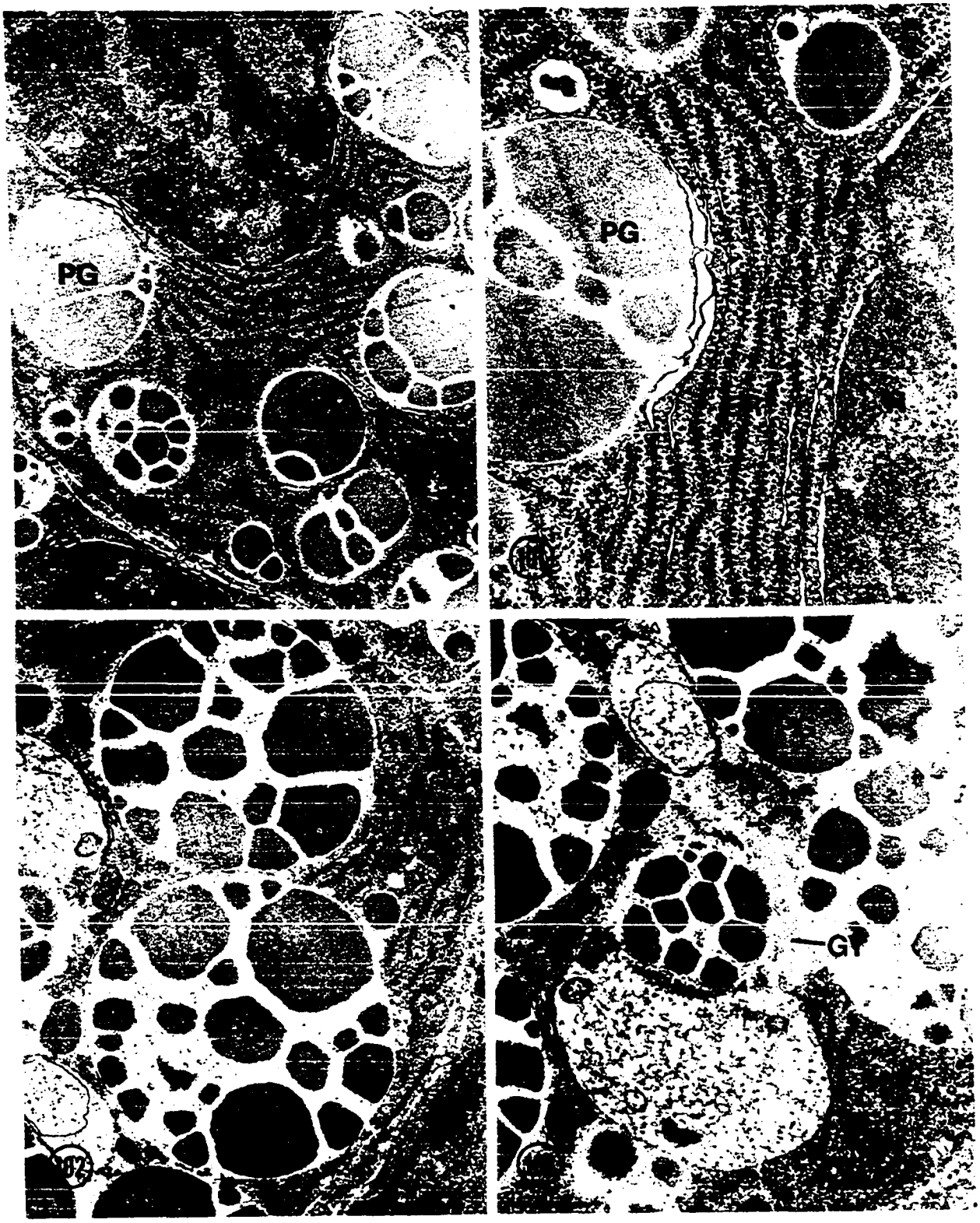
PG
PG
GT

Plate XXX

Fig. 104. Uterus of Q. quinqueserialis. Uterine wall is formed by thin epithelium. Note elongate nucleus (N) of epithelial cell. Parenchymal cell (PA) is interspersed between adjacent uterine walls. (X 13,500)

Fig. 105. Epithelium of uterus. Cytoplasmic components include extensive system of granular endoplasmic reticulum (ER) and numerous Golgi complexes (G). Large electron-dense secretory granules (SG) lie in uterine lumen. (X 21,500)

Plate XXXI

Figs. 106-109. Uterine epithelium of Q. quinqueserialis.

Fig. 106. Adjacent epithelial cells are separated by septate desmosome (D). Note filiform cytoplasmic extension (CE) projecting into lumen. (X 36,000)

Fig. 107. Infolding of epithelium. Granular endoplasmic reticulum (ER), free ribosomes (R), Golgi complexes (G), and mitochondria (M) occur in cytoplasm. Note basal lamina (B) and thin layer of muscle (MU) underlying basal membrane. Fibrous secretory material (FS) is found in lumen. (X 25,300)

Fig. 108. Mitochondria (M) in epithelium. Note also extensive endoplasmic reticulum (ER) and free ribosomes (R). (X 30,000)

Fig. 109. Infolding of epithelium. Note secretory granules (SG) lying within cytoplasm and in infolding. (X 21,700)

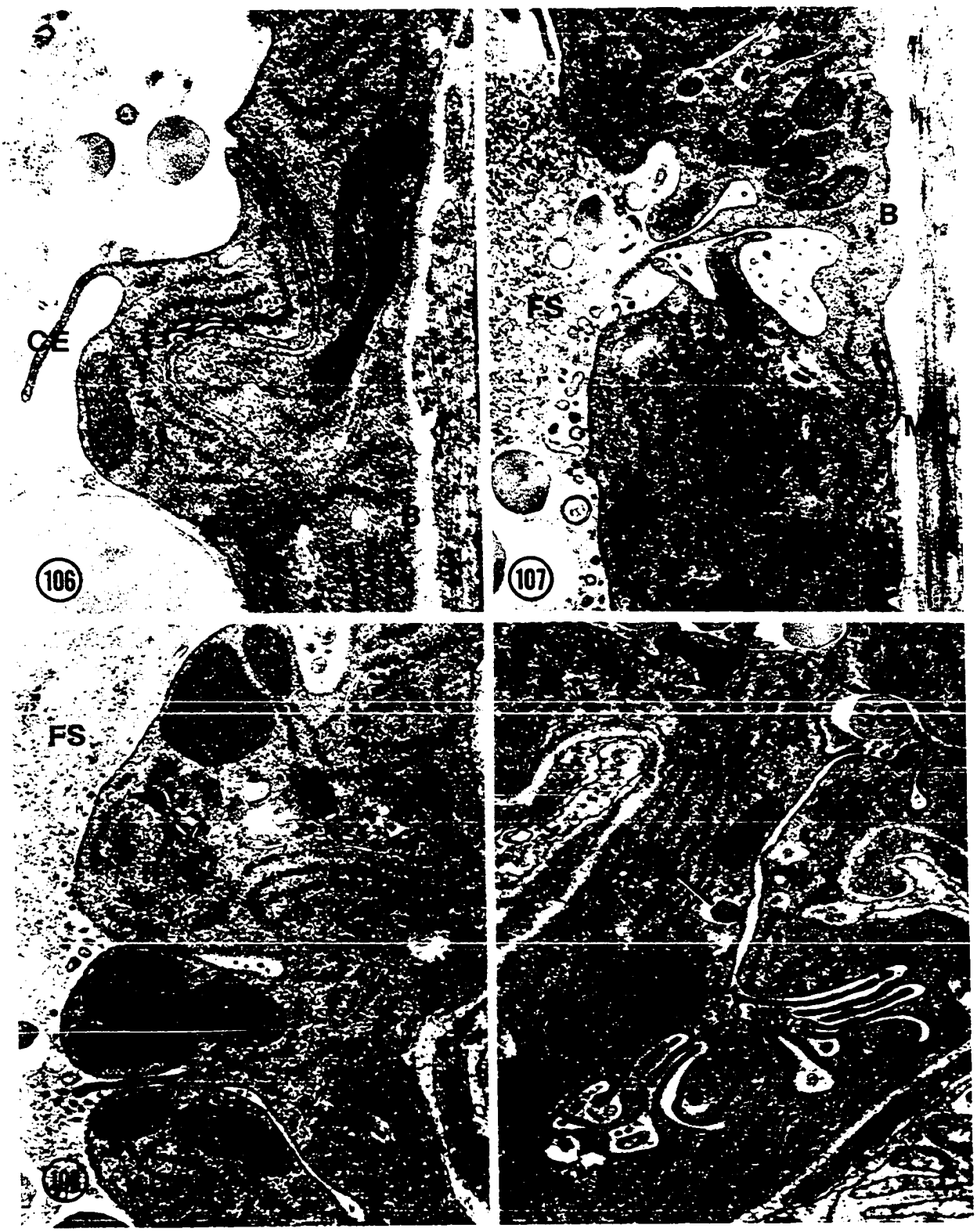
106
E
B
107
FS
B
FS

Plate XXXII

Figs. 110-113. Egg of *Quinqueserialis quinqueserialis*.

Fig. 110. Light micrograph of eggs. Note long bipolar filaments (EF) extending from egg capsule (EC). (X 350)

Fig. 111. Scanning micrograph of egg. Note sculpturing of egg capsule (EC) and smooth surface of filaments (EF). (X 3,250)

Fig. 112. High magnification scanning micrograph of egg capsule surface. Note numerous crater-like pits. (X 7,300)

Fig. 113. Transmission micrograph of egg capsule layers. Inner layer (IL) is thick and electron-dense. Outer layer (OL) appears reticulate. (X 50,000)

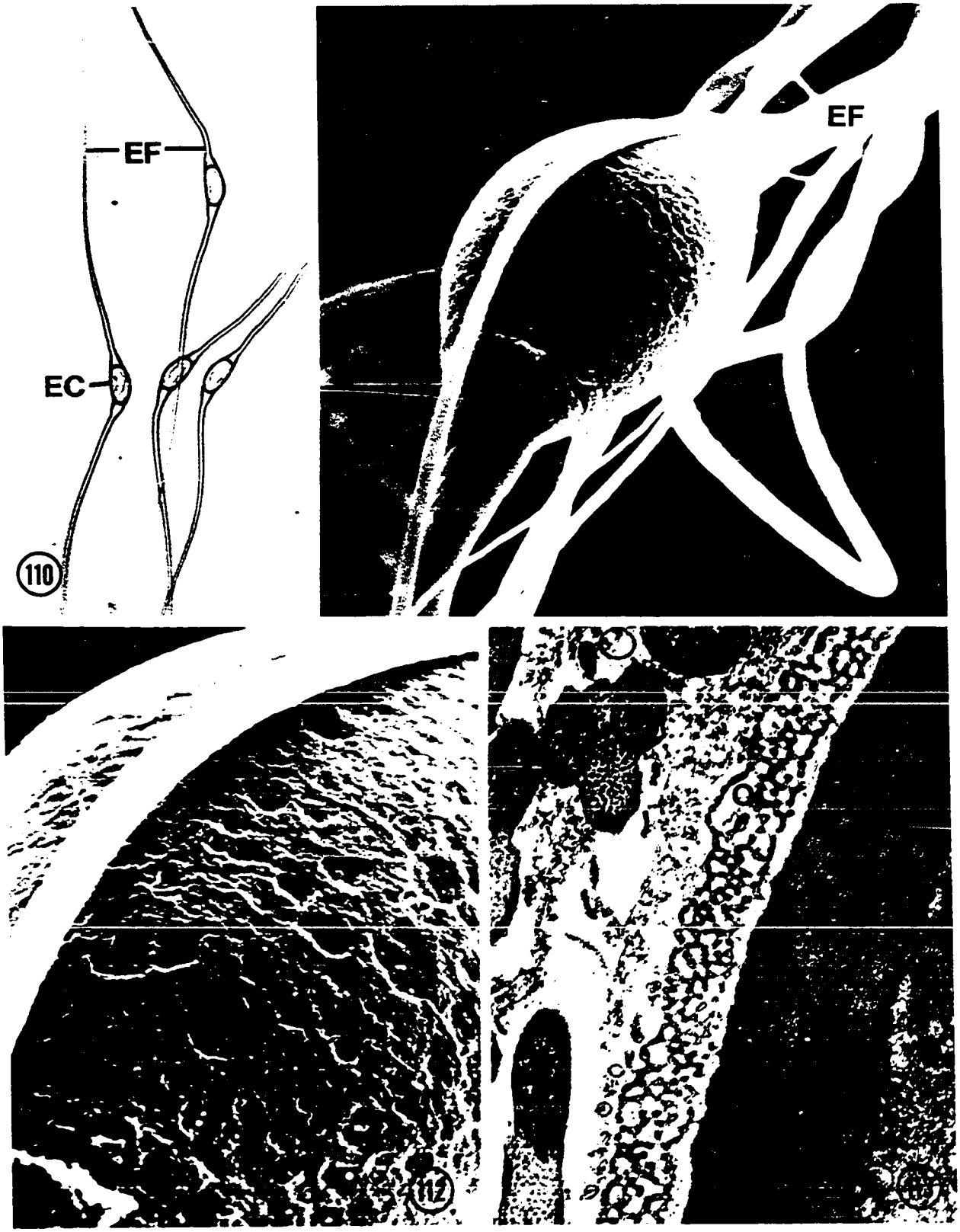
EF
EC
110
EF
112

Plate XXXIII

Fig. 114. Intrauterine egg. Note distinct outer (OL) and inner (IL) egg capsule layers. Developing embryo (miracidium) lies within capsule. Fertilization has occurred as evidenced by presence of nucleus of spermatozoan (S). Lying in uterine lumen are numerous spermatozoa. (X 24,000)


S
OL
FS
S
114

Plate XXXIV

Fig. 115. Spermatogonial cell in testis. Note large nucleus (N) and small amount of cytoplasm containing mitochondria (M) and Golgi complex (G). (X 11,300)

Fig. 116. Spermatogonial cell. Undifferentiated cytoplasm contains narrow cisternae of smooth endoplasmic reticulum (ER) and occasional mitochondria (M). Patches of heterochromatin (H) occur in nucleoplasm. (X 26,250)

Fig. 117. Spermatocyte. Note circular nucleus (N) containing scattered heterochromatin. Large volume of cytoplasm contains mitochondria (M), smooth endoplasmic reticulum (ER), Golgi complexes (G), and secretory vesicles (SG). (X 13,900)

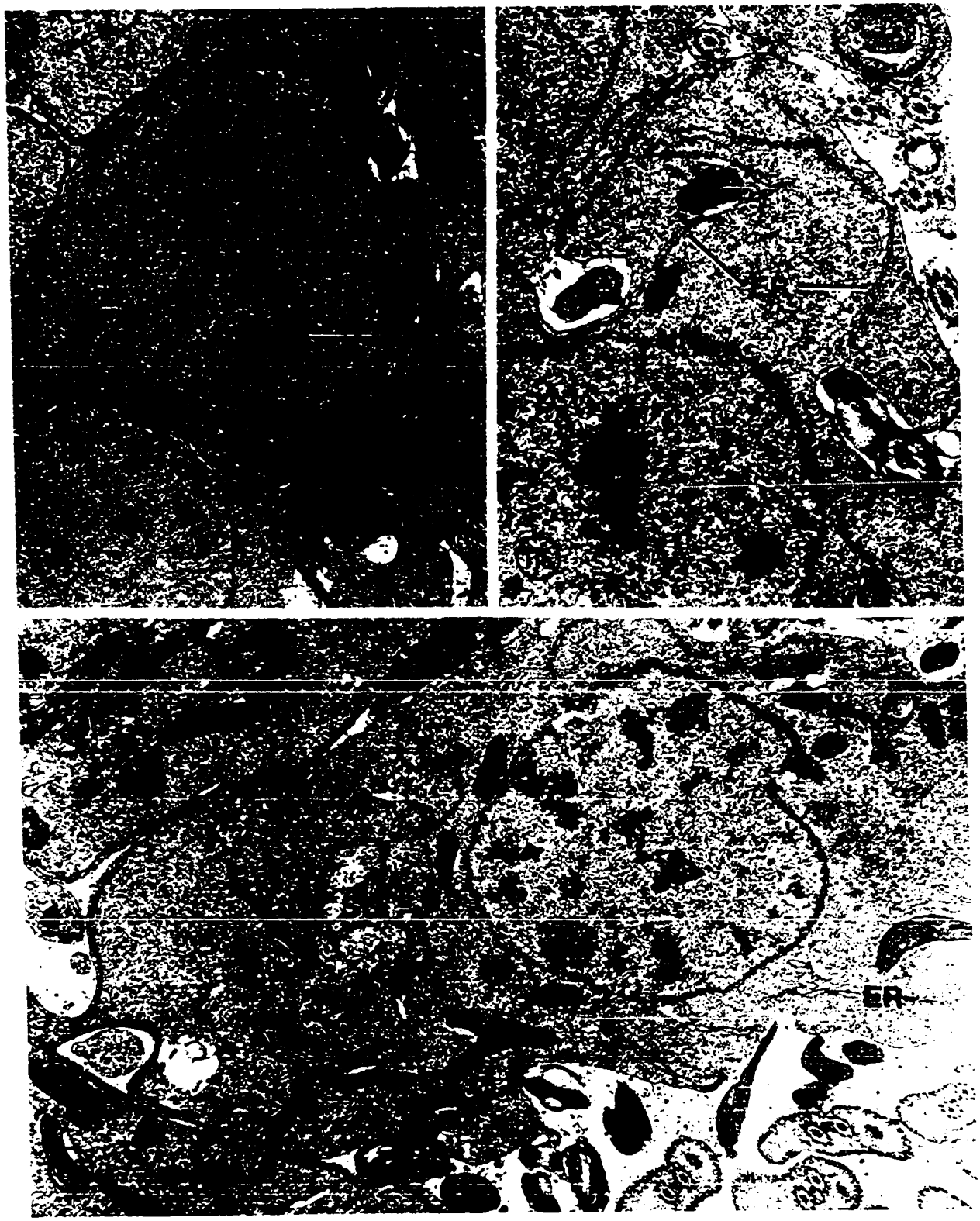
ER

Plate XXXV

Fig. 118. Cytophores (arrows) connect spermatocytes in rosette pattern. Note thin cisternae of endoplasmic reticulum (ER) lying within outer plasma membrane. Undifferentiated chromosomes (CH) occur in cytoplasm. (X 15,200)

Fig. 119. Early spermatid. Note elongate nucleus (N) coiled throughout cytoplasm. Chromatin material is condensed into thin strands. (X 23,300)

Fig. 120. Early spermatid. Golgi complex consists of numerous thin saccules (GS) and ovoid vesicles (GV). Note dense sheets of chromatin in nucleus (N). (X 40,800)

Fig. 121. Microtubule-organizing center (MTC) of early spermatid. Ciliary rootlets (RT) which eventually form axonemes lie on each side of MTC. Note peripheral position of nucleus (N). (X 31,100)

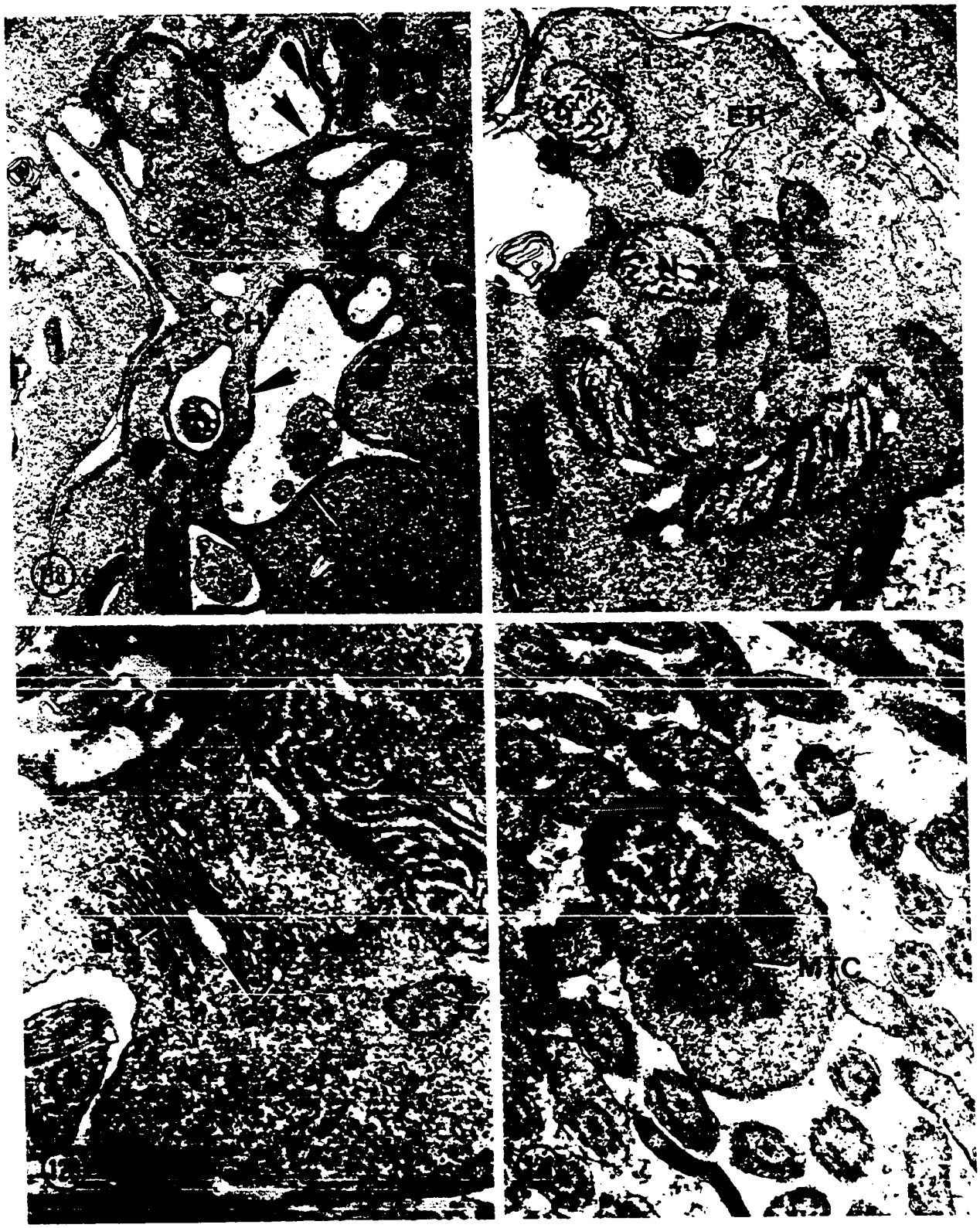
CH
ER
MTC

Plate XXXVI

Fig. 122. Early and late spermatids. Note smooth endoplasmic reticulum (ER) in cytoplasm of early spermatid. Numerous late spermatids are characterized by large, dense nuclei (N). (X 25,560)

Fig. 123. Cytoplasmic projections of developing spermatids include two axonemes separated by mid-piece (MP). Note 9+1 arrangement of axial units (AU) around central core (CC) in each axoneme. Cortical microtubules (MT) lie in single row along expanded ends of mid-piece. Eventually, these three projections will fuse to form mature spermatozoan. (X 54,000)

Fig. 124. Head region of late spermatid. Note two axonemes (A) separated by central nucleus (N). (X 62,500)

Fig. 125. Middle region of late spermatid. Nucleus is displaced by mitochondrial rod (M). Central region of axoneme consists of central core (CC) surrounded by cortical sheath (CSH). Spokes radiate outward from sheath and connect with axial units (AU). (X 46,000)

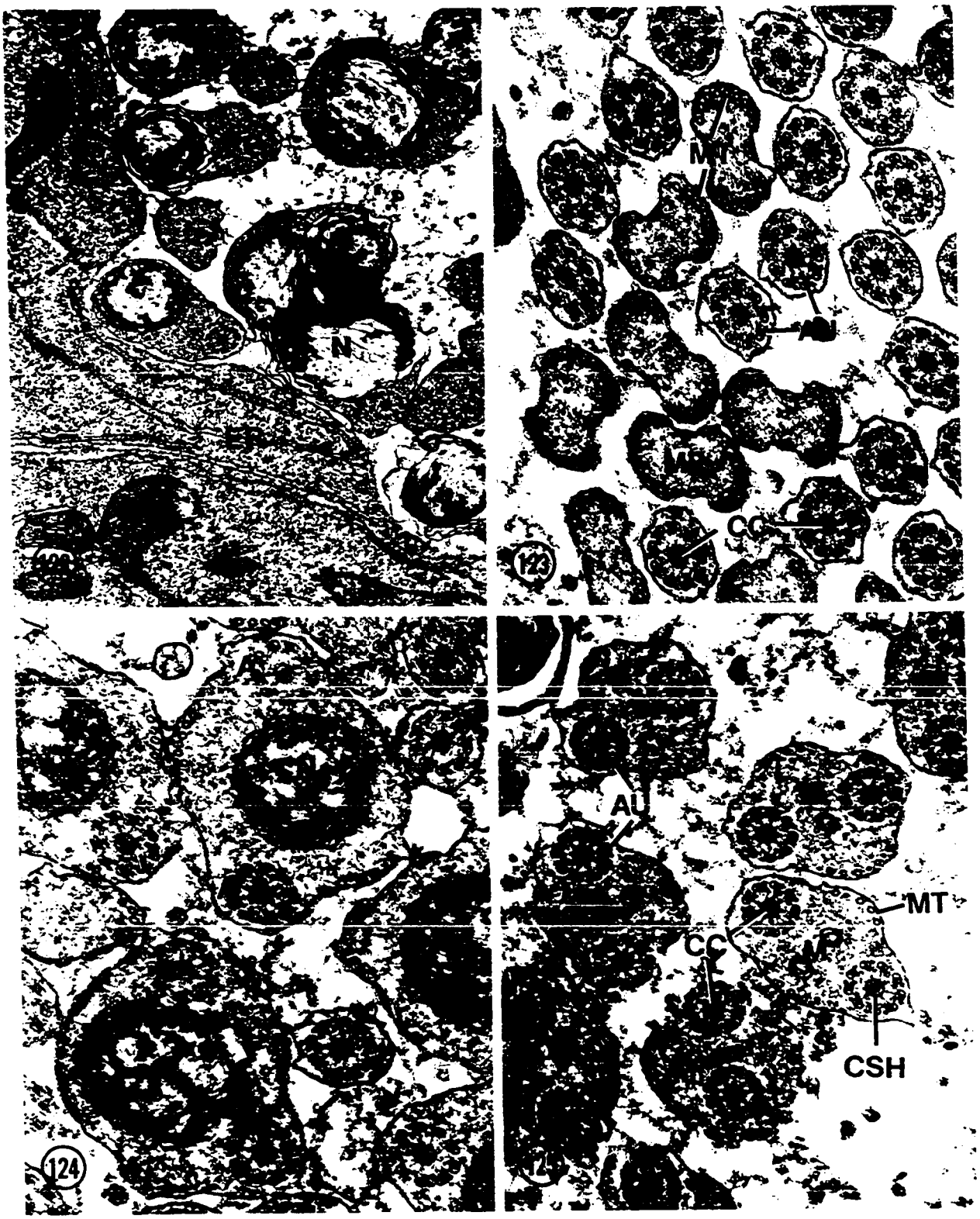
N
ER
MT
AU
MT
CC
123
AU
MT
CC
CSH
124

Plate XXXVII

Fig. 126. Late spermatid. Nucleus (N) has migrated from center of spermatid and replaced one axoneme. Mitochondrial rod (M) lies between single axoneme (A) and nucleus. (X 52,000)

Fig. 127. Head region of mature spermatozoan. Note single axoneme containing nine doublet axial units (AU) surrounding central core (CC). Nucleus (N) lies opposite axoneme. Cytoplasm contains central mitochondrial rod (M), glycogen (GY), and cortical microtubules (MT). (X 97,000)

Fig. 128. Middle region of mature spermatozoan. Nucleus (N) is displaced to center by second axoneme (A). Note large amount of glycogen (GY) in cytoplasm. (X 70,000)

Fig. 129. Tail region of mature spermatozoan. Two axonemes (A) are separated by cytoplasmic glycogen (GY). (X 60,000)

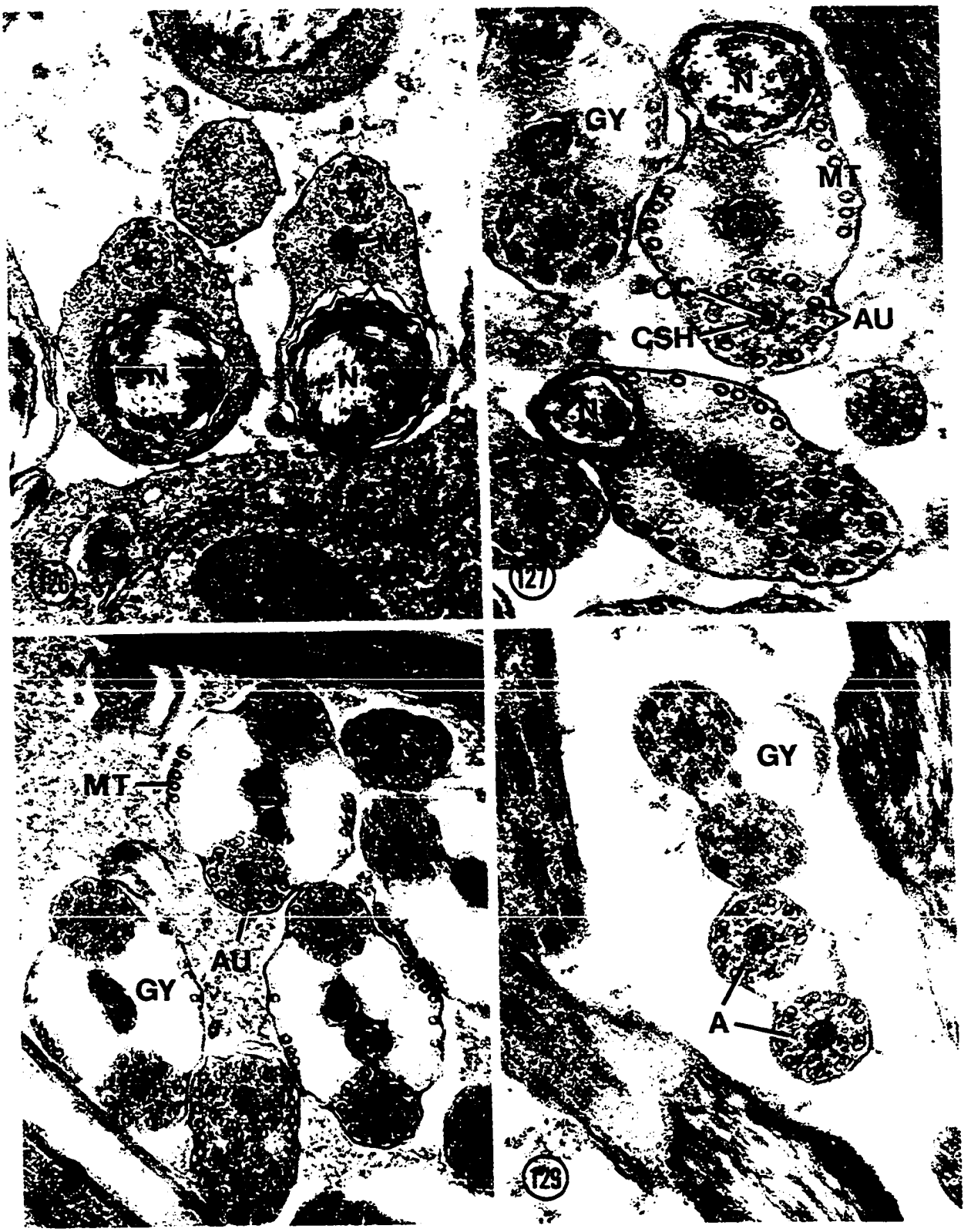
N
N
126
GY
N
MT
CC
AU
CSH
N
127
MT
GY
AU
GY
A
129

Plate XXXVIII

Fig. 130. Vas efferens. Wall is formed by thick epithelium. Numerous spermatozoa (S) lie in lumen. Epithelium is surrounded by fibrous interstitial tissue (F) and layer of circular muscle (CM). (X 11,100)

Fig. 131. Epithelium of vas efferens. Lumenal surface contains numerous cytoplasmic extensions (CE). Golgi complexes (G) and mitochondria (M) occur in cytoplasm. (X 20,000)

Fig. 132. Vas efferens containing spermatogonial cells which have migrated from testis. (X 8,600)

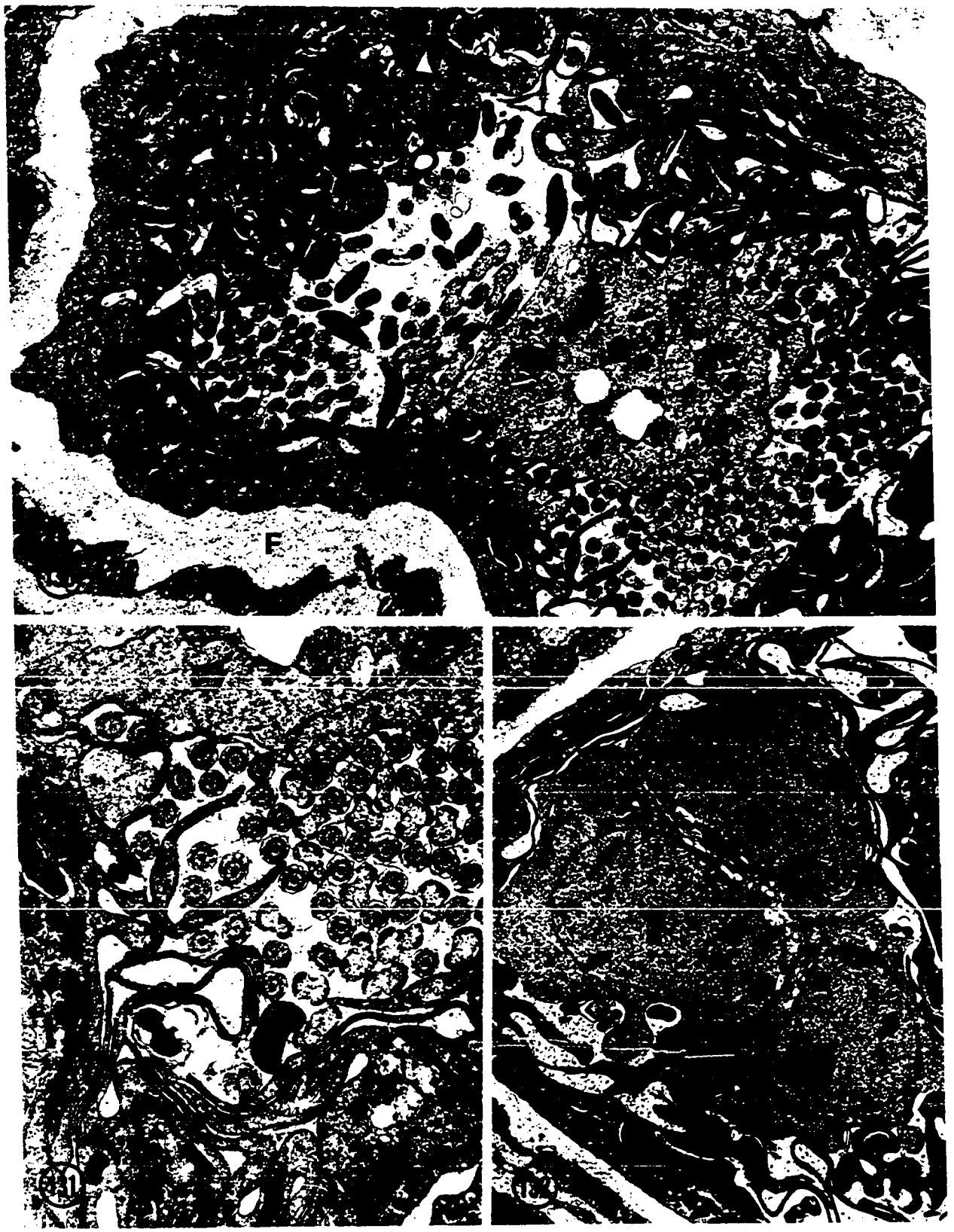
F

Plate XXXIX

Fig. 133. Survey micrograph of seminal vesicle. Wall of seminal vesicle (SV) is formed by thin epithelium. Numerous bands of circular muscle (CM) underlie epithelium. (X 5,000)

Fig. 134. Vas deferens. Epithelium contains mitochondria (M) and extensive granular endoplasmic reticulum (ER). Cytoplasmic layer is distended to accommodate irregular nucleus (N). Spermatozoa in lumen lie in fibrous secretory material (FS). (X 15,300)

Fig. 135. Epithelium of seminal vesicle. Cytoplasm contains extensive system of granular endoplasmic reticulum (ER), mitochondria (M), and Golgi complex (G). (X 35,500)

Fig. 136. Epithelium of seminal vesicle. Septate desmosome (D) separates individual cells. Lumenal surface consists of cytoplasmic extensions (CE) projecting into lumen and often surrounding spermatozoa (S). (X 49,000)

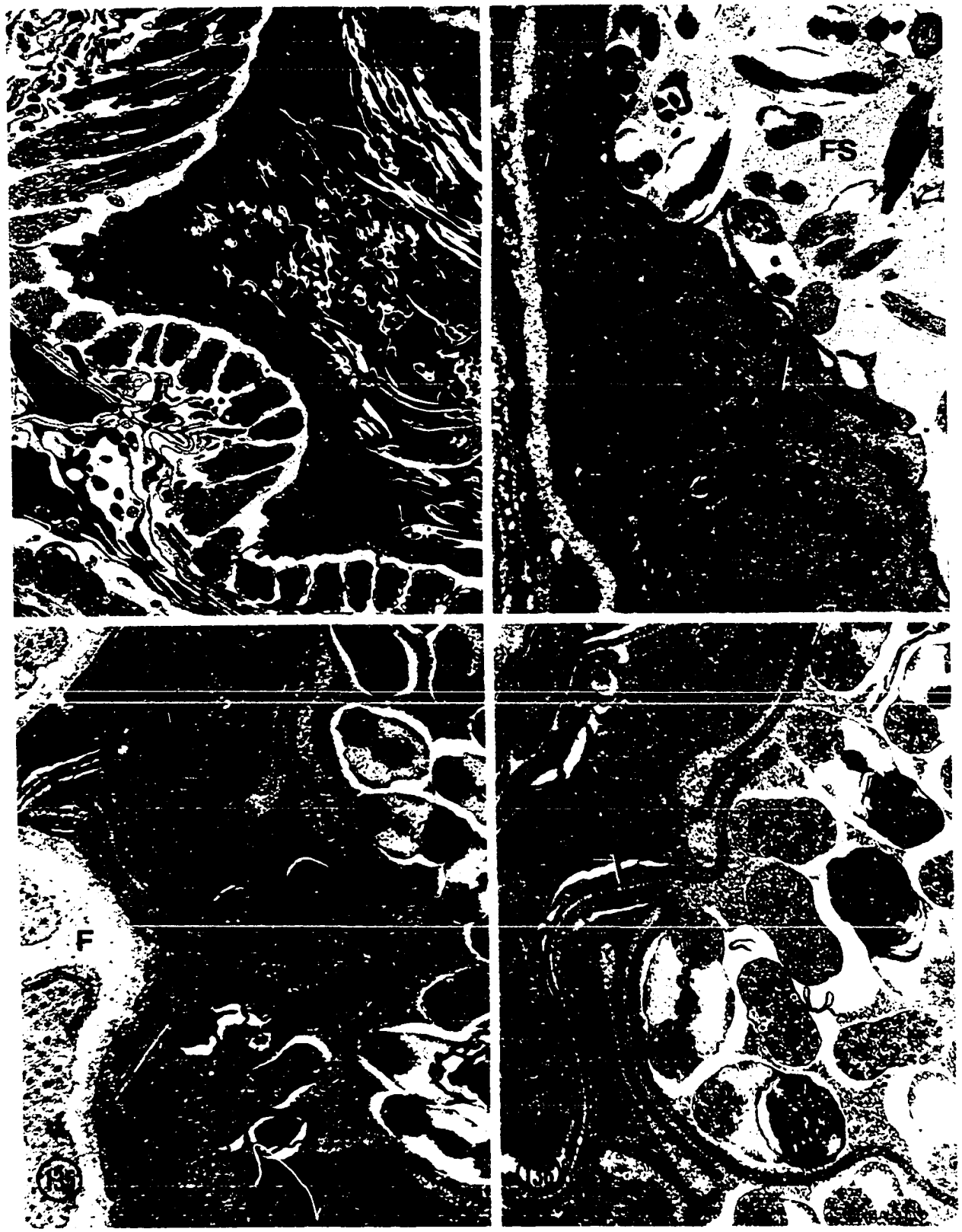
FS
F

Plate XL

Fig. 137. Prostate gland cell. Irregular nucleus (N) containing granular nucleolus (NU) lies near cell base. Cytoplasm contains Golgi complexes (G), mitochondria (M), granular endoplasmic reticulum (ER), and large secretory granules (SG). (X 30,000)


SG
N

Plate XLI

Fig. 138. Golgi complexes in prostate cytoplasm. Each complex consists of elongate saccules (GS) and ovoid vesicles (GV). (X 52,300)

Fig. 139. Prostate gland cytoplasm. Secretory granules (SG), closely associated with Golgi complexes (G), are electron-dense containing small areas of greater density. Granules of this type are the most common prostate secretory product. (X 34,000)

Fig. 140. Prostate secretory granules. This type of granule (SG) contains a large central dense area. Note Golgi complex (G). (X 30,000)

Fig. 141. Prostate secretory granules. Vesicular secretions, containing granular residue (arrow), are common in the anterior portions of prostate gland and ejaculatory duct. These may represent phagocytized secretory granules. (X 17,250)

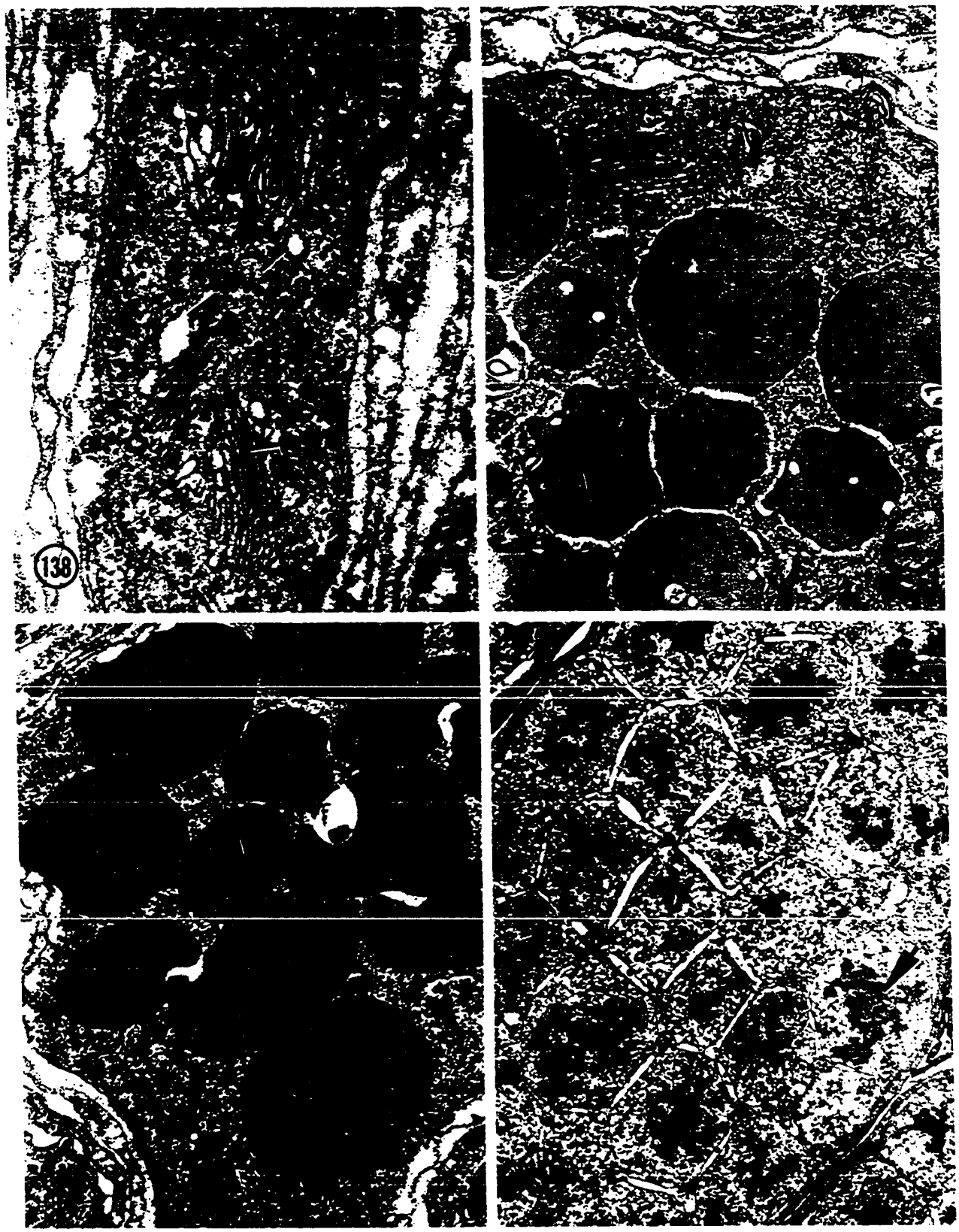
138

Plate XLII

Fig. 142. Prostate gland cytoplasm. Lakes of endoplasmic reticulum (EL) commonly occur in peripheral cytoplasm. Note numerous free ribosomes (R) and Golgi complex (G). (X 35,300)

Fig. 143. Autophagosome (AP) in prostate cytoplasm. This organelle contains remnants of granular endoplasmic reticulum. Note Golgi complex (G) and thick cisternae of endoplasmic reticulum (ER) lying in adjacent cytoplasm. (X 38,700)

Fig. 144. Autophagosome (AP) containing mitochondrion (M). (X 31,250)

Fig. 145. Autophagosome in prostate gland cytoplasm containing secretory granule (SG). (X 33,500)

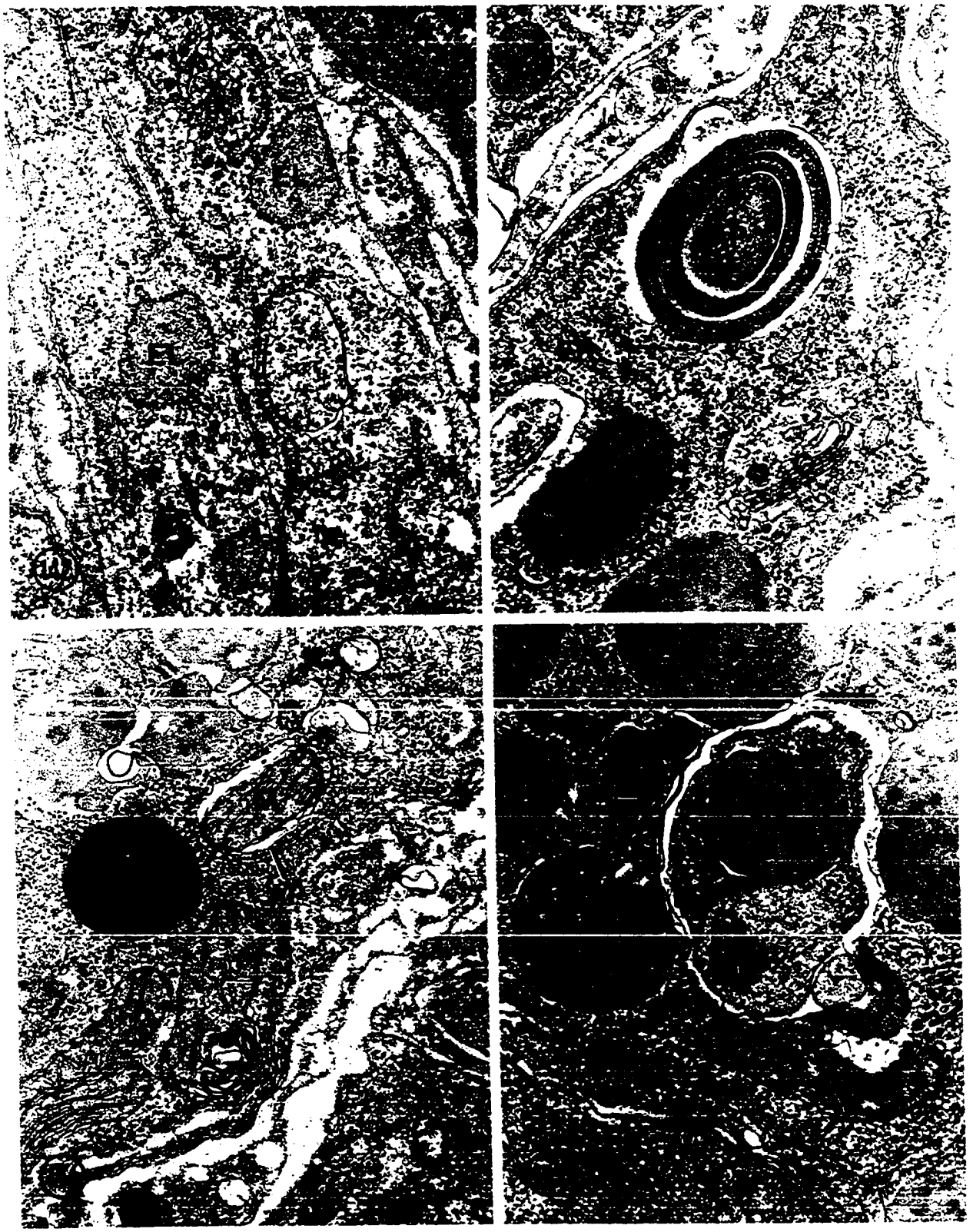

Plate XLIII

Figs. 146-148. Ejaculatory duct of Q. quinqueserialis.

Fig. 146. Ejaculatory epithelium containing irregular nucleus (N). Bands of circular muscle (CM) and layer of longitudinal muscle (LM) support epithelium. Note cytoplasmic extension (CE) surrounding group of prostate secretory granules. (X 11,800)

Fig. 147. Junctional complexes (J) connecting adjacent epithelial cells. (X 45,000)

Fig. 148. Lumenal surface of ejaculatory epithelium containing numerous cytoplasmic extensions (CE). Note prostate ducts (PD) extending through circular muscle (CM) and ejaculatory epithelium. Secretory granules (SG) migrate from prostate gland via prostate ducts into ejaculatory lumen where they accumulate. (X 13,000)

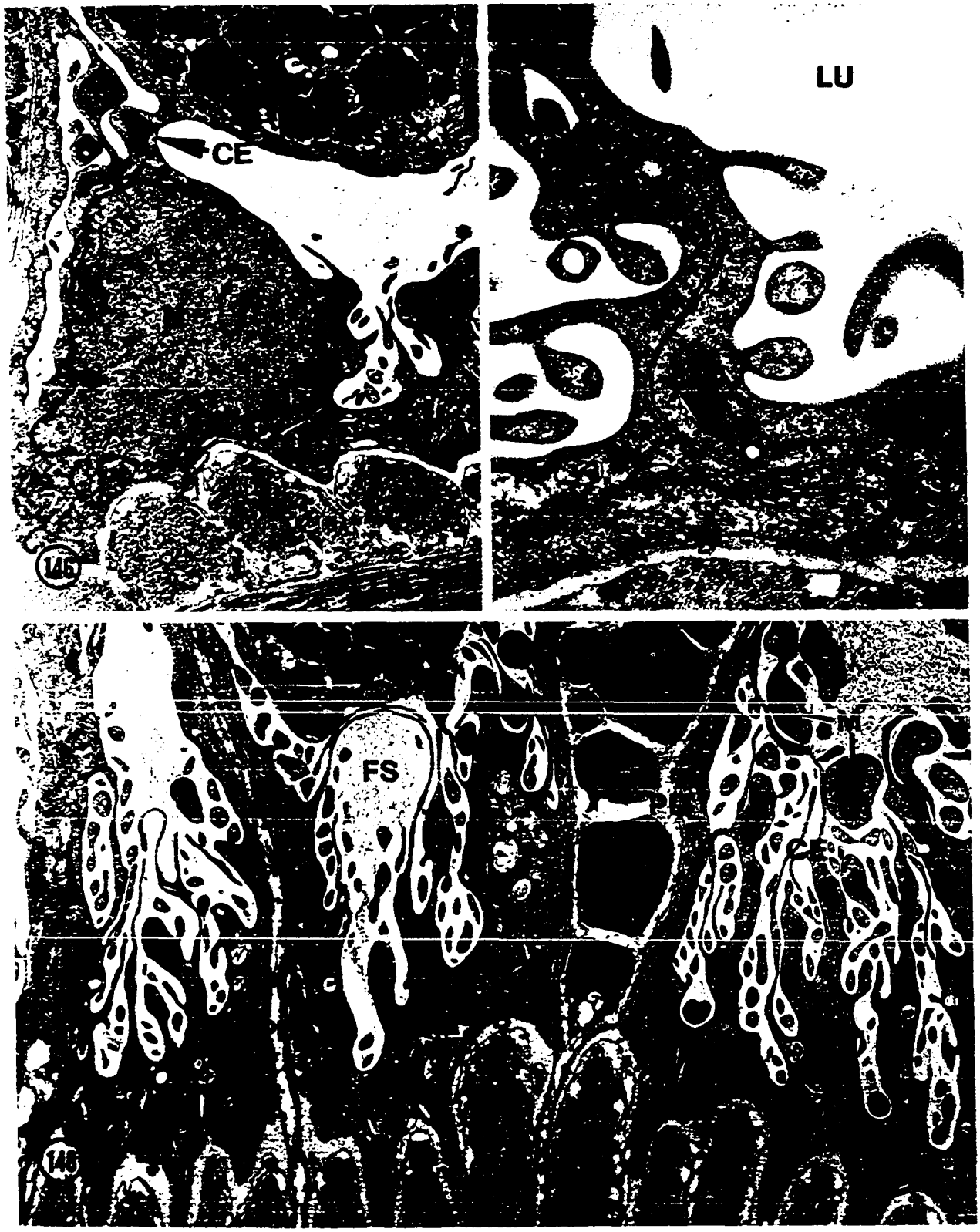
CE
LU
FS
C
146
148

Plate XLIV

Fig. 149. Prostate duct extending through ejaculatory epithelium is supported by microtubules (MT). Note thick basal lamina (B) underlying epithelium. (X 27,750)

Fig. 150. Anterior portion of ejaculatory duct is formed by syntegument (ST). Note underlying circular muscle bands (CM) and layer of longitudinal muscle (LM). This region represents transitional zone between ejaculatory epithelium and cirrus syntegument. (X 16,700)

Fig. 151. Scanning micrograph of cirrus. Note numerous spinelike protuberances on surface. (X 450)

Fig. 152. High magnification scanning micrograph of spinelike protuberances of cirrus. Note numerous small evaginations. (X 10,000)

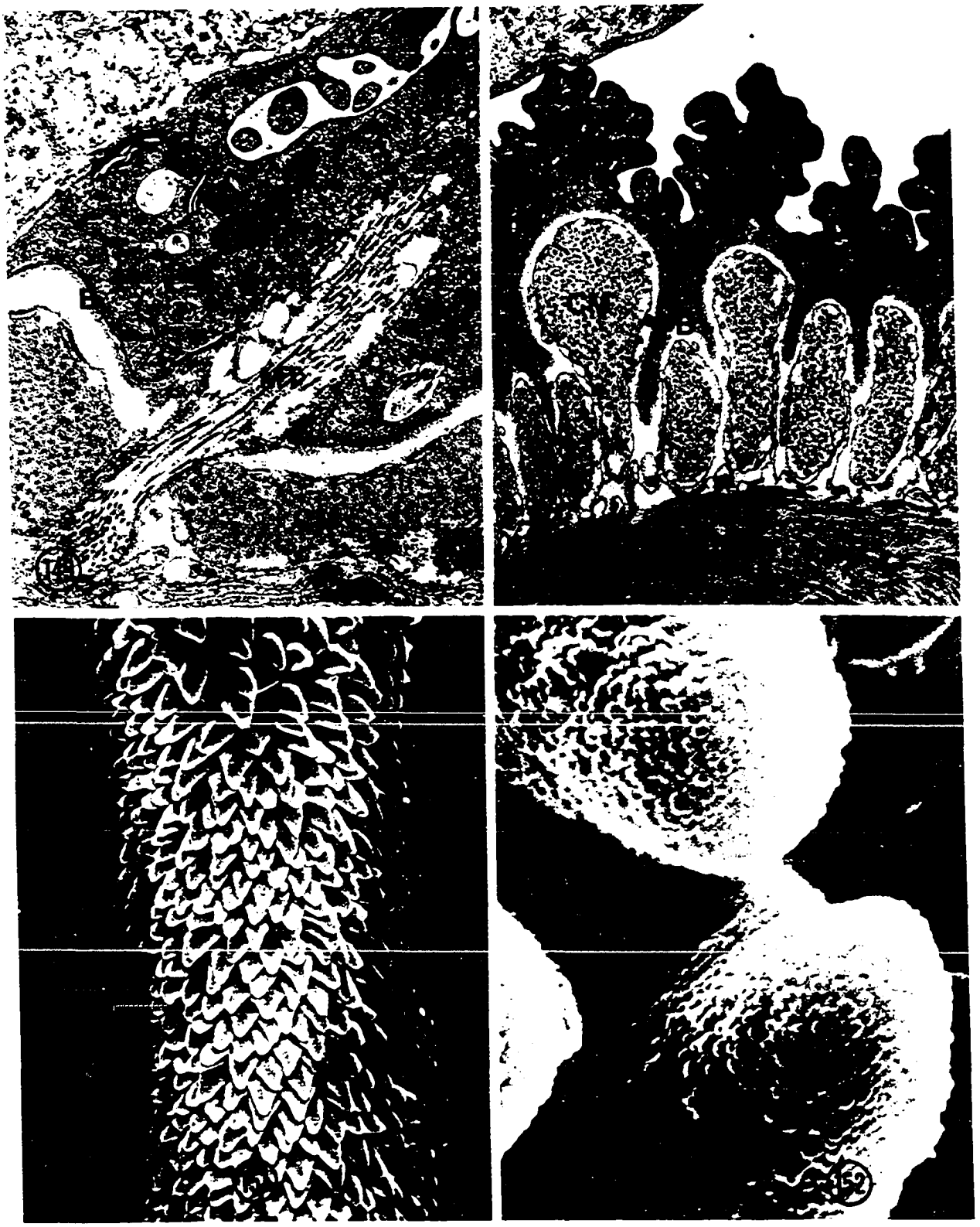

Plate XLV

Fig. 153. Transmission micrograph of cirrus. Spinelike protuberances are formed by modified syntegument (ST) containing numerous vesicular tegumental inclusions (VB) and few mitochondria (M). Circular muscle (CM) and longitudinal muscle (LM) lie below syntegument in fibrous interstitial tissue (F). Cytotegument (CT) consists of thin cytoplasmic cisternae. Internuncial process (IP) of cytotegument extends through tegumental musculature. (X 13,350)

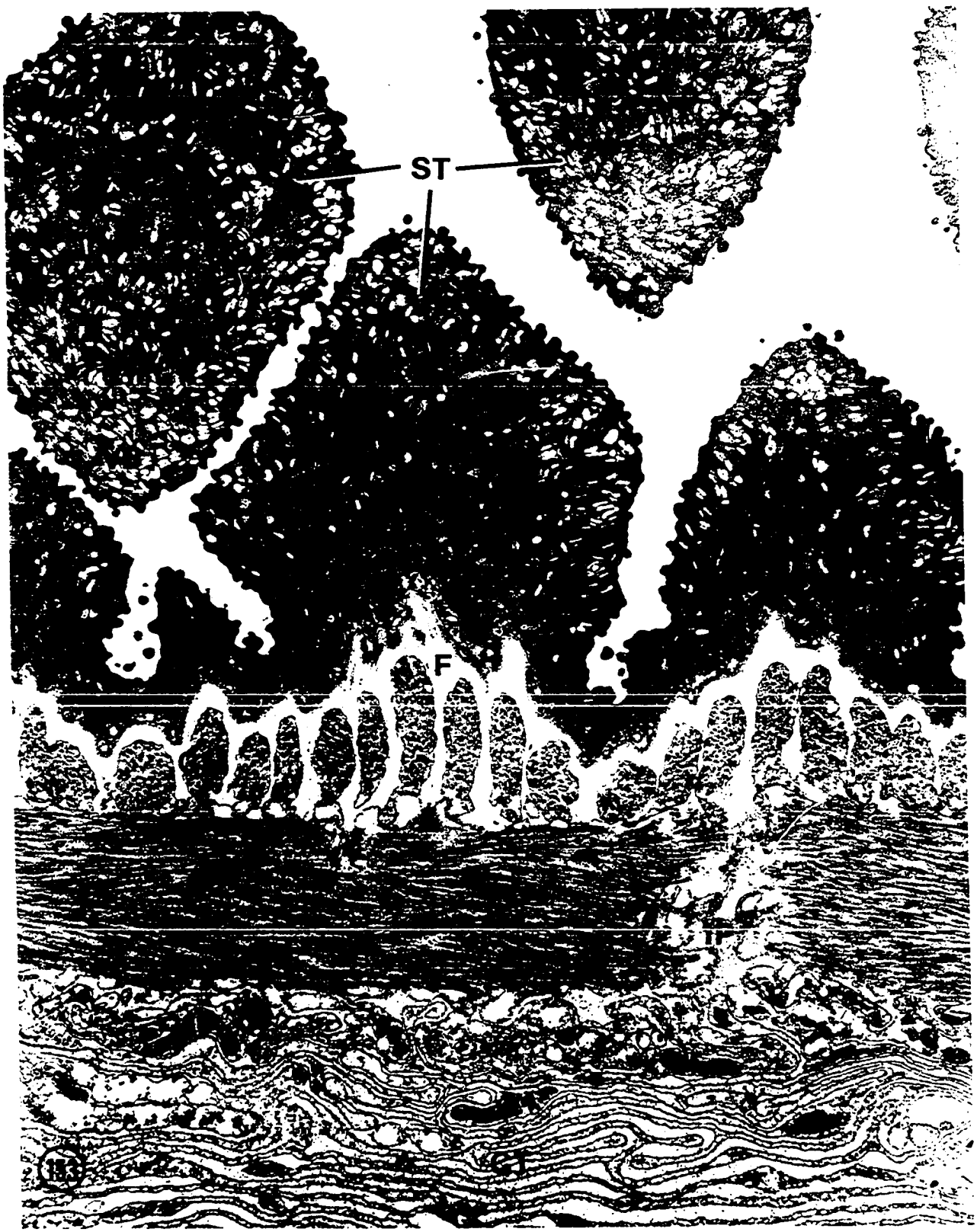
ST
F
TF